Coherence Analysis: Methods, Solutions and Problems

A thesis submitted for the degree of
Doctor of Philosophy

By
Memon Irfan

School of Information Systems, Computing and Mathematics
Brunel University
August 2008

Abstract

A coherence function is a measure of the correlation of two signals and may be used as a measure for functional relationship between brain areas. In studying functional relationships, referenced EEG (REEG) coherence analysis yields important new aspects of brain activities, which complement the data obtained by power spectral analysis. However, REEG-based coherence tends to show a false high value due to volume conduction from uncorrelated sources (VCUS). Existing signal processing methods address this issue using a Fourier coherence function of scalp Laplacian. Although this method has been proved useful to reveal correlation between EEG signals with minimum VCUS effects, it only provides frequency-domain analysis. Since EEG signals are highly non-stationary, it is more appropriate to use time-frequency methods for coherence analysis of scalp Laplacian. Thus this research applies the wavelet transform on coherence analysis of scalp Laplacian.

To verify our technique, already recorded EEG data of event related potentials were obtained from a study of two large groups of alcoholic and abstinent alcoholic subjects, performing visual picture-recognition tasks. The proposed coherence method successfully detected time-frequency correlation between EEG signals with minimum VCUS effects. It showed significant spatial specificity and revealed detailed coherence patterns. Some new important results regarding time-frequency characteristics of VCUS effects on wavelet and short-time Fourier transform (STFT) coherence analysis of REEG signals were deduced. The proposed coherence method was also compared to a conventional wavelet coherence method of REEG signals in the study of coherence difference between coherences of alcoholic and abstinent alcoholic EEG signals. Results of this study provided substantial evidence that VCUS effects are not additive and therefore can not be ignored in comparison of different brain states between groups of subjects.

Contents

List of Figures

Acknowledgements

I am very thankful to Dr Tony Elliman, Reader at the School of Information Systems, Computing and Mathematics, Brunel University, West London, for giving me the opportunity to work under his direction and for his experienced advice in the development of my work.

I am also thankful to Ex-Professor Paul Nunez at the Department of Biomedical Engineering, Tulane University, Professor Lagerlund, Associate Professor of Neurology at the Mayo Clinic Rochester Campus and Dr Yongmin Li, Senior Lecturer at the School of Information Systems, Computing and Mathematics, Brunel University, West London for their guiding about my work. I would like to thank the one who introduce me in this fascinating world of brain signals, the one who encouraged and supported a new student coming up with crazy ideas about EEG and the brain. My very special thanks to Dr Lampros Stergioulas. My special thanks to Dr Henri Begleiter at the Neurodynamics Laboratory at the State University of New York Health Center at Brooklyn for providing the EEG data. I am also thankful to the Dr Gonzalo Alarcon, Director of the MSc Course in Epileptology, Department of Clinical Neurophysiology King's College Hospital for providing sound basis for my research.

List of abbreviations

AD: Alzheimer's disease

ADHD: Attention deficit hyperactivity disorder

AWSC: Averaged wavelet squared coherency

CSF: Cerebral spinal fluid

CWT: Continues wavelet transform

EEG: Electroencephalography

ERP: Event related potential

REEG: Referenced electroencephalography

STFT: Short-time Fourier Transform

ms: Milliseconds

MRI: Magnetic resonance imaging

MEG: Magnetoencephalography

SCD: Scalp current density

SC: Squared coherency

SL: Scalp Laplacian

VCUS: Volume conduction from uncorrelated sources

Glossary of symbols

$\boldsymbol{a}$: The scale parameter in wavelet transform

$\boldsymbol{b}$: The translation parameter in wavelet transform

$\boldsymbol{C_{xy}(\omega)}$: The Fourier coherence function between continuous time series $x(t)$ and $y(t)$ at frequency ω

$\boldsymbol{C_{xy}(m)}$: The Fourier coherence function between discrete time series $x(n)$ and $y(n)$ at discrete frequency m

$\boldsymbol{C_{xy}(m,n)}$: The STFT coherence function between discrete time series $x(n)$ and $y(n)$ at discrete frequency m and discrete time n

$\boldsymbol{f_a}$: The frequency of wavelet in Hertz related to scale a

$\boldsymbol{i}$: The imaginary number

$\boldsymbol{l_E}$: The SL based on Perrin method at electrode position E

$\boldsymbol{l_x(n)}$: The SL based on Hjorth method at electrode position x

$\boldsymbol{m}$: The discrete frequency variable

$\boldsymbol{M}$: The number of segments of signal $x(t)$

$\boldsymbol{N}$: Total number of samples present in time series $x(n)$.

$\boldsymbol{n}$: The discrete time variable

$\boldsymbol{N_c}$: The number of samples in the interval over which the coherence functions are estimated.

$\boldsymbol{P_{xy}(\omega)}$: The continuous Fourier cross-spectrum between time series $x(t)$ and $y(t)$ at frequency ω

$\boldsymbol{P_{xy}(m,n)}$: The discrete STFT cross-spectrum between time series x (n) and $y(n)$ at frequency m and time n

$\boldsymbol{P_{xx}(m,n)}$: The discrete STFT auto-spectrum of time series x (n) at frequency m and time n

$\boldsymbol{q}$: The order of Legendre polynomial

$\boldsymbol{R}$: The number of the repeated trials present in the EEG data

$\boldsymbol{r}$: The number of scalp electrodes used for recoding EEG

$\boldsymbol{s}$: The degree of Legendre polynomial

$\boldsymbol{SL}$: The scalp Laplacian based on Hjorth method

$\boldsymbol{t}$: Used as the superscript to indicate transpose operation on matrices

$\boldsymbol{x(t)}$: The continuous time series at time t

$\boldsymbol{x(n)}$: The discrete time series at discrete time n

$\boldsymbol{X(\omega)}$: The Fourier transform of signal $x(t)$ at frequency ω

$\boldsymbol{X(m)}$: The Fourier transforms of discrete time series at discrete frequency variable m

$\boldsymbol{X(t,\omega)}$ The STFT of continuous signal $x(t)$ at frequency ω and time t

$\boldsymbol{*}$: It stands for complex conjugate operation.

$\boldsymbol{\gamma_n^{xy}(a,b)}$: The wavelet coherence of time series x (n) and y (n) at scale a and translation parameter b

$\boldsymbol{\omega}$: The continues frequency variable

Chapter 1

Introduction

1.1 Motivation of the research

Wavelet coherence analysis of referenced EEG (REEG) signals is one of important signal processing tools that has many neurocognitive and clinical applications. For example, significant increase in the value of wavelet coherence of REEG signals at the ictal phase of epilepsy has been reported by various studies (Blanco, et al., 1997; Bahcivan et al., 2001; Hassanpour et al., 2004; Xiaoli Li et al., 2006). It has been also used to study various neurocognitive processes, including attention, memory, learning, comprehension, and decision making (Shaw, 1981; Lamer et al., 1994; Saiwaki et al., 1997; Nunez et al., 1999). However, volume conduction from uncorrelated sources (VCUS) in the head is a serious problem during wavelet coherence analysis of REEG signals. It alters coherence estimates by introducing artificial coherence between a corresponding pair of electrodes. Existing signal processing methods developed so far to address this issue are only useful for frequency-domain methods of EEG coherence analysis. Therefore, this study addresses this issue by introducing a signal processing technique based on a wavelet coherence method of scalp Laplacian (SL). This signal processing method reveals EEG correlation with minimum VCUS effects and a satisfactory time-frequency resolution.

An important clinical application of the proposed coherence method arises in the study of coherence analysis of seizure EEG. EEG signals of such a disorder are highly time-varying and show important seizure signatures in both low and high frequency ranges (Blanco, et al., 1997; Zarjam and Mes-

bah, 2003; Hassanpour et al., 2004). A wavelet coherence method of REEG signals has been found useful for such kind of signals, as it offers an optimal time-frequency resolution in all frequency ranges. However, VCUS effects present in the brain can be a major problem during its use. To the best of our knowledge, to date no solution has been proposed to overcome this problem. However, this problem can be solved using the proposed method based on the wavelet coherence analsysis of SL, because it detects low and high frequency correlations with an optimal time-frequency resolution and minimum VCUS effects.

1.2 Thesis Introduction

Chapter 1 first presents a brief literature review and background theory required for the understanding of our research problem by rising the following questions in mind:

1. How the problem arises?
2. What is the state-of-the-art and its criticisms?

The subsequent sections of Chapter 1 present a research problem, proposed solution, significance and motivation of research and finally objectives of the research. Chapter 2 presents a review of coherence methods of REEG signals from Fourier-based signal processing methods to wavelet-based signal processing methods. Chapter 3 presents a review of various signal processing methods that are developed to minimize VCUS effects on coherence analysis of REEG signals. At the end, it introduces new signal processing methods based on STFT and wavelet coherences of SL. Chapter 4 presents an overview of our research methodology. Chapter 5 presents a detailed discussion on signal processing and statistical techniques which are used to develop wavelet and STFT coherence methods of SL. Chapter 6 explains the ability of these developed methods in detecting EEG correlation with minimum VCUS effects in the time-frequency domain. In addition, it also deduces some important results regarding time-frequency characteristics of VCUS effects on EEG correlation. At the end, this chapter presents a comparison of performances between the wavelet and STFT coherence methods of SL. Chapter 7 examines consequences of avoiding VCUS effects on EEG coherence analysis by comparing the proposed method based on the wavelet coherence of SL to a conventional wavelet coherence method of REEG signals. In addition, it also

presents a discussion on alcoholic effects on EEG correlation in the context of VCUS effects. Overall, this chapter demonstrates the importance of our proposed method in EEG signal processing. Finally in Chapter 8, the thesis is concluded by giving summary of major findings with their clinical applications, the limitations of the research performed, and the recommendations for future research.

1.3 Introduction of research

This section first presents a brief literature review and background theory required to understand a research problem. Then, overview of the research problem including its objectives, and its major contributions is discussed.

1.3.1 Short literature review of background theory

Electroencephalography is the study of the small, constantly changing electric potentials from the brain and is abbreviated as EEG. Dr Hens Berger made the measurement of small potentials on the the scalp and published the first recording in 1929. He used two large sheets of tinfoil, which served as electrodes, one on the forehead and one on the back of the head. EEG is nowadays recorded by affixing many electrodes to the scalp, and measuring the voltage between pairs of these electrodes, which are then filtered, amplified, and recorded. EEG recorded by affixing many electrodes to the scalp is called REEG or scalp EEG in EEG signal processing. These signals provide an important source of information for studying underlying brain processes. Current research in many fields investigates the potential use of REEG signals for psychiatric/physiological diagnosis as well as for evaluation of sensory experiences. A raw REEG signal provides information in the time-domain but its frequency-domain characteristics are also important. Therefore a given REEG signal is usually transformed into the frequency-domain using different methods, among them the most common method is called the Fourier transform. In the Fourier transform, a given signal $x(t)$ is transformed into the frequency-domain by describing the signal $x(t)$ as linear superposition of sines and cosines characterized by their frequency ω using the following equation:

$$X(\omega) = \int_{-\infty}^{\infty} x(t)e^{-i\omega t}dt, \tag{1.1}$$

where $X(\omega)$ is the Fourier transform of the signal $x(t)$ at the frequency ω, and i stands for the imaginary number. One of important applications of the Fourier transform in signal processing is a coherence function, which reveals the degree of linear correlation between EEG signals in the frequency-domain. The coherence function between signals $x(t)$ and $y(t)$ is defined by the following relation (Nunez et al., 1997):

$$C_{xy}(\omega) = \frac{P_{xy}(\omega)}{\sqrt{P_{xx}(\omega) \cdot P_{yy}(\omega)}}, \tag{1.2}$$

where $P_{xx}(\omega)$ and $P_{yy}(\omega)$ are the auto-spectra of the signals $x(t)$ and $y(t)$ respectively, and $P_{xy}(\omega)$ is the cross-spectrum of these signals. Auto and cross spectra are usually estimated on the basis of averages drawn from individual spectra of segments of a corresponding signal.

Coherence analysis of REEG signals has brought reliable results for a wide range of neurocognitive and clinical studies that corroborate the validity of this method. For example, it has been used to locate a epileptogenic focus from epilepsy patients (Mormann et al., 2000), to identify neuroanatomic pathways for a seizure propagation (Tsai et al., 1995; Sherman et al., 1997), and to detect a seizure activity (Brazier, 1972; Gotman, 1983; Bahcivan et al. (2001); Xiaoli Li et al. (2006)).

Fourier-based coherence analysis provides only frequency-domain information of signals, therefore it is suitable when time-domain information of signals is not required. However, a wide range of EEG signals encountered in biomedical applications fall into the category of non-stationary signals which contain important signatures both in time and frequency domains. Therefore, EEG coherence methods need to be studied in the time-frequency domain. Existing signal processing methods to study EEG coherence in the time-frequency domain are based on the STFT and wavelet transform. In the STFT, a given signal is divided into equal small segments such that the assumption of the stationarity holds for each segment (Chui, 1992; Cohen, 1995). The time evolution is provided by moving through each segment using some fixed window function. However one critical limit arises, when windowing a signal, due to the uncertainty principle. According to this principle, if a window width is very narrow, a frequency resolution will be poor, and if a window width is very wide, a time resolution will be poor (Cohen, 1995). Therefore we can conclude that for a signal having slow frequencies, a wide window width will be more appropriate and for a signal having fast frequen-

cies, a narrow window width will be more appropriate. Then, owing to its fixed window width, the STFT is not suitable for analyzing a signal involving important signatures in both low and high frequency ranges. The wavelet transform has been introduced in order to overcome this problem. A window width in the wavelet transform is not fixed. It is wide for slow frequencies and narrow for fast ones. Therefore the wavelet transform provides an optimal time-frequency resolution in all frequency ranges. The wavelet transform can be considered as an extension of the STFT incorporating the compromise between a time and frequency resolution. We can think of the STFT as filtering a signal by a filter function, which is shifted in time to provide information about time. Similarly, we can consider the wavelet transform as passing a signal through a filter function, which is not only shifted in time to provide information about time but also its width varies as frequency of the signal varies.

1.3.2 Overview of the research problem

Although wavelet coherence analysis of REEG signals has been found a useful time-frequency coherence method, VCUS effects are major problem during its use. VCUS effects biases its results by introducing artificial coherence in its true value (Srinvans et al., 1998; Nunez and Srinivasan, 2005). Few signal processing techniques have been developed to address a issue of VCUS effects on EEG coherence analysis. These techniques use SL to estimate a coherence function rather than REEG signals. The SL, which is radial scalp current density is less affected by VCUS effects, therefore a coherence function estimated using the SL reveals EEG correlation with minimum VCUC effects. However, existing SL-based coherence methods are based on the Fourier transform and therefore do not resolve the issue of VCUS effects on wavelet coherence analysis. Therefore, this research addressing this issue has proposed a wavelet coherence method of SL. This coherence method not only reveals EEG correlation with an optimal time-frequency resolution, but also minimizes VCUS effects on it.

The proposed coherence method is not a complete alternative to conventional coherence methods of REEG signals. This restriction arises due to sensitivity of the SL and REEG signals to different spatial properties (depth and orientation) of EEG sources. The SL emphasizes the contribution of superficial radial sources and at the same time deemphasizes the contribution of deeper EEG sources. This results in filtering out of coherences due to deeper sources. In contrast to the SL, REEG signals contain more contributions

generated by deeper sources, but at the same time they also contain volume-conducted activity generated by uncorrelated cortical sources. Therefore, each coherence method has its advantages and disadvantages. However, use of the proposed coherence method with conventional coherence methods will provide more useful information than is obtained by considering either in isolation.

1.3.3 Objectives of the research

The main aim of this research is to develop signal processing techniques for the following objectives:

- To detect correlation between EEG signals with minimum VCUS effects in the time-frequency domain.

- To detect low and high frequency correlations between EEG signals with minimum VCUS effects and optimal time-frequency resolutions.

- To find time-frequency characteristics of VCUS effects on EEG correlation.

- To examine consequences of avoiding VCUS effects in the study of coherence difference between coherences of different EEG activities

1.3.4 Contributions of the proposed method

- Since EEG signals are non-stationary, information regarding time evolution of coherence estimation is also important for clinical applications of REEG-based coherence analysis. Existing signal processing methods offer various time-frequency methods of REEG-based coherence analysis, which can efficiently detect time-varying coherences. However, presence of artificial coherence due to VCUS effects is still a serious issue during the use of these coherence methods. The proposed coherence method in this thesis has an advantage of detecting highly time-varying and short-duration coherences with minimum VCUS effects. Moreover it offers a satisfactory time-frequency resolution in all frequency ranges.

An important application of the proposed coherence method arises in the study of event related potentials (ERPs), which are highly non-stationary

EEG signals. During the recoding of such signals, subjects are asked to listen or see some stimulus. A recorded signal is usually called ERPs and contains important signatures of different cognitive or mental activities. These signatures are called ERP components and their time of appearance after the stimulus is usually referred as their latency. Among REEG-based coherence methods, A wavelet coherence method has been been found more useful during ERP analysis of various brain disorders and neurocognitive processes (Bianchi et al., 1998; Ta-Hsin Li and Klemm, 2000; Markazi et al., 2005; Klein et al., 2006). This is because, wavelets have ability to detect very short duration ERP components with an optimal time-frequency resolution. However, a major difficulty arises when VCUS effects significantly biases its results by introducing artificial coherence between a corresponding pair of electrodes. To the best of our knowledge, no solution to this problem has been reported so far in literature, whereas the coherence method proposed in this thesis overcomes this problem by introducing a method based on wavelet coherence of SL.

• Another application of the proposed method arises in coherence analysis of seizure EEG. These signals are highly time-varying and contain important seizure signatures in low and high frequency components. Conventional wavelet coherence analysis of REEG signals has been proved effective in detecting these seizure signatures (Bahcivan et al., 2001; Hassanpour et al., 2004). However, this coherence method can provide insignificant results due to the presence of significant VCUS effects at the corresponding pair of electrodes. In such a situation, the use of the proposed coherence method is appropriate, as it can simultaneously detect low and high frequency coherences with optimal time-frequency resolutions and minimum VCUS effects.

• This study aims to deduce characteristics of VCUS effects on EEG correlation in the time-frequency domain. These characteristics can lead to better understanding of VCUS effects on EEG correlation than those discussed in EEG coherence literature which are based on only frequency-domain characteristics of VCUS effects (Nunez, 1995; Nunez et al., 1997; Srinivasan et al., 1998; Nunez and Srinivasan, 2005).

• This study also aims to compare a conventional wavelet coherence method of REEG signals with the proposed coherence method using the REEG data set of alcoholic and abstinent alcoholic subjects. Results will be proved useful in order to assess the importance of minimizing VCUS effects during EEG coherence analysis.

Chapter 2

Review of REEG-based coherence analysis: signal processing methods and clinical applications

2.1 Introduction

This chapter presents a review of existing REEG-based coherence methods, with their clinical applications and limitations in EEG signal processing. In addition, it discusses statistical methods used to assess performance of these coherence methods.

2.2 Background theory of coherence analysis in EEG studies

REEG-based cross-correlation analysis is a time-domain method of measuring the degree of correlation between EEG signals, usually from different recording sites. The cross-correlation function of time series $x(n)$ and $y(n)$ at discrete time n is given by the following relation (Lynn, 1992):

$$R_{xy}(d) = \frac{1}{N} \sum_{n=1}^{n=N} x(n)y(n+d), \tag{2.1}$$

where N is the total number of samples present in each of these time series, and d is the time-shift of time series $y(n)$ with respect to time series $x(n)$. When a cross-correlation function is first computed from time series which have had the mean removed, and is then normalized by the product of the square root of the variance of each signal, the normalized cross-correlation coefficient is produced. The maximum value of this coefficient is always one. Two signals with identical patterns have a cross-correlation coefficient of 1 at zero time-shift, even if they have different overall amplitudes. REEG-based cross-correlation analysis has been used to study the relationship of EEG activity between different cortical regions, and between cortical and subcortical regions of the brain. It has shown the high degree of bilateral symmetry and synchronization over homologous location on each side of the scalp (Brazier and Casby, 1952; Barlow, 1959a; Barlow and Freeman, 1959b). It has been used to measure the time-shift between signals (Daniel, 1966; Liske et al., 1966). In Parkinson's disease, REEG-based cross-correlation analysis has been used to investigate the relationship between the cortex and deep structures as well as between the cortex and the limb tremor (Brazier and Barlow, 1956). A possible relationship between cortical rhythms and tremor activity[1] in essential tremor has also been explored by it (Barlow, 1967). One of major disadvantages of REEG-based cross-correlation analysis is that, it is based on only time-domain analysis of REEG signals. Both frequency and time-domain information of REEG signals have been proved very useful in EEG signal processing (Vincent et al., 1995; Demiralp et al., 1998; Akin, 2002).

Therefore, REEG-based cross-spectrum analysis was introduced in order to measure the degree of correlation between EEG signals in the frequency-domain (Gath et al., 1992; Ferri et al., 2000; Ning and Trinh, 2004). The cross-spectrum function of two discrete time series $x(n)$, and $y(n)$ whose Fourier transforms are $X(m)$ and $Y(m)$ respectively is given by the following relation:

$$P_{xy}(m) = X(m)Y^*(m), \tag{2.2}$$

where m is the frequency variable, and asterisk stands for the complex conjugate operation. When $x(n)$ is equal to $y(n)$, for all values of n, Eq. (2.2) is called the auto-spectrum of time series $x(n)$ or $y(n)$.

[1]Uncontrollable shaking (tremor) of the hands and head and sometimes other parts of the body

2.3 Fourier coherence analysis

The Fourier-based cross-spectrum in Eq. (2.2) is a complex measure, it can be described by an amplitude and a phase. In order to get a normalized and real magnitude value between 0 and 1, the cross-spectrum of time series $x(n)$ and $y(n)$ in Eq. (2.2) is normalized by dividing it with the square root of the product of the auto-spectra of these time series. Then, the square of the normalized cross-spectrum is taken. The normalized cross-spectrum is called the Fourier coherence and its square is called the Fourier squared coherency in EEG studies.

$$C_{xy}(m) = \frac{P_{xy}(m)}{\sqrt{P_{xx}(m) \cdot P_{yy}(m)}}, \tag{2.3}$$

$$C^2_{xy}(m) = \frac{\mid P_{xy}(m) \mid^2}{P_{xx}(m) \cdot P_{yy}(m)}, \tag{2.4}$$

where $C_{xy}(m)$, and $C^2_{xy}(m)$ represent the Fourier coherence and Fourier squared coherency functions respectively. If we have an appropriately pair of data recording we could estimate $P_{xy}(m)$, $P_{xx}(m)$ and $P_{yy}(m)$ by the Fourier transform to obtain,

$$P_{xx}(m) = a + ib, \quad P_{yy}(m) = c + id, \quad P_{xy}(m) = (a + ib)(c - id)$$

If these equations are substituted into Eq. (2.4), we get value of squared coherency equal to unity for all values of m. This is perhaps no surprise when we consider that the cross-spectrum is merely a complex product of the two constituent spectra, and that the coherence function is normalized by placing a not dissimilar product in the denominator. Why then are coherence functions of use to the analyst? The answer is that calculation of coherence by means of averaged estimates based on segments of the original signal indeed yields meaningful quantitative measures of similarity between them, and these measures take values between zero and unity. Thus auto-spectra and cross-spectrum for Fourier coherence analysis of REEG signals are usually estimated on the basis of averages drawn from the individual spectra of the segments.

A coherence function measures the degree of correlation between signals in terms of their relative phase and relative amplitude (Nunez et al., 1997). However, a phase coherence function can be used to measure the degree of

correlation between signals in terms of their relative phase, independent of amplitude fluctuations. It is given by the following relation (Marple, 1987):

$$\Upsilon_{xy}(m) = \frac{\mid U_x(m)V_y^*(m) \mid^2}{\mid U_x(m)U_x^*(m)V_y(m)V_y^*(m) \mid}, \tag{2.5}$$

where $U_x(m)$ and $V_y(m)$ can be obtained by taking the ratio between real component to the imaginary component of time series $x(n)$ and $y(n)$ respectively. Another important kind of REEG-based coherence analysis is based on a partial coherence function. It is used to measure the coherence between time series $x(n)$ and $y(n)$, after removing the common influence of another time series $w(n)$ (Gardner, 1992). To calculate a partial coherence function, first we need to compute the partial cross-spectrum function, which is the cross-spectrum of signals $x(n)$ and $y(n)$ with the effects of signal $w(n)$ removed and is given by (Gardner, 1992),

$$P_{xy,w}(m) = P_{xy}(m)P_{ww}(m) - P_{xw}(m)P_{yw}^*(m). \tag{2.6}$$

When $x(n) = y(n)$ for all values of n, Eq. (2.6) is called the partial auto-spectrum of time series $x(n)$ or $y(n)$. The partial coherence of time series $x(n)$ and $y(n)$ is given by the following relation (Gardner, 1992):

$$C_{xy,w}(m) = \frac{P_{xy,w}(m)}{\sqrt{P_{xx,w}(m)P_{yy,w}(m)}}. \tag{2.7}$$

2.3.1 Statistical procedures

As mentioned earlier that robust coherence estimates require an averaging over the segments of original signals involved in coherence analysis. Therefore the first step when computing a coherence function using the Fourier transform is to divide given time series $x(n)$ and $y(n)$ into M segments of short and equal intervals.

The disadvantage of Fourier coherence is that it requires fairly long observation time about 30 seconds or more to achieve a good spectral resolution but this results in a poor time resolution. This limitation simply follows from the uncertainty principle, which states that if Δt and Δf are the standard deviations in time t and frequency f of signal $x(t)$ respectively then (Cohen, 1995),

$$\Delta t \Delta f \geq \frac{1}{4\pi} \tag{2.8}$$

Eq. (2.8) simply means that frequency and time resolutions are inversely proportional to each other. Another disadvantage is increase in bias and variance of coherence estimates due to long segments. There is thus a compromise required in the choice of segment length. It must be long enough to provide an adequate frequency resolution and short enough to allow sufficient segments in the average to control bias and variance. In addition each segment must be extracted using a time-window to control slidelobes in the frequency-domain functions and thereby limit the bias which arises due to the resulting leakage. Conflicting requirements of number of segments and segment length can be resolved to some extent by overlapping segments as this permits more averages to be taken while maintaining the same frequency resolution. However, this is effective up to a point because the improvement declines due to greater correlation between segments. Computational overheads also increase with increased overlap. In general, there is no rule to control these statistical errors. However over the years, few techniques have been developed, which can be used to minimize these statistical errors to some extent. For example, Carter et al. (1973) derived following two approximations assuming an ideal Hanning window applied to each segment and no overlap between segments. Signals involved in coherence estimate were assumed zero-mean stationary Gaussian processes.

$$Bias \approx \frac{\left(1- \mid C_{xy}^2(m) \mid^2\right)^2}{M}, \tag{2.9}$$

$$Variance \approx \frac{2 \mid C_{xy}^2(m) \mid^2 \left(1- \mid C_{xy}^2(m) \mid^2\right)}{M}, \tag{2.10}$$

where M is the number of segments used in the estimation of squared coherency $C_{xy}^2(m)$. Approximations in Eqs.(2.9) and (2.10) are valid when squared coherency is greater than zero. For zero value of the squared coherency these approximations lead to a constant value of the variance, which is equal to inverse of M. Another important method to control statistical errors in coherence estimate is based on the confidential interval of a coherence function. It is defined as the "probability that the true coherence at a certain time lies within a certain interval about the estimated coherence". The approximate relation for the 95 % confidence interval for Fourier coherence is given in terms of standard error e in coherence estimate $C_{xy}^2(m)$ (Bendat and Piersol, 2001):

$$\frac{C_{xy}^2(m)}{1+2e} \leq coh^2 \leq \frac{C_{xy}^2(m)}{1-2e}, \tag{2.11}$$

where

$$e = \sqrt{\frac{2}{N_c}} \frac{1 - C_{xy}^2(m)}{\mid C_{xy}(m) \mid}. \tag{2.12}$$

N_c is the number of samples in the interval over which the coherence function is estimated. Eq. (2.11) can be used to find number of the samples required for the satisfactory value of a coherence function.

2.3.2 Recording strategies

Apart from statistical constraints, the choice of reference electrode has also great implications when coherence between REEG signals is estimated (French and Beaumont, 1984; Gavins, 1989). Electrical activity generated by reference electrodes can yield an increase as well as decrease of REEG-based coherence as activity at reference electrodes contributes to both signals involved in REEG-based coherence analysis (Fein et al., 1988).

The use of EEG recording systems based on the linked ear, average reference and bipolar techniques (see Appendix C for detail) substantially reduces the problem of reference electrode. However, performance of these techniques against each other depends upon the specific EEG application. With the small number of recording electrodes, the bipolar and linked ear techniques are best options than the average reference technique (Nunez and Srinivasan, 2005). This is because, accuracy of the average reference technique depends upon the number of recording electrodes. As the number of electrodes increases, the error in its accuracy is expected to decrease. However EEG recording system of at least 64 electrodes based on this technique shows better performance than those which are based on the bipolar and linked ear techniques (French and Beaumont, 1984; Nunez, 1981). As far as choice between the linked ear and bipolar techniques is concerned, the linked ear technique has shown the better performance than the bipolar technique (Fein et al., 1988; Bendat and Piersol, 2001; Nunez and Srinivasan, 2005). The main reason is the poor conduction properties of tissues between the temporal and the ear lobes, which are linked by a wire to serve as the reference in the linked ear technique.

2.3.3 Applications

Fourier coherence analysis of REEG signals has become an important tool to study the functional relationship between EEG signals on the assumption that higher the correlation, the stronger the functional relationship between EEG signals (Nunez and Srinivasan, 2005). Its applications include studies of human pain (Andrew et al., 1998; Baltas et al., 2002), abnormal EEG during the epilepsy (Brazier, 1972; Gotman, 1983; Tsai et al., 1995; Sherman et al., 1997; Mormann et al., 2000; Bahcivan et al., 2001; Xiaoli Li et al., 2006), EEG of spilt brain patients (Nunez, 1981), brain development and cognitive processes (Tucker et al., 1985; Marosi et al., 1992).

Epilepsy

One of most important clinical applications of Fourier coherence analysis of REEG signals is observed for the epilepsy. Epilepsy is a physical condition that occurs when there is a sudden, brief change in how the brain works. When brain cells are not working properly, a person's consciousness, movement, or actions may be altered for a short time. These physical changes are called epileptic seizures. Epilepsy is therefore sometimes called a seizure disorder. Fourier coherence analysis of REEG has been used to identify neuroanatomic pathways for a seizure propagation. For example, it was used for clonic seizure using the assumption that anterior thalamus and cortex are coherent, if the seizure activity spreads from the subcortical to the cortical brain (Tsai et al., 1995; Sherman et al., 1997). Results showed that thalamus and cortical regions of the brain were highly coherent during clonic seizure. In other words Fourier coherence was found larger between the thalamus and cortical regions. Fourier coherence can be useful to locate a epileptogenic focus from epilepsy patients. For example, Mormann et al. (2000), used it to analyze intracranial EEG activity of 17 epilepsy patients undergoing presurgical diagnostics. Results showed increase in mean phase coherence function near the epileptogenic focus.

Alzheimer's disease

Alzheimer's disease (AD) is characterized by loss of function and the death of nerve cells in the several areas of the brain leading to loss of the cognitive function such as memory and language (Abasolo et al., 2006). The cause of the nerve cell death is unknown but the cells are recognized by the

appearance of unusual helical protein filaments in the nerve cells and by degeneration in cortical regions of the brain, especially frontal and temporal lobes. Fourier coherence analysis of REEG signals has greatly contributed to a better definition of modification of EEG in the early stages of this disease: these changes consist in a slowing of the peak of an alpha band and in an increase of the power of a theta band (Coben et al., 1985; Leuchter et al., 1987; Jelic et al., 1997; Locatelli et al., 1998; Knott et al., 2000; Adler et al., 2003). For example, Adler et al. (2003) examined REEG signals of 31 AD patients and 17 healthy subjects using Fourier coherence function. The ages of all subjects were above 60 years. Their finding was the decrease of the left temporal alpha band of coherence and the decrease of the interhemispheric theta band of coherence in AD patients with a sensitivity of 87% and specificity of 77 %. The decrease in coherence for the alpha band in AD patients can be related to the alternations in the cortico-cortical connections (Locatelli et al., 1998). In more advanced stages of AD patients, increase of Fourier coherence in a delta band with decrease of the alpha band of coherence has also been reported (Coben et al., 1985).

Human pain

Fourier coherence analysis of REEG signals has been used to examine effects of human pain on the correlation of EEG signals. Andrew et al. (1998) examined effects of human pain on cerebral EEG activity using Fourier coherence. The pain test was pain stimulation by a ice cube on the right hand of a subject. Higher coherence during pain was examined between frontal and parietal positions. Baltas et al. (2002) examined effects of pain on Fourier coherence of REEG signals. The pain test was the repeated heat stimuli in the form of laser pulses which were delivered to the right forearm of a subject by laser cannon. The study showed significant value of coherence during pain.

2.4 STFT coherence function

The non-stationary nature of EEG signals makes it necessary to use signal processing methods which have ability to quantify their spectral components as a function of time. Fourier coherence analysis lacks of such ability, because of the Fourier transform which is based on only frequency-domain analysis. For analyzing such signals, time-frequency methods of coherence analysis are

more appropriate, therefore STFT coherence analysis has been introduced as an alternative to Fourier coherence analysis (Lachaux et al., 2002; Sun et al., 2003; Bruns, 2004; Markazi et al., 2005; Zhan et al., 2006).

In STFT, to study properties of the continuous signal $x(\tau)$ at time t, the signal is multiplied by a window function, $w(\tau\text{-}t)$. The effect of the window function is to keep the signal less unaltered around the time t but to suppress the signal for times distant from time of interest. Since the product between the signal and the window function emphasizes the signal around the time t, the Fourier transform will reflect the distribution of frequency around that time,

$$X(\omega, t) = \int_{-\infty}^{\infty} x(\tau) w(\tau - t) e^{-i\omega\tau} d\tau, \tag{2.13}$$

The STFT in Eq. (2.13) is defined for the continuous signal, for a discrete signal $x(k)$, the discrete STFT is defined as (Semmlow, 2004):

$$X(m, n) = \sum_{k=1}^{N} x(k) w(k - n) e^{-i2\pi km/N}, \tag{2.14}$$

where N is the total number of samples present in time series $x(k)$, n is the discrete time variable and m is the discrete frequency variable, representing integers from 0 to N-1. The STFT cross-spectrum of time series x (k) and $y(k)$ is given by the relation (Semmlow, 2004):

$$P_{xy}(m, n) = X(m, n).Y^*(m, n) \tag{2.15}$$

The cross-spectrum of two equal time series, i.e., $x(k) = y(k)$ for all values of k, is usually called an auto-spectrum. The STFT coherence and STFT squared coherency functions of time series $x(k)$ and $y(k)$ are given by the following relations:

$$C_{xy}(m, n) = \frac{P_{xy}(m, n)}{\sqrt{P_{xx}(m, n) P_{yy}(m, n)}}, \tag{2.16}$$

$$C_{xy}^2(m, n) = \frac{\mid P_{xy}(m, n) \mid^2}{P_{xx}(m, n) \cdot P_{yy}(m, n)} \tag{2.17}$$

Even though STFT coherence provides useful information in the time-frequency domain, major disadvantage of the STFT is the window function

of the fixed width which results either in a poor frequency resolution or in a poor time resolution. This limitation simply follows from the uncertainty principle, according to which, frequency and time resolutions of a signal are inversely proportional to each other (for details see Section §2.3).

2.5 Wavelet coherence analysis

Like STFT, the wavelet transform also allows us to study the signal $x(t)$ in time and frequency domains. The major advantage of the wavelet transform is that it has a varying window width, being wide for slow frequencies and narrow for the fast ones, thus leading to an optimal time-frequency resolution in all the frequency ranges. By contrast, in the STFT, once we choose a particular width for the window function, that window is the same for all frequencies. Many signals require a more flexible approach, where we can vary the window width to determine more accurately for either time or frequency.

The continuous wavelet transform (CWT) of the signal $x(t)$ in terms of the basic function $\psi_{a,b}(t)$ is given by the following relation (Cohen, 1995):

$$W_t^x(a,b) = \frac{1}{\sqrt{a}} \int_{-\infty}^{\infty} x(t)\psi_{a,b}^*(t)dt, \tag{2.18}$$

provided that,

- The wavelet must have finite energy:

$$E = \int_{-\infty}^{\infty} \mid \psi(t) \mid^2 dt < \infty \tag{2.19}$$

- If $\Psi(\omega)$ is the Fourier transform of $\psi(t)$ then the following condition must hold:

$$C_g = \int_0^{\infty} \frac{\mid \Psi(\omega) \mid^2}{\omega} d\omega < \infty \tag{2.20}$$

$\psi_{a,b}(t)$ can be obtained from a single prototype wavelet called the mother wavelet $\psi(t)$ by

$$\psi_{a,b}(t) = \frac{1}{\sqrt{a}} \psi\left(\frac{t-b}{a}\right), \tag{2.21}$$

where a and b are the scale and translation parameters respectively. As scale a changes, the shape of the wavelet is compressed or stretched to cover

different frequency ranges and by varying translation parameter b, the mother wavelet is displaced in time. In this way, the wavelet transform provides a time-frequency description of the signal $x(t)$.

2.5.1 Estimation of wavelet coherence

Using Eq. (2.18), the wavelet transform of discrete time series $x(n)$ is given by,

$$W_n^x(a,b) = \frac{1}{\sqrt{a}} \sum_{n=1}^{N} x(n)\psi_{a,b}^*(n), \tag{2.22}$$

It is possible to compute the wavelet transform in the time-domain using Eq (2.22). However it is much simpler to use the fact that wavelet transform is the convolution between time series $x(n)$ and wavelets $\psi_{a,b}^*(n)$, and to carry out the wavelet transform in Fourier space using the fast Fourier transform (FFT). Unlike the convolution, the FFT method allows the computation of all n points simultaneously. In the Fourier domain, the wavelet transform is given by,

$$W_n^x(a,b) = \frac{1}{\sqrt{a}} \sum_{m=0}^{N-1} X(m)\Psi_{a,b}^*(m)e^{i2\pi nm/N}, \tag{2.23}$$

where $X(m)$ and $\Psi_{a,b}^*(m)$ denote the Fourier transforms of $x(n)$ and $\psi_{a,b}^*(n)$ respectively. Given two time series $x(n)$ and $y(n)$, with wavelet transforms $W_n^x(a,b)$ and $W_n^y(a,b)$, the wavelet cross-spectrum $W_n^{xy}(a,b)$ and the wavelet auto-spectrum $W_n^{xx}(a,b)$ are given by,

$$W_n^{xy}(a,b) = W_n^x(a,b) \cdot W_n^{*y}(a,b), \tag{2.24}$$

$$W_n^{xx}(a,b) = W_n^x(a,b) \cdot W_n^{*x}(a,b), \tag{2.25}$$

The wavelet coherence is given by,

$$\gamma_n^{xy}(a,b) = \frac{W_n^{xy}(a,b)}{\sqrt{W_n^{xx}(a,b) \cdot W_n^{yy}(a,b)}} \tag{2.26}$$

2.5.2 Applications

This section describes applications of wavelet coherence analysis of REEG signals in neuroscience.

Epilepsy

Bahcivan et al. (2001) using wavelet coherence examined REEG signals of three male epileptic rats. Results showed significant level of coherence at the ictal phase of seizure. Phase coherence analysis can be used to know the phase information in EEG signals. Xiaoli Li et al. (2006) used wavelet phase coherence of REEG to measure the phase information during the pre-ictal and the ictal stage of seizures in 12 rats. Results showed increase in phase coherence from the pre-ictal stage to the ictal stage for high frequency components which indicates that frequency components tend to couple from the pre-ictal stage of seizure to the ictal stage in phase.

Cognitive processes

Mental functions such as learning, memory, imagination, comprehension and decision making are usually called cognitive processes in psychology. Various studies have conformed the usefulness of wavelet coherence analysis of REEG signals in cognitive studies (Shaw, 1981; Lamer et al., 1994; Saiwaki et al., 1997; Nunez et al., 1999; Ta-Hsin Li and Klemm, 2000; Minfen et al., 2002; Kelly et al., 2003; Meinicke et al., 2004; Srinivasan, 2004; Markazi et al., 2005; Klein et al., 2006). For example, in cognitive processes the human brain recognizes various spatially distributed elements of stimulus into a meaningful way after detecting a silent relationship and binding these various distributed elements into a meaningful way (Ta-Hsin Li and Klemm, 2000). This process is also called cognitive binding. Ta-Hsin Li and Klemm (2000) proved the mechanism of cognitive binding as a result of neuronal synchronization using wavelet coherence. In their experiment, 17 subjects were selected and were shown 10 various ambiguous figures, this is because ambiguous figures are the best way to induce cognitive binding in the human brain (Ta-Hsin Li and Klemm, 2000). Results showed significant increase in the coherence when subjects tried to recognize alternate images, i.e, when the cognitive binding occurred. Therefore, process of cognitive binding was assumed due to the increase in neuronal synchronization. In another study, Klein et al. (2006) using wavelet and Fourier coherences studied ability of

the brain to learn associations among different stimuli. These stimuli were shown to the subjects during the recording of ERPs which were later analysed using wavelet and Fourier coherences. Subjects, involved in associative learning by receiving two classes of stimuli (visual and electrical) showed the larger value of wavelet coherence in a gamma band as compared to the subjects not involved in the associative learning procedure. This supported the idea that changes in coherence observed in the learner group were due to the associative learning. On the other hand the Fourier coherence revealed no significant changes in the gamma band for subjects involved in the associative learning. Markazi et al. (2005) used wavelet coherence analysis of scalp ERPs in the study of change blindness and change detection. Change blindness is a phenomenon in visual perception in which very large changes occurring in full view are not noticed (Markazi et al., 2005). The scalp ERPs of the change detection and the change blindness were recorded by showing frames of different pictures to the 9 subjects whose ages ranged from 19 to 55 years. Results showed the significant amount of change in wavelet coherence values between change blindness and change detection.

Chapter 3

Coherence of SL

3.1 Introduction

The issue of VCUS effects on REEG-based coherence analysis has been addressed in this chapter after reviewing the background theory of the SL including its applications in neuroscience. It ends with the discussion of our proposed coherence method.

3.2 Interpretation of the SL

Existing signal processing methods to minimize the VCUS effects on coherence analysis of REEG signals are based on the SL. Before we discuss these methods, it would be useful to discuss some basics of the SL.

3.2.1 Scalp current density

According to the four concentric spherical shells model of the head, the human head is divided into four parts: the brain, cerebral spinal fluid (CSF), skull and scalp as shown in Figure 3.1.

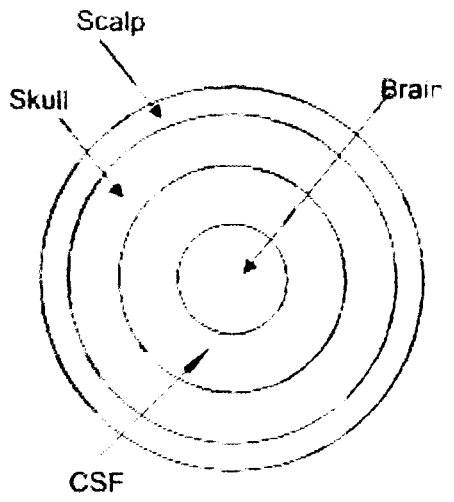

Figure 3.1: Four concentric spherical shells model of the head is based upon the assumption that human head is composed of four concentric spherical shells: the brain, CSF, skull and scalp. Nunez and Srinivasan, 2005

Each region of the brain obeys the Ohm's law, which is the fundamental assumption of this model (Srinivasan et al., 1996, 1998). The CSF is a water like fluid that surrounds and baths the brain and the spinal cord. The brain's outer layer is called the cerebral cortex. It is assumed in this model that the scalp, skull and CSF are charge free regions, containing no generating current sources and there is a constant rate of flow or volume conduction for these three tissues of the brain. In other words, these tissues serve purely as the volume conductor for brain current generators. The current generators are assumed in this model as equipotential dipoles. The current is generated in the brain and reaches to the scalp by flowing through CSF and skull[1] such that the most of the current in the skull is radial which spreads tangentially when enters into the scalp (Nunez and Srinivasan, 2005). This radial current flowing per unit volume is called the scalp current density (SCD) in EEG studies.

Perrin et al. (1987) reported that potentials from deeper sources in the brain at a depth of half the radius of the head are not reflected in the SCD. The SCD is sensitive to superficial sources, with sensitivity falling off at approximately r^4, where r is the distance from the current source to the scalp

[1]As Compared to the scalp, skull is very poor conductor of the brain and current falls off by two order of magnitude within the thickness of the skull because of its poor conductivity, therefore REEG is blurred considerably as compared to the cortical potential (Nunez and Srinivasan, 2005).

surface (Oostendorp and Van Oosterom, 1996; Pernier et al., 1988). The implication is that superficial cortical sources will have greater impact on the SCD than deeper sources. Due to this important characteristic, the SCD has an ability to eliminate much of the VCUS effects from distant sources[2], and electrical activity generated by reference electrodes (Gavins et al., 1991).

3.2.2 The SL: physical basis and applications

The SL is the second order spatial derivative of the potential on the scalp surface. It turns out that if the skull conductivity is less than at least 20 % of cortical conductivity, it provides good estimate of both SCD and cortical potentials (Nunez, 1981). The proof of this is included in Appendix B. It is a simple technique and shows most of important characteristics of the SCD. Therefore, it is frequently used in applications of the SCD in EEG signal studies. It provides various important applications in neuroscience. For example, Hjorth and Rodin (1988) reported that difference of superficial activity estimated by the SL and REEG signals can be used to differentiate superficial EEG generators from deep EEG generators. Based on this study, Yoshinaga et al. (1996) studying two cases of epilepsy, demonstrated that secondary bilateral synchrony is generated from a deep cerebral area of the brain. The secondary bilateral synchrony is an ictal bilaterally synchronous EEG signal at the location in the brain exactly contralateral to the discharge caused by lesion (Tukel and Jasper, 1952).

The SL has been also used to minimize blurring effects of the scalp and skull on REEG signals. For example, Wallin and stalberg (1980); Nunez (1989) compared REEG and SL results obtained in the study of complex partial seizure. Scalp Laplacain-based plots provided better spatial resolution of ictal activity than REEG-based plots. Wang and Begleiter (1999) compared SL-based and REEG-based plots obtained using EEG signals of alcoholics (more than 8 years) and long-term abstinent alcoholics (average 8 years of abstinence). SL-based plots showed more distinct and clear difference between the abstinent alcoholics and the alcoholic subjects than those plots obtained using REEG signals.

[2]These sources are not close (less than 2cm) to the electrodes at which the SCD is calculated.

3.2.3 Methods for estimating SL

Methods to calculate the SL or the SCD are divided into two classes: Local methods (Hjorth, 1975; Wallin and Stalberg, 1980; Katznelson, 1981; Gevins et al., 1990; Le and Gevins, 1993; Wang and Begleiter, 1999) and global methods (Perrin et al., 1987, 1989; Nunez, 1989; Law et al., 1993).

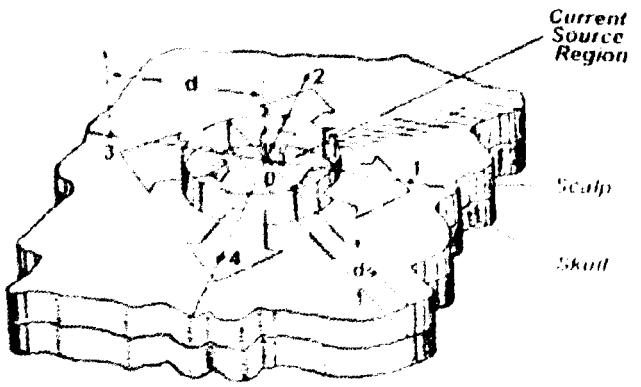

Figure 3.2: The brain region is divided into two parts: skull and scalp. d_s is a thickness of a small cylinder with principal axis perpendicular to the scalp surface. Electrode 0 is placed at the scalp position right above the EEG source, and electrodes labeled 1 to 4 are equally placed from this electrode. Katznelson, 1981

The so-called local methods use only potentials at nearest neighbor electrodes in which the SL is computed by finite difference scheme (Hjorth, 1975; Katznelson, 1981). A typical example of local methods is Hjorth's second order finite difference scheme (Hjorth, 1975), which is also called a nearest neighborhood method or Hjorth method in EEG studies. This method approximates SL at electrode 0 as the sum of the potentials at the four nearest neighbors to electrode 0 minus four times the potential at electrode 0. It has been assumed that electrode 0 is placed at the scalp position right above the EEG source, located inside the brain as shown in Figure 3.2. A small cylinder of scalp tissue of thickness d_s with principle axis perpendicular to the scalp surface is assumed. Four more electrodes labeled 1 to 4 from electrode 0 at equal distance d are assumed here. Using simple mathematical approaches, the SL at electrode 0 can be approximated as the sum of the potentials at the four nearest neighbors (electrodes 1 to 4) to electrode 0 minus four times

the potential at electrode 0, that is,

$$l_x(n) = x_0(n) - \frac{x_1(n) + x_2(n) + x_3(n) + x_4(n)}{4}, \tag{3.1}$$

where $x_0(n)$, $x_1(n)$, $x_2(n)$, $x_3(n)$, and $x_4(n)$ are time series of EEG signals at electrodes 0, 1, 2, 3, and 4 respectively. A proof of Eq. (3.1) is included in Appendix B. It is very difficult to meet conditions for the Hjorth method for all electrodes in EEG recording. For example in 10-20 electrode system, the Hjorth method is well fitted for some of electrodes such as Cz whose neighbors Fz, C_3, C_4 and Pz are nearly equidistant as shown in Figure 3.3.

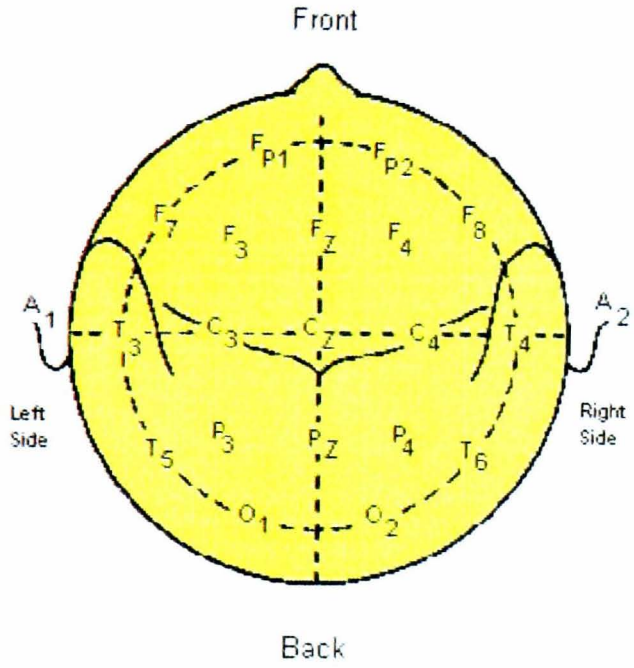

Figure 3.3: Electrodes, C_3, C_4, Fz, and Pz are nearly equidistant from electrode Cz

The Hjorth method tends to be more accurate as the distance between adjacent electrodes becomes smaller. This is because, the SL for large interelectrode distances can be contaminated by more distant, independent features rather than reflecting only the immediate surrounding potential. The smaller interelectrode distance can be achieved by using the larger number of electrodes but the recording may be more difficult to handle. The Interelectrode distance of 3.2cm is required for the satisfactory estimation of the SL, which can be achieved by using the EEG recording systems based on the extended 10/20 system of at least 64 electrodes (Nunez, 1981). When the distances

from an electrode to all of its neighbors are not equal, the Hjorth method can be modified by multiplying each potential in the average by the reciprocal of the distance. That is, each neighboring electrode potential is divided by the distance between that electrode and the center electrode, results are summed, and from this sum one subtracts the potential at the center electrode multiplied by the sum of the reciprocal distances (Babiloni et al., 1995; Lagerlund et al, 1995). If three neighbors are available, an average of these may be used. Alternatively, additional electrodes may be placed on the head in a circle passing through the nasion (Nz), inion (Iz), and the points just anterior to the tragus of the ears (T9 and T10). These electrodes may be used in the calculation of SL at the fronto polar, lateral frontal, temporal, and occipital electrode positions.

In the global methods, an imaginary surface is used to approximate SL using various interpolation techniques. The imaginary surface is generated using the projected positions and the measured potentials at the corresponding original electrodes. SL is then calculated by applying direct differentiation to a resulting interpolation function. The simplest interpolation technique is based on a linear interpolation method. It is based on the assumption that the rate of change between unknown values is constant and can be computed using a simple slope formula. However the main disadvantage of this method is its performance which tends to decline as the degree of polynomials increases (Jaffrey, 2004). A spline interpolation technique has been introduced to overcome this problem (Law et al., 1993). The idea underlying this method is to approximate a given function by the set of low degree polynomials (Jaffrey, 2004). Different spline interpolation techniques have been introduced over the years, including two-dimensional rectangular surface splines (Perrin et al., 1987; Nunez, 1989), three-dimensional rectangular splines (Law et al., 1993; Srinivasan et al., 1996), spherical surface spline (Perrin et al., 1989; Babiloni et al., 1995), and spherical harmonic expansion (Lagerlund et al., 1995).

The global methods provide a useful estimation of the SL even when neighboring electrodes are not available for a central electrode. The major disadvantage of the global methods is artificially high coherence which results due to spline coefficients (Biggins et al., 1991, 1992; Biggins and Fein, 1993; Lagerlund et al., 1995). These methods also produce a large level of interpolation noise. However, this noise level can be reduced using averaging techniques (Nunez and Srinivasan, 2005). Few researchers have developed spline interpolation techniques based on the scalp surface model constructed from MRI of a subject, which provides more distinct and sharp images than

a mathematically generated model (Le and Gevins, 1993; Gevins et al., 1994; Babiloni et al., 1996).

3.3 Fourier coherence of SL

As mentioned earlier that the SL is sensitive mostly to superficial sources and suppresses volume-conducted activity from distant generators. This implies that SL-based coherence can be a useful measure to detect correlation between EEG signals with minimum VCUS effects. Based on this important characteristic of the SL, some important results regarding VCUS effects on coherence of REEG signals were deduced by Nunez and Srinivasan (2005). According to these results, conventional REEG-based coherence due to VCUS effects does not depend on frequency and decreases as interelectrode distance decreases. Figure 3.4 shows results of this study in more detail. This figure shows coherences of SL and REEG signals between electrode labeled X and a ring of electrodes at progressively greater distances from X labeled 1-3. The estimated coherence between electrode X and electrode n is labeled X:n. The REEG-based coherence shown in this figure has strong qualitative similarity to the coherence effects predicated by VCUS effects of uncorrelated sources activity (Nunez and Srinivasan, 2005). The level of this coherence that is independent of frequency systematically decreases as interelectrode distance increases and is also lower in value than the corresponding coherence of SL. Therefore, there is strong evidence that most of the frequency independent coherence of REEG signals shown in Figure 3.4 is due to VCUS effects. On the other hand, the corresponding SL-based coherence shown in Figure 3.4 does not show any similarity to the coherence due to VCUS effects. The results shown in Figure 3.4 provide sufficient evidence that SL-based coherence is a useful method to detect EEG correlation with minimum VCUS effects. Various other studies have reported the ability of SL-based coherence to detect EEG correlation with minimum VCUS effects (Nunez and Pilgreen, 1991; Nelson and Nunez, 1993; Nunez and Westdorp, 1994; Srinvans et al., 1998; Srinvans, 1999).

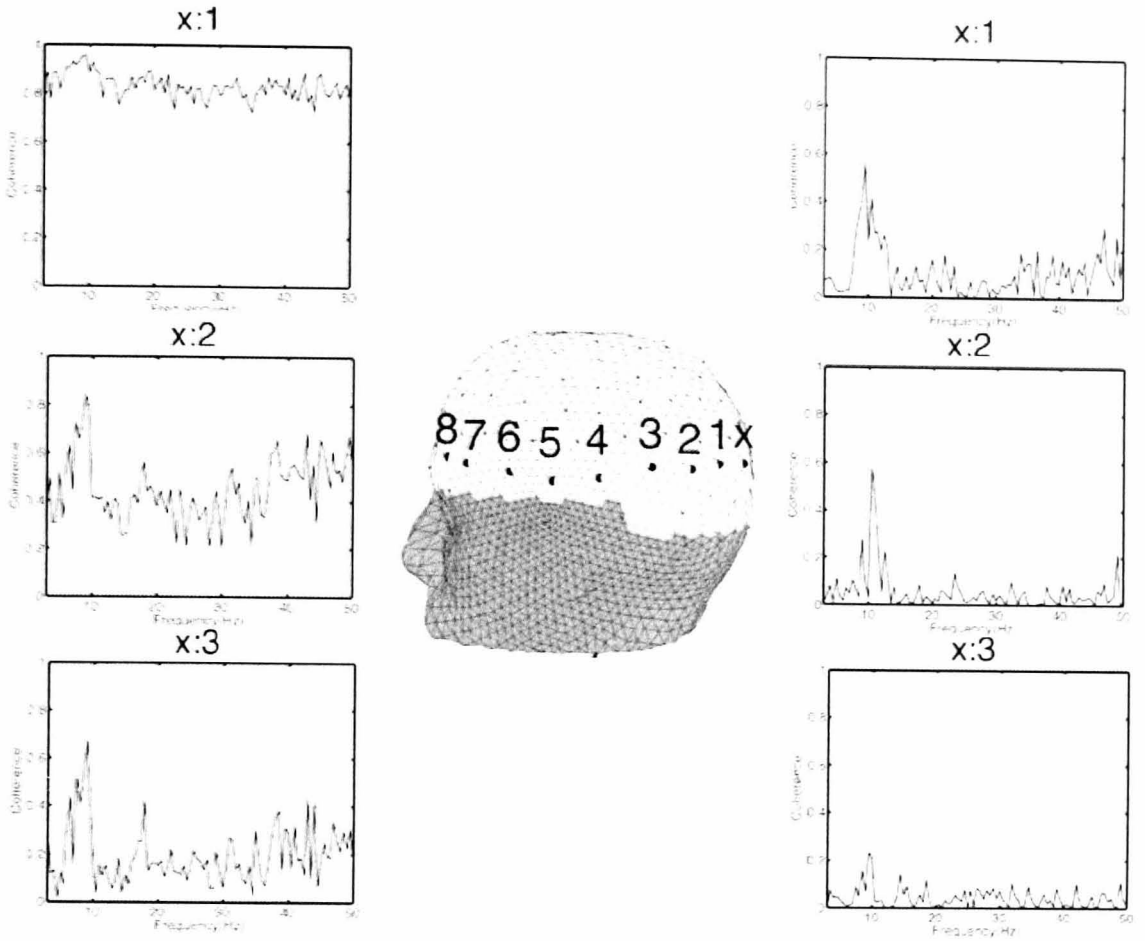

Figure 3.4: The graph between REEG-based coherence (left side of figure) and SL-based coherence for the subject at rest with eyes closed. Nunez and Srinivasan, 2005

3.4 Proposed solution: wavelet coherence of SL

SL-based coherence methods discussed in Section §3.3 are based on the Fourier transform, therefore they do not provide time evolution of coherence spectra. To the best of our knowledge, time-frequency methods of SL-based coherence have not been developed to date. Most kind of EEG signals are non-stationary and contain important signatures in time and frequency domains. Time-frequency methods of SL-based coherence are more appropriate for such kind of EEG signals. Therefore, this research proposes a time-frequency method of SL-based coherence.

The proposed coherence method is based on wavelet coherence of SL. It can detect EEG correlation with minimum VCUS effects and a satisfactory time-frequency resolution. In addition, it minimizes electrical activity generated by reference electrodes during EEG coherence analysis. Detailed theoretical background of wavelet coherence and SL methods have been already discussed in Chapters 2 and 3 respectively and its mathematical formalization will be developed in Chapter 5.

Chapter 4

Research methods

4.1 Introduction

This chapter presents a discussion on research methodology used in our study. Four major stages of this research are discussed. First stage presents a discussion on methodology required to choose already recorded particular REEG data. Second and third stages involve discussion on data reformatting and feature extraction respectively. Finally, performance and quality of various extracted features are discussed.

4.2 Research methodology

The overall strategy of our method is shown in the following diagram.

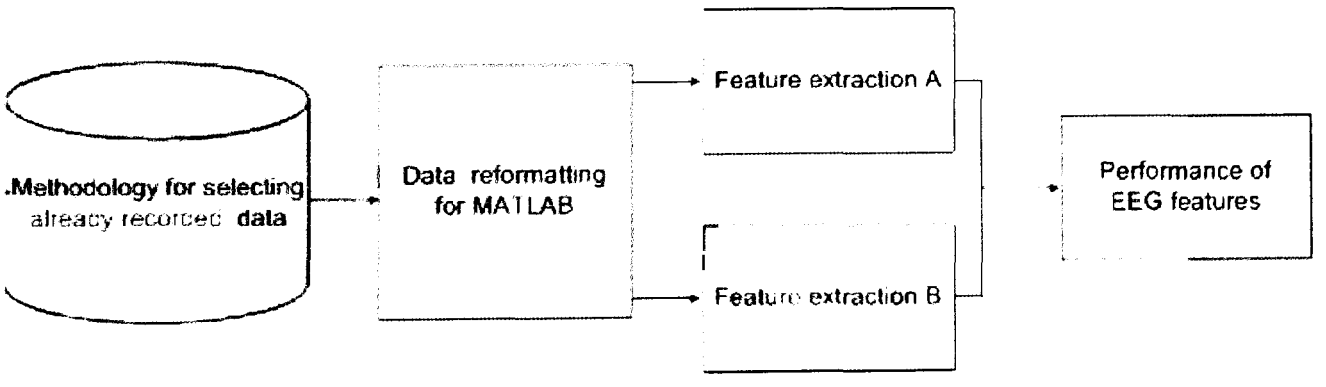

Figure 4.1: An overview of research strategy

4.2.1 Methodology for selecting already recorded data

This study uses the already recorded REEG data, which was donated by Dr Henri Begleiter at the Neurodynamics Laboratory of New York Health Center at Brooklyn. It was also publicly available at the web page http://kdd.ics.uci.edu//databases/eeg/eeg.html. The data consists of ERPs recorded from alcoholics and abstinent alcoholics subjects (average 10 years of abstinence). Alcoholics subjects had a history of alcoholism of at least 10 years. Further detail on this data is included in Appendix C. It was selected according to the following criteria:

(1) *ERPs*

This study uses ERPs, because these signals are highly time-varying and contain important signatures in both time and frequency domains. The use of ERPs for existing coherence methods of SL does not provide most of important information, contained in these signals. Contrary to this, the proposed coherence method in this research is developed for such highly time-varying signals, therefore the use of this data provides the opportunity to check its performance.

(2) *Interelectrode distance between recording electrodes*

Satisfactory estimates of the SL require the average interelectrode distance of at most 3.5 cm (Nunez et al., 1997). Therefore, we used the REEG data based on the extended 10-20 recording system of 64 electrodes, because the average interelectrode distance for such recording system is 3.2cm (Gevins, 1987c). However, SL estimates can be further improved by decreasing interelectrode distance more than 3.5 cm. Large interelectrode distance can be contaminated by more distant independent features rather than reflecting only the immediate surrounding potential (Nunez and Srinivasan, 2005).

(3) *The number of repeated trials*

The number of repeated trials must be sufficient to cause ERPs to be clearly distinguishable from unrelated background EEG. This is because, ERPs compared to background EEG are very small in magnitude, therefore ERPs are enhanced when many trials are averaged together. The signal to noise ratio is thus improved in proportion to the square root of the number of trials averaged (Cooper, 1974). Therefore, the ERP data chosen for this research

consists of the large number of repeated trials, i.e, at least 100 trials per subject.

(4) *Choice of subjects*

This study will also examine consequences of avoiding VCUS effects on coherence analysis based on difference in coherence between coherences of alcoholic and abstinent alcoholic REEG activities. This is because, most of REEG-based coherence studies on alcoholic effects have avoided the issue of VCUC effects on REEG signals (Ellis and Oscar, 1989; Ciesielski et al., 1995; Moselhy et al., 2001; Winterer et al., 2003; De Bruin et al., 2004; Marsdlek et al., 2006). Results of this study will help to assess the importance of minimizing VCUS effects on conventional REEG-based coherence analysis. Therefore, REEG signals of alcoholics and long-term abstinent alcoholics will be used in this study. Further detail about the history of subjects is explained in Appendix C.

(5) *Artifact-free data*

Various kinds of artifacts are observed during the recording of REEG signals. These artifacts contaminate the actual brain activity. Therefore the REEG data has been carefully selected keeping in mind all important precautions required for artifact-free data. Further detail on the selected REEG data and its recording procedure is included in Appendix C.

4.2.2 Data reformatting

The huge amount of data will be used in this study which requires vast amounts of computation time. The computational language MATLAB best suits for such data, because it is better at handling large data set and contains various signal processing tools compared to other languages. Therefore, the selected data, which is in the ASC11 file format, will be converted into readable MATLAB files. Later these files will be used to extract various EEG features.

4.2.3 Feature extraction

Using the MATLAB, various codes will be developed to extract EEG features. These EEG features are STFT and wavelet coherencies of Hjorth method-

based SL (Hjorth, 1975) and Perrin method-based SL (Perrin et al., 1989). In addition, EEG features based on STFT and wavelet coherencies of REEG signals will also be computed.

4.2.4 Performance of EEG features

Performance of EEG features depends upon their accurate estimates, therefore it is first discussed and then the methods used to assess the performance of that estimated features will be addressed.

Estimates of a EEG-based coherence function can be biased due to VCUS effects, reference electrode effects, filtering of genuine EEG signals by SL, and statistical errors. First two issues will be resolved using SL-based coherence, because the SL eliminates most of VCUS and reference electrodes effects. Third issue arises when we use SL-based coherence, because the SL filters out EEG signals due to distant sources. This issue will be resolved using REEG-based coherence, because REEG activity picks up signals from local and distant sources. As for statistical errors, this problem will be resolved using some statistical techniques. For example, noise and other un-correlated sources, present in coherence estimates, will be removed by averaging techniques. Statistical errors in coherence estimates also depend on the number of samples used in the coherence estimate. In this study, the number of samples for robust coherence estimates will be determined by 95 % confidence intervals[1].

As for as accuracy of SL estimates are concerned, they depend on the number of recording electrodes. As mentioned before that an EEG recording system based on at least 64 electrodes, produces satisfactory estimates of the SL. Therefore this study has selected REEG data which was recorded using the 64-electrode system. Another important issue when estimating the SL, is its algorithm. Among various algorithms of the SL, the Hjorth method based on local methods (Hjorth, 1975) and the Perrin method based on spherical interpolation methods (Perrin et al., 1989) are most successful (Pernier et al., 1988; Perrin et al., 1989; Tandonnet et al., 2005). This study aims to compare performance of both these methods and a method will be used whose estimates show more consistency to the characteristics of the true SL.

[1]Confidence interval is defined as the probability that the true coherence at a certain time lies within a certain interval about the estimated coherence

As far as performance of estimated EEG features is concerned, it will be evaluated by comparing their results to the existing literature on EEG coherence methods. For example, according to existing coherence methods, REEG-based coherence due to VCUS effects does not change with frequency (Nunez and Srinivasan, 2005).

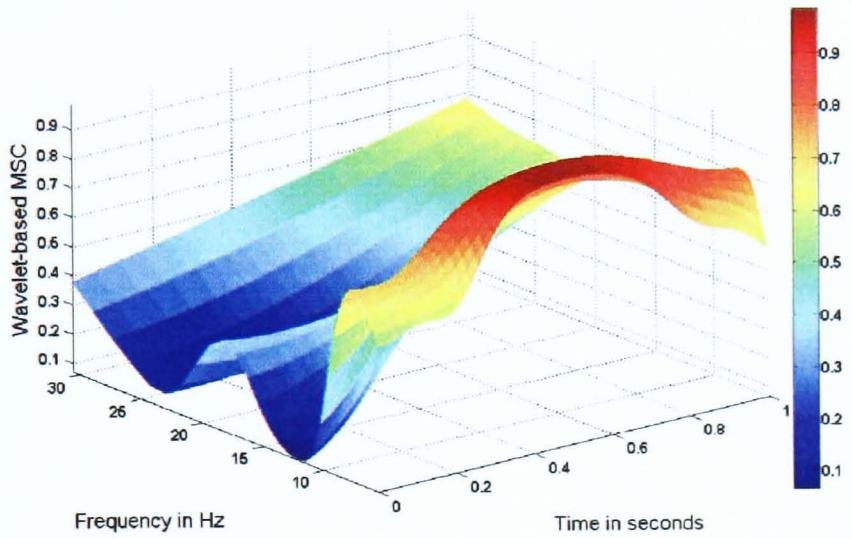

Figure 4.2: Subject c381: wavelet squared coherency of SL between electrode's position C3 and C5.

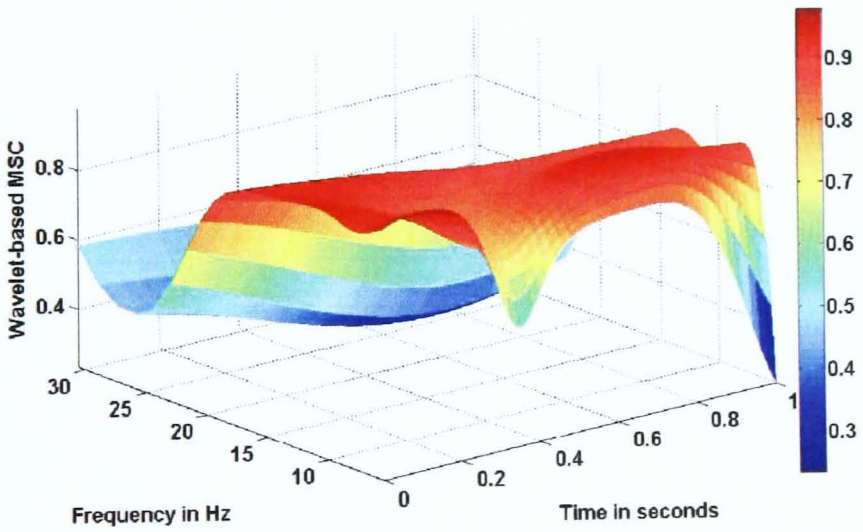

Figure 4.3: Subject c381: wavelet squared coherency of REEG between electrode's position C3 and C5.

Using this important result, the wavelet squared coherency of SL, shown in Figure 4.2, can be proved less affected by VCUS. This is due to the fact that this coherency is highly dependent on its frequency. Contrary to this, the wavelet squared coherency of REEG shown in Figure 4.3 is highly affected by VCUS, because most of its part is independent of frequency. Therefore, performance of the SL-based coherency seems to be satisfactory as compared to the REEG-based coherency as shown in Figures 4.2, and 4.3.

Chapter 5

Time-frequency coherence analysis of SL: methodology

5.1 Introduction

Wavelet and STFT squared coherencies of SL are developed in this chapter. Finally, this chapter presents a discussion on statistical methods which are used to assess performances of these coherence methods.

5.2 STFT and wavelet squared coherencies based on Hjorth method

Let X and Y be two electrode positions whose nearest neighbored are given by: [X_1, X_2, X_3, X_4] and [Y_1, Y_2, Y_3, Y_4] respectively. Time series recorded at these nearest neighbored electrode positions are $[x_1(n), x_2(n), x_3(n), x_4(n)]$ and $[y_1(n), y_2(n), y_3(n), y_4(n)]$ respectively. If $x(n)$ and $y(n)$ are time series recorded at electrode positions X and Y respectively then using Eq. (3.1) (Section §3.2 of Chapter 3), SLs of these time series are given by,

$$l_x(n) = x(n) - \frac{x_1(n) + x_2(n) + x_3(n) + x_4(n)}{4}, \tag{5.1}$$

$$l_y(n) = y(n) - \frac{y_1(n) + y_2(n) + y_3(n) + y_4(n)}{4}, \tag{5.2}$$

Using Eqs. (2.16) and (2.26) (sections §2.4, and §2.5 respectively of Chapter 2), the STFT and wavelet coherences of these SLs are given by the following relations,

$$C_{l_x l_y}(m,n) = \frac{P_{l_x l_y}(m,n)}{\sqrt{P_{l_x l_x}(m,n) \cdot P_{l_y l_y}(m,n)}}, \tag{5.3}$$

$$\gamma_n^{l_x l_y}(a,b) = \frac{W_n^{l_x l_y}(a,b)}{\sqrt{W_n^{l_x l_x}(a,b) \cdot W_n^{l_y l_y}(a,b)}}, \tag{5.4}$$

where $C_{l_x l_y}(m,n)$ and $\gamma_n^{l_x l_y}(a,b)$ are the STFT and wavelet coherences, and $P_{l_x l_y}(m,n)$, and $W_n^{l_x l_y}(a,b)$ are STFT and wavelet cross-spectra respectively. STFT and wavelet squared coherencies can be obtained by taking the square of their respective absolute values.

5.2.1 Statistical considerations

In Fourier coherence, cross and auto spectra are estimated using a periodogram method. In this method, two time series are divided into equal number of segments. Auto and cross spectra of each segment are then estimated. Averages of these spectra provide the required cross and auto spectra for the estimation of a coherence function. However, this method makes sense only if coherence analysis of stationary time series is required. Averaging the spectral estimates of non-stationary segments would provide a possibly meaningless average values (Cohen, 1995). Therefore, following different approach has been used for the robust estimates of the STFT and wavelet squared coherencies.

First, any two trails are randomly selected and transformed into SLs, and then STFTs and wavelet transforms of these transformed SLs are estimated. These transformed SLs are then used for the estimation of their corresponding STFT and wavelet based cross and auto-spectra. This procedure is repeated for each pair of repeated trials. In next step, averages of all estimated cross and auto-spectra for each transform are estimated and finally these averaged cross and auto-spectra are used in the square of the absolute values of Eqs. (5.3) and (5.4) in order to estimate the STFT and wavelet squared coherencies respectively.

The statistical significance of these time-frequency coherencies is examined by the confidence intervals. In Fourier coherence, confidential interval is set by assuming that two time series are stationary and Gausssian distribution is used to approximate the probability density of data. However such an assumption can not be used for time-frequency methods of coherence. Therefore, statistical significance of these coherencies is assessed by using the method of Gish and Cochran (1988), which is not based on stationary assumption of EEG signals. It is given by the following relation,

$$P_t = 1 - (1-t)^{R-1}, \; where \; 0 \leq t \leq 1 \tag{5.5}$$

Where t is the detection threshold, R is the number of repeated trials, and P_t is the desired level of confidence. For a 95 % confidence interval,

$$1 - (1-t)^{R-1} = 0.95 \tag{5.6}$$

or

$$t_{95\%} = 1 - 0.05^{1/R-1} \tag{5.7}$$

Any estimate of these coherence less than the $t_{95\%}$, will not be considered as the significant value. In addition to SL-based estimates of squared coherencies, the conventional STFT and wavelet squared coherencies of REEG signals are estimated following the procedure from Eqs. (5.3) to (5.7).

5.2.2 Time-frequency resolution

In order to find a suitable time-frequency resolution, three different time resolutions of 0.1s, 0.2s and 0.3s corresponding to frequency resolutions of 10 Hz, 5Hz and 3.3Hz respectively were used for STFT. These time-frequency resolutions correspond to Hanning windows of lengths: 25, 51, and 75 respectively and can be calculated by the relation $\Delta F_r = F_s/N_w$ and $\Delta T_r = N_w/F_s$, where N_w and F_s stand for window length and sampling frequency respectively.

In order to achieve time-frequency representation of wavelet coherence, first wavelet scale a was transformed into frequency scale f_a in Hertz. The scale level was incrementally changed from 1 (higher frequency) to 50 (lower frequency) in every single step. Finally the Morlet wavelet of center frequency 0.8125 Hz was scaled in this study so that f_a ranged from 1 Hz to 50 Hz.

5.3 STFT and wavelet squared coherencies based on Perrin method

Perrin's method of spline spherical interpolation technique is used here to estimate SL (Perrin et al., 1989). This technique involves three important steps.

- The projection of scalp electrode position on the sphere.
- To determine the value of the potential at the sphere.
- To determine the value of the SL.

Let v_i be the potential value measured at the ith electrode. The projection of ith electrode position into spherical system is denoted by E_i. The value at electrode position E of the spherical spline U which interpolates the $v_i s$ at the $E_i s$ is given by,

$$U(E) = c_o + \sum_{i=1}^{r} c_i g(cos(E, E_i)), \tag{5.8}$$

where r is the number of scalp electrodes used for recording scalp potentials or REEG. The coefficients $c_i s$ (elements of matrix C) can be determined from the following matrix equations:

$$GC + TC_o = V \tag{5.9}$$

$$T^t C = 0, \tag{5.10}$$

where superscript t stands for transpose operation, V is a column vector of r rows whose elements $v_i s$ are scalp potentials at any strategy at r electrode positions, G is a r by r square matrix of spline coefficients $g_{ij} s$, T is a column vector of r rows whose all elements are one, and C is a column vector of r rows whose elements are spline coefficients $c_i s$. The coefficients $g_{ij} s$ of the square matrix G are equal to $g(\cos(E_i,E_j))$, which is the cosine of the angle between the electrode projections E_i and E_j. The value of the $g(\cos(E_i,E_j))$ can be found from the function:

$$g(x) = \frac{1}{4\pi} \sum_{s=1}^{\infty} \frac{2s+1}{s^q (s+1)^q} P_s(x) \tag{5.11}$$

$P_s(x)$ is the Legendre polynomial of degree s and order q. If (x_E,y_E,z_E) and (x_F,y_F,z_F) are the cartesian coordinates of electrode positions E and F, then

for the unit sphere of radius one,

$$cos(E,F) = 1 - \frac{(x_E - x_f)^2 + (y_E - y_f)^2 + (z_E - z_f)^2}{2} \tag{5.12}$$

Let l_E be Perrin method-based SL at the electrode position E. According to Ohm's law, it is proportional to the gradient of the interpolated potential on the spherical surface at the electrode position E,

$$l_E \propto -\nabla U(E) \propto -\nabla(C_o + \sum_{i=1}^{r} C_i g(cos(E,E_i))), \tag{5.13}$$

$$l_E \propto -\nabla(\sum_{i=1}^{r} C_i g(cos(E,E_i)), \tag{5.14}$$

Substituting the value of $g(cos(E,E_i))$ into Eq. (5.14), using Eq. (5.11)

$$l_E \propto -\nabla(\sum_{i=1}^{r} C_i \frac{1}{4\pi} \sum_{s=1}^{\infty} \frac{2s+1}{s^q(s+1)^q} P_s(cos(E,E_i)) \tag{5.15}$$

Using the property that 2-dimensional spherical Laplacian of the Legendre polynomials is the multiple of same Legendre polynomials (Perrin et al., 1989)

$$\nabla P_s = -(2s+1)P_s \tag{5.16}$$

Therefore, using Eq. (5.16), we can write Eq. (5.14) as,

$$l_E = \sum_{i=1}^{r} C_i h(cos(E,E_i)) \tag{5.17}$$

Where $h(cos(E,E_i))$ is given by,

$$h(cos(E,E_i)) = -\frac{1}{4\pi} \sum_{s=1}^{\infty} \frac{(2s+1)^2}{s^q(n+1)^q} P_s(cos(E,E_i)) \tag{5.18}$$

Similarly Perrin method-based SL at electrode position F can be estimated following the same procedure. Using the procedure described in Sections §2.4, and §2.5 of Chapter 2, STFT and wavelet squared coherencies of these SLs are estimated respectively.

Chapter 6

Time-frequency coherence analysis of SL: Results and discussion

6.1 Introduction

Using the techniques developed in Chapter 5, and already recorded ERP data (Detail on this data is included in Appendix C), various important results regarding performance of the STFT and the wavelet coherence methods of SL have been derived in this study. Time-frequency characteristics of VCUS effects on EEG correlation have been also examined. This chapter presents a discussion on the results of this study.

6.2 STFT coherence analysis of SL

In order to obtain satisfactory estimates of the SL, performance of the Hjorth method based on local methods (Hjorth, 1975) and the Perrin method based on spline spherical interpolation technique (Perrin et al., 1989) were compared in this study. The SL estimates based on the Hjorth method were found more consistent to the true SL than those obtained using the Perrin method. Therefore, results in this study were obtained using the SL based on the Hjorth method. Following is the discussion on the results of this study.

STFT coherence analysis of SL has been proved useful in studying EEG

correlation with minimum VCUS effects in the time-frequency domain. This result is illustrated in Figures 6.1 and 6.2, where the STFT squared coherencies of SL and REEG signals, estimated using the same electrode's positions and the subject, are shown. The STFT squared coherency of SL in Figure 6.2 is showing changes across all frequencies, whereas the corresponding STFT squared coherency of REEG in Figure 6.1 is almost constant across all frequencies. In addition, the frequency independent part of the REEG-based squared coherency is larger in the value than the corresponding SL-based squared coherency. The Coherence spectra shown in Figure 6.1 have strong qualitative similarity to coherence effects predicted by VCUS.

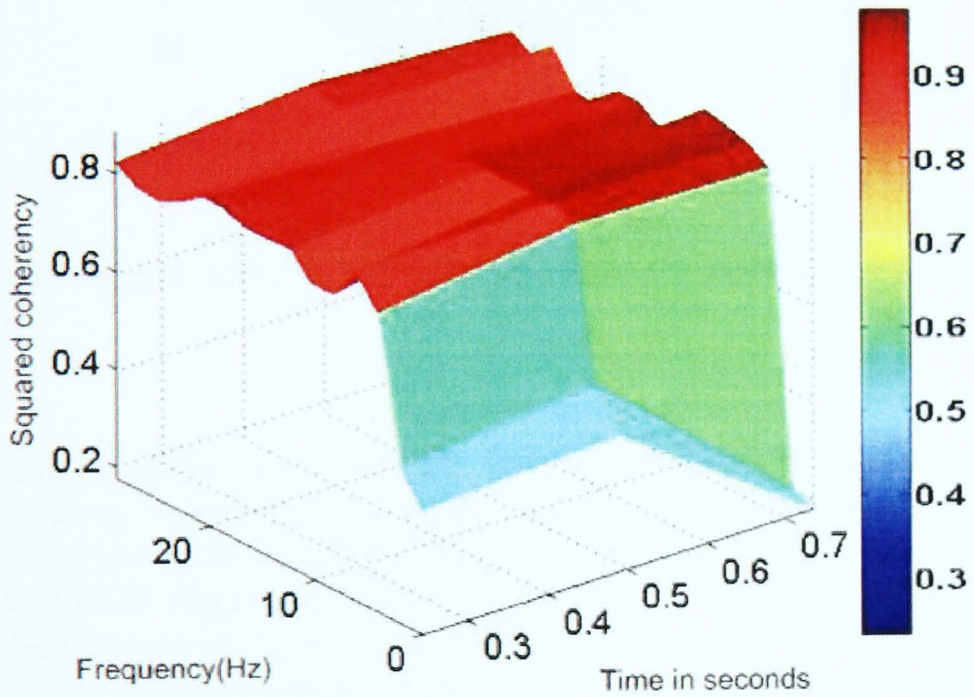

Figure 6.1: Subject c381: STFT squared coherency of REEG signals between electrodes c_3 and c_5.

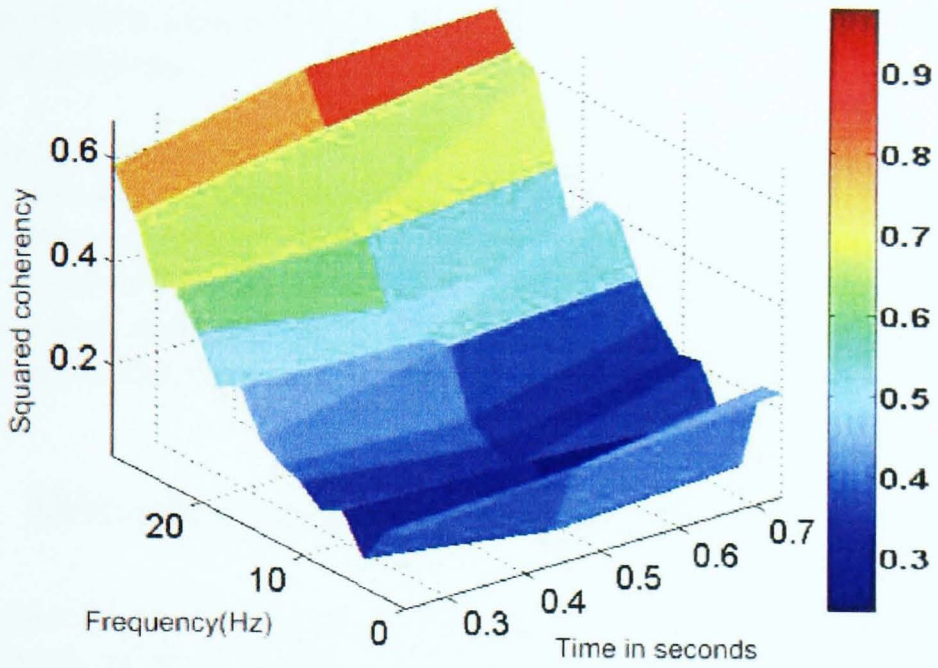

Figure 6.2: Subject c381: STFT squared coherency of SL between electrodes c_3 and c_5.

As mentioned earlier that coherence due to VCUS effects does not change with frequency, therefore it is almost certain that the frequency independent part of the conventional REEG-based squared coherency in Figure 6.1 is due to VCUS effects. On the other hand, there is strong evidence that the SL-based squared coherency in Figure 6.2 is very less affected by VCUS effects. Thus, STFT coherence analysis of SL provides EEG correlation with minimum VCUS effects. Moreover, it proved to be useful in detecting significant correlation by comparing various time-varying correlations at same frequency. Figure 6.2 illustrates this result, where the SL-based squared coherency reveals EEG correlations at 0.3, and 0.7 seconds at frequency of 20 Hz. This coherence at 0.3 seconds is less than 0.2, which is not significant as it is very low in value. However, it detects significant coherence of around 0.4 value at 0.7 seconds.

During this study, it was found that *the coherence, which is independent of some frequency range, is also independent of corresponding time.* This result is illustrated in Figure 6.1, where it is clearly shown that level of frequency independent coherence is constant at each instance of time. Since coherence, which is constant across some frequency range, is mainly due to

VCUS effects, we can conclude that coherence due to VCUS effects is independent of both time and frequency. This important result was noticed for all the 30 subjects.

As discussed earlier in Chapter 3 (Section §3.3) that coherence due to VCUS effects decreases as interelectrode distance increases. This characteristic of VCUC effects was also observed during STFT coherence analysis in this study. However, it was observed for those interelectrode distances which were increased along a fixed direction[1]. This important result is discussed in more detail in the next section using wavelet coherence analysis.

6.3 Wavelet coherence analysis of SL

The results discussed in Section §6.2 were based on STFT coherence analysis of SL, study of these results using a more advance technique like wavelet coherence can provide better understanding of VCUS effects on EEG correlation. Therefore, this section using the wavelet squared coherencies of SL and REEG signals discusses these results again. Performance of wavelet coherence analysis of SL as compared to STFT coherence analysis of SL has been also assessed here.

One of important results found in the previous section that *STFT coherence due to VCUS effects is independent of both time and frequency domains* was also observed during wavelet coherence analysis. This result is illustrated in Figure 6.4, where wavelet squared coherency of REEG signals between electrodes CP_3 and PO_4 is shown. Figure 6.4 clearly shows that the level of the frequency independent coherence around 30 Hz is also independent of the corresponding time. Applications of this results are important. For example, this result is useful in order to detect VCUS effects on REEG-based coherence when only its time-domain part is known. This is because, existing knowledge about VCUS effects on EEG coherence analysis is limited to only frequency-domain characteristics (Nunez and Srinivasan, 2005).

According to the results of this study, wavelet coherence analysis of SL was found to be highly dependent on frequency. It indicates that the wavelet coherence of SL efficiently reveals EEG correlation with minimum VCUS effects in the time-frequency domain. Majority of results showed larger values of wavelet squared coherency of REEG as compared to the wavelet squared

[1]Direction is considered here along a straight line joining two adjacent electrodes

coherency. Increase in REEG-based coherence values was probably due to VCUS effects. However some results showed larger values of the wavelet squared coherency of SL than those obtained using the wavelet squared coherency of REEG signals. This is because, smaller correlated EEG sources usually make smaller contribution to corresponding coherence of REEG signals and at same time these sources make larger contributions to coherence of SL (Nunez, 1981). In other words, as scale of correlated sources increases, sensitivity of REEG-based coherence increases whereas sensitivity of SL-based coherence decreases at same time. Therefore higher coherence can be observed in either REEG or SL depending on the size of coherent source activity.

Dependance of coherence due to VCUS effects on interelectrode distance was also examined in this study using the wavelet squared coherencies of SL and REEG signals. It was found that coherence due to VCUS effects does not always decrease as interelectrode distance increases. However decrease in coherence was always observed when interelectrode distance was along some fixed direction.

It is important to mention here that existing studies on EEG coherence analysis also predict decrease in coherence due to VCUS as interelectrode distance increases (Nunez, 1981; Srinvans et al., 1996; Nunez et al., 1997; Srinvans et al., 1998; Nunez and Srinivasan, 2005). However, these studies do not mention effects of the direction between corresponding electrodes. Most of results of these studies have been derived using EEG signals of electrodes attached to the scalp of a subject along some fixed direction.

Figures 6.3 and 6.4 illustrate the result of our study for effects of interelectrode distance on coherence due to VCUS effects. These figures represent the estimated wavelet squared coherencies of REEG for same subject a681. Figure 6.3 clearly shows that there is no level of the coherence at electrodes CP_3 and P_1 which is affected by VCUC. However, VCUS effects on the coherence are observed, when the interelectrode distance is increased from CP_3 to Po_4 in the different direction than the direction between CP_3 and P_1. Figure 6.4 clearly shows presence of the coherence due VCUS effects at electrodes CP_3 and Po_4 between 10 to 20 Hz. This result is contrary to the fact that coherence due to VCUS effects decreases as interelectrode increases.

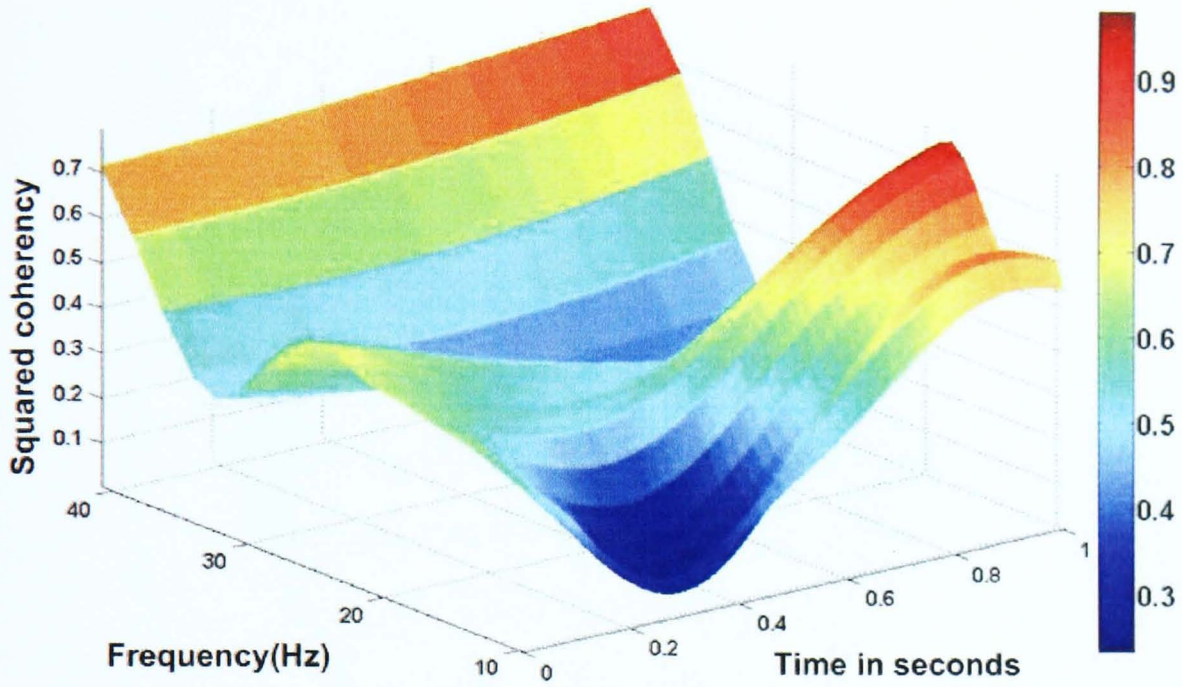

Figure 6.3: Subject a681: wavelet squared coherency of REEG between electrodes CP_3 and P_1.

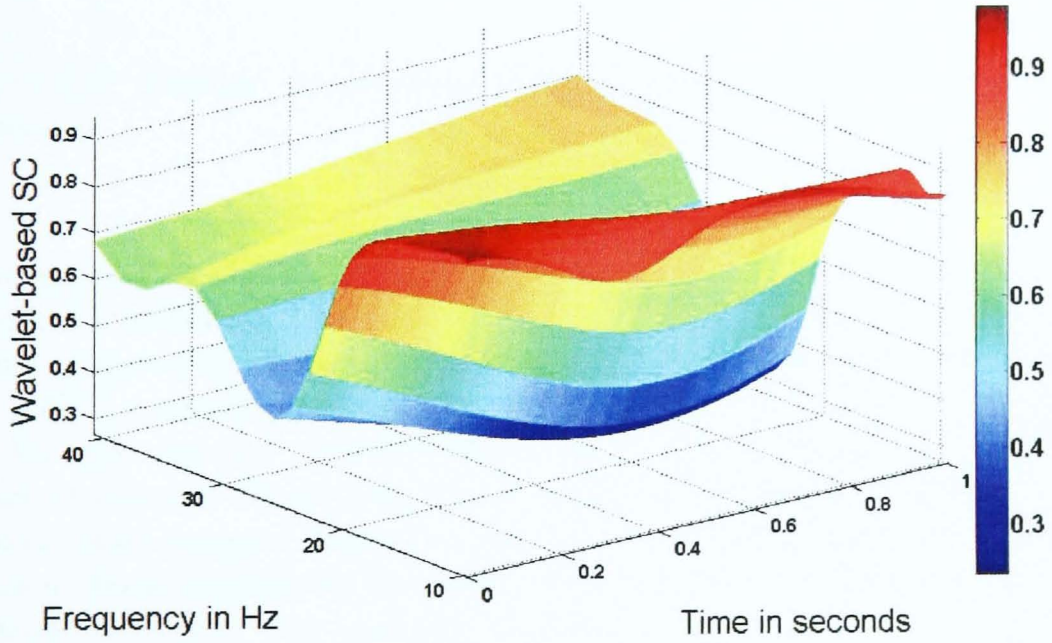

Figure 6.4: a681: wavelet squared coherency of REEG between electrodes CP_3 and PO_4.

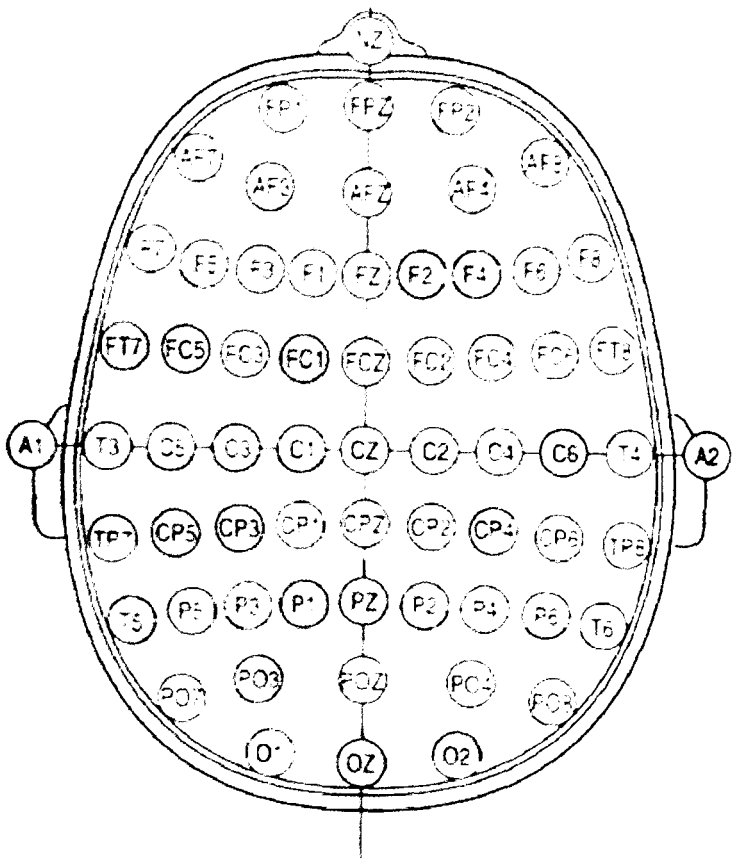

Figure 6.5: Position of electrodes based on EEG recording system of 64 electrodes.

As compared to the STFT coherence of SL, the wavelet coherence of SL provided a better time and frequency resolution in low and high frequency ranges. Figures 6.6 and 6.7 illustrate this result in more detail, where wavelet and STFT squared coherencies of SLs between same electrode's positions and for same subject a364 are shown. Both figures show some significant values of squared coherencies at low and high frequencies. However, the wavelet-based squared coherency provides more sharp and well separated values at these frequencies than those obtained by the corresponding STFT squared coherency. For example, Figure 6.6 clearly indicates the wavelet squared coherency of 0.4, and 0.55 values at 60 Hz for 0.3 and 0.8 seconds respectively. On the other hand, values of the STFT squared coherency at 60 Hz as shown in Figure 6.7, appear to be ambiguous or almost same throughout the entire corresponding time axis. Similarly at lower frequencies, the wavelet-based squared coherency provides more information than the STFT squared coherency.

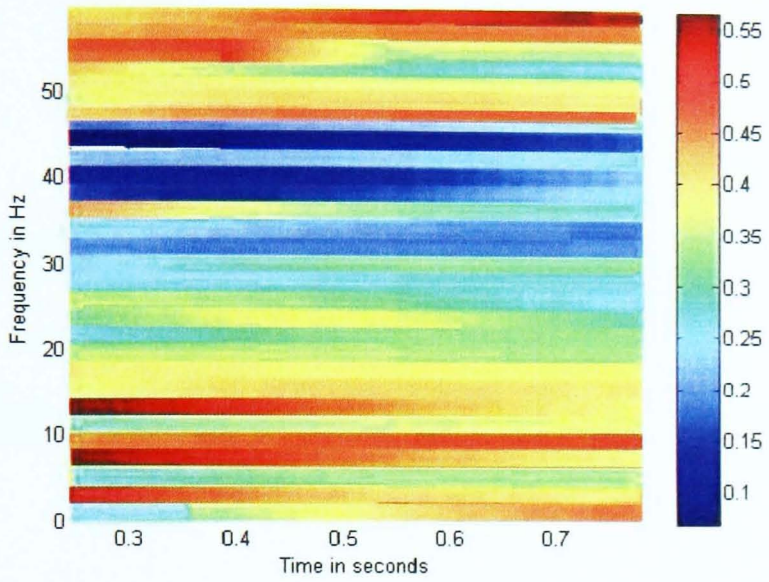

Figure 6.6: Subject a364: wavelet squared coherency of SL between electrodes C3 and C5.

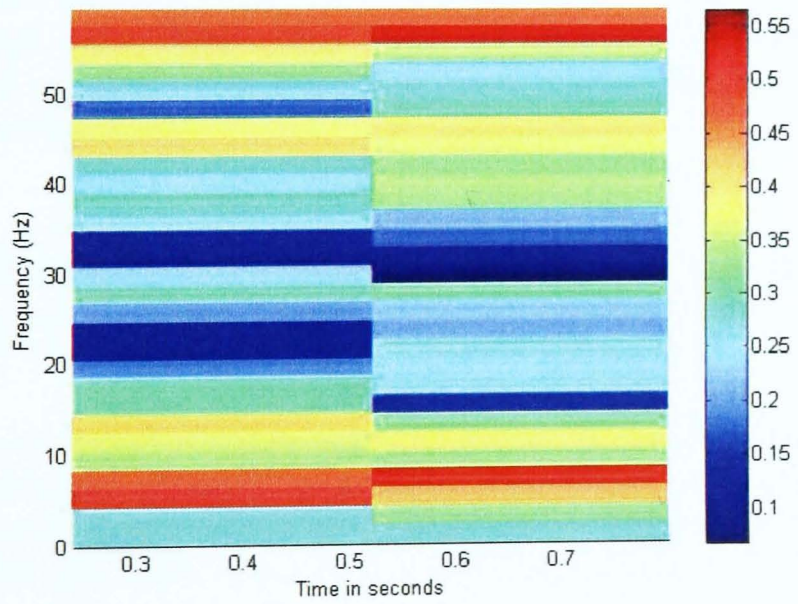

Figure 6.7: Subject a364: STFT squared coherency of SL between electrodes C3 and C5.

Chapter 7

Applications

7.1 Introduction

Great majority of REEG coherence methods applied to examine alcoholic effects on the brain are based on coherence difference between coherences of alcoholic and non-alcoholic REEG activities (Ellis and Oscar, 1989; Ciesielski et al., 1995; Moselhy et al., 2001; Winterer et al., 2003; De Bruin et al., 2004; Marsdlek et al., 2006). This study will assess the importance of minimizing VCUS effects on such coherence method using the proposed wavelet coherence method of SL.

7.2 Wavelet coherence analysis of alcoholic EEG

The already recorded ERP data from the groups of long-term alcoholics and long-term abstinent alcoholics was used in this study. The abstinent alcoholics group consisted of 15 males with no history of alcoholism for the last 10 years. The alcoholics dependent group also consisted of 15 males who had a history of alcoholism of at least 10 years. Further detail on this data set is included in Appendix C. Following method of wavelet coherence analysis was used in this study: First, wavelet squared coherency of SL using the procedure described in Section §5.2 of Chapter 5 was estimated. Next, the squared coherency ranging between 100-200ms was separated from the estimated squared coherency. Finally average of the separated squared co-

herency was taken across its samples, which is later used in this study to examine alcoholic effects on the brain.

Choice of the sample length around 100-200ms (which corresponds to ERP component C110) was made, because it indicated the difference between alcoholics and abstinent alcoholics subjects more efficiently than other sample lengths or ERP components. Figures 7.1 and 7.2 illustrate this in more detail, where averaged wavelet squared coherencies (AWSCs) of REEG signals for abstinent alcoholic subject c364 and alcoholic subject a364 are shown.

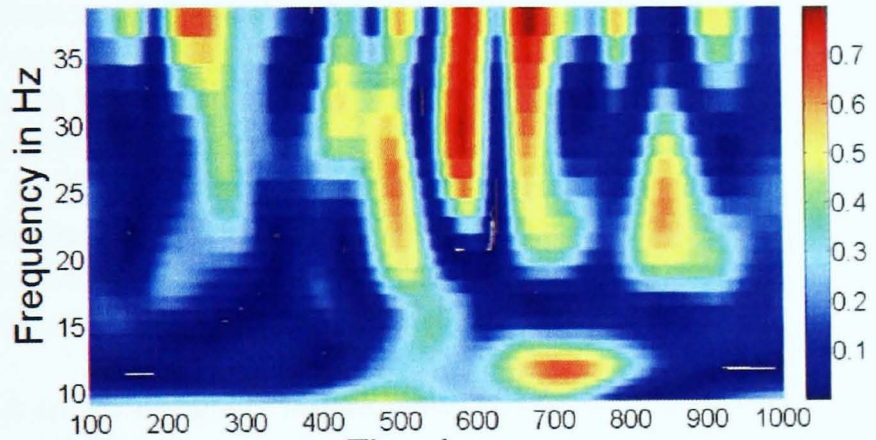

Figure 7.1: Abstinent alcoholic subject c364: AWSC of REEG between electrodes F3 and P3

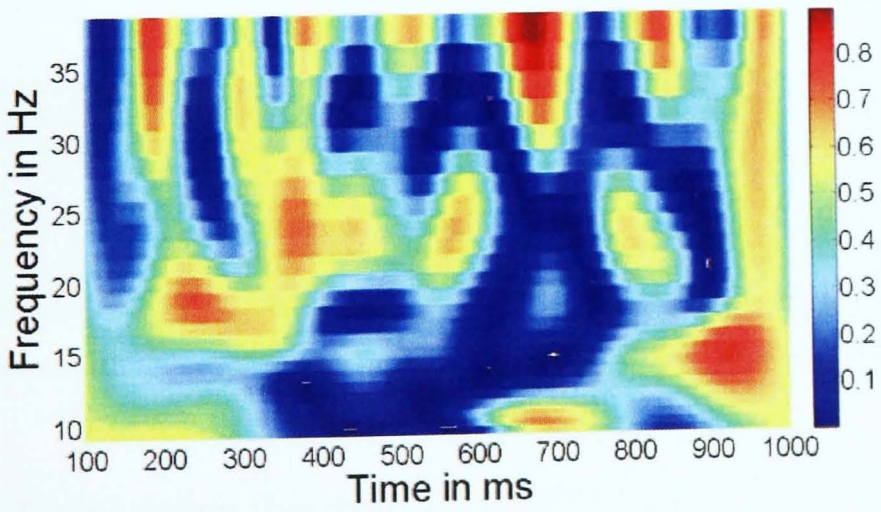

Figure 7.2: Alcoholic subject a364: AWSC of REEG between electrodes F3 and P3

These figures clearly show that squared coherency around 100-200ms significantly differentiates EEG activities of alcoholic and abstinent alcoholic subjects than coherencies around other ERP components. AWSC of REEG was estimated using the same procedure described above for AWSC of SL.

7.3 Results and discussion

The AWSC of REEG signals was found larger for alcoholic subjects as compared to abstinent alcoholic subjects. This larger coherence was mostly observed for parietal-parietal, parietal-frontal, and parietal-temporal electrode pairs. Results were also consistent with existing studies on REEG-based coherence analysis for alcoholics (Moselhy et al., 2001; Winterer et al., 2003; Marsdlek et al., 2006). Results obtained using the AWSC of REEG signals were again examined for the parietal lobe of the brain using the AWSC of SL. Most of results obtained using the AWSC of SL were not consistent with those obtained before using the AWSC of REEG.

Figures 7.3 to 7.6 illustrate one of these results in more detail, where AWSCs of REEG and SL for alcoholic subject a364 and abstinent alcoholic subject c364 are shown. These averaged coherences were estimated between electrode Pz and the electrodes mentioned in Table 7.1.

Table 7.1: *Set of electrodes used for the estimation of AWSCs of REEG and SL*

Alphabetical representation	Numerical representation	Location
F_3, F_4, AF_3,F_2	7,9,8,5,6	Frontal Lobe
Cz,C_1,C_3,C_4,FC_2,FC_1,FC_4,FC_3	16,52,17,18,12,13,39,40	Central lobe
CPz,P_Z,P_1,P_2,P_3,P_4,CP_3,CP_4	61,25,60,59,23,24,48,49	Parietal lobe
C_5,FC_6,FC_5,CP_5,CP_6,P_5,P_6	42,10,11,19,20,50,51	Temporal lobe
POz	57	Occipital Lobe

Figures 7.3 and 7.4 show that most of the AWCSs of alcoholic REEG activity are larger in the value than those obtained using the AWCSs of abstinent alcoholic REEG activity. However the AWSCs of SL for these same subjects a364 and c364 are not consistent with these results. This result is illustrated

in Figures 7.5 and 7.6, where most of the AWSCs of SL for abstinent alcoholic subject c364 are larger in the value than those obtained using the AWSCs of SL for alcoholic subject a364. Results shown in Figures 7.3 to 7.6 provide the strong evidence that increase in REEG-based coherence was due to artificial coherence which resulted due to VCUS effects.

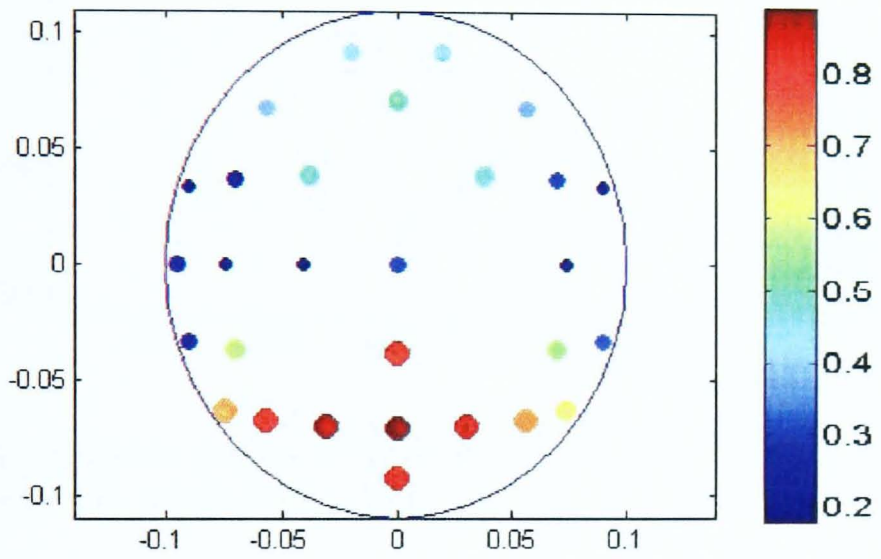

Figure 7.3: Alcoholic subject a364: AWSC of REEG signals between electrodes Pz and rest of electrodes, mentioned in Table 7.1.

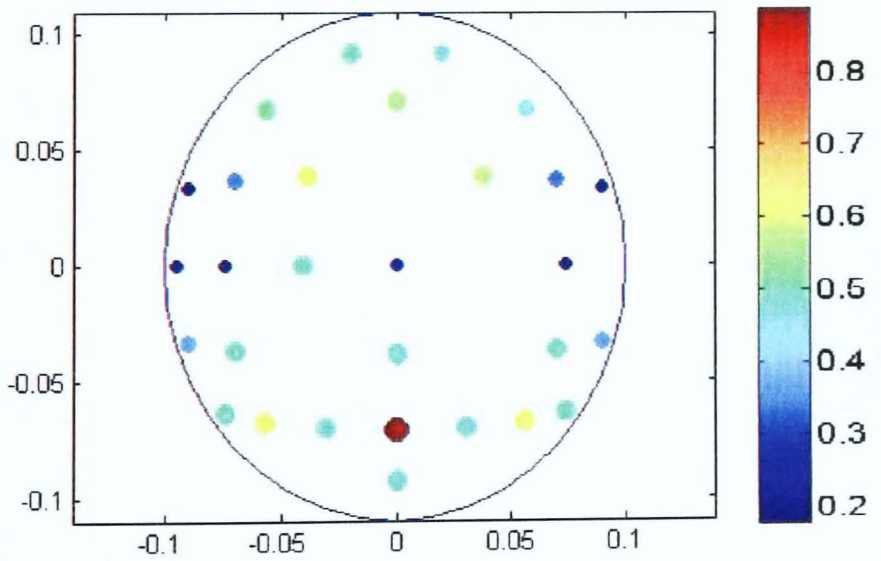

Figure 7.4: Abstinent alcoholic subject c364: AWSC of REEG signals between electrodes Pz and rest of electrodes, mentioned in Table 7.1.

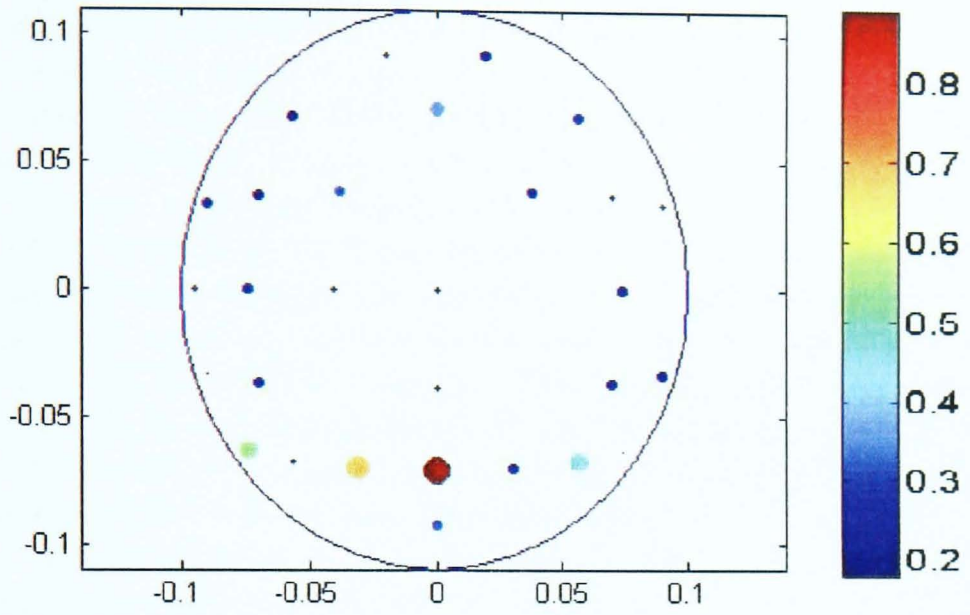

Figure 7.5: Alcoholic subject a364: AWSC of SL between electrodes Pz and rest of electrodes, mentioned in Table 7.1.

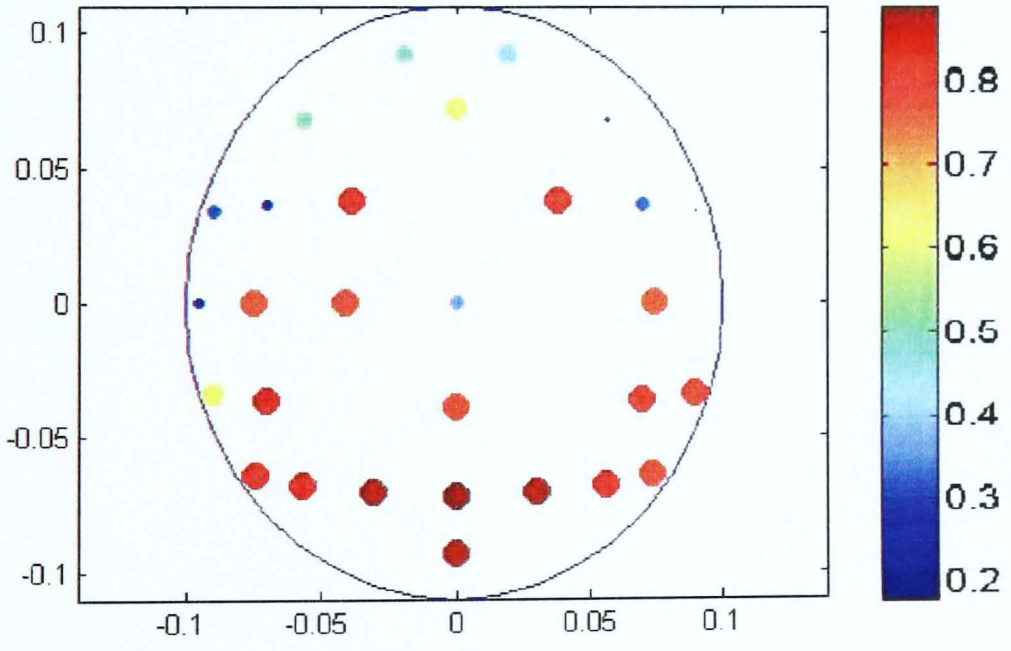

Figure 7.6: Abstinent alcoholic subject c364: AWSC of SL between electrodes Pz and rest of electrodes, mentioned in Table 7.1.

The next part of this study is based on statistical analysis of the results discussed in this section for the parietal lobe of the brain. Statistical significance of these results was assessed using the t-test. It was first performed on the results obtained using the AWSC of REEG signals. More than 95 % significance level of difference was obtained as p value was found between 0.02 and 0.05. T-test was again performed on the results obtained using the AWSC of SL, which resulted in 50 % significance level of difference. There is the significant difference between this significance level and the significance level obtained before using the conventional wavelet coherence method of REEG signals, i.e., AWSC of REEG signals. These results lead to the conclusion that VCUS effects significantly biases results of conventional wavelet coherence analysis of REEG signals by introducing artificial coherence between a corresponding pair of electrodes. They also imply that VCUS effects are not additive and therefore can not be ignored in comparison of different EEG activities. The results discussed in this chapter are included in Appendix C.

Chapter 8

Conclusions and perspectives

8.1 Introduction

This thesis considered the use of signal processing methods based on wavelet and STFT coherences of SL with the goal of detecting EEG correlation with minimum VCUS effects in the time-frequency domain. Using these methods, various important results were obtained. This chapter first presents a summary and clinical applications of the results obtained throughout the thesis. Then, finally limitations of this research are discussed followed by discussion on future research related to this study.

8.2 Summary of main findings

• The proposed wavelet coherence method of SL successfully revealed correlation between EEG signals with minimum VCUS effects in the time-frequency domain. Coherence spectra obtained using it had strong qualitative similarity to true coherence of EEG signals. Most of this spectra were highly dependent on frequency, which provided strong evidence about the absence of VCUC effects on them.

• Performance of the proposed wavelet coherence method was compared with the STFT coherence method of SL. STFT coherence analysis of SL revealed EEG correlation with minimum VCUS effects, but due to a use of a fixed window function in the STFT, its time-frequency resolution was not satisfactory as compared to the proposed wavelet coherence method. However,

STFT coherence analysis of SL can be proved useful when correlation between slowly time-varying EEG signals (at least in the order of minutes or hours) is under consideration. This is because, the STFT is computationally very fast (Kiymik et al., 2005) and produces effectively equivalent results to wavelet-based methods for slowly-varying EEG signals (Bruns, 2004; Zhan et al., 2006).

• The proposed wavelet coherence method of SL proved to be a useful technique for detecting EEG correlations of very short-duration ERP components with minimum VCUS effects[1]. Later, these short-duration correlations proved to be a useful tool for examining alcoholic effects on EEG correlation. Existing coherence methods for detecting EEG correlation with minimum VCUS effects lack of ability to detect such short-duration correlations. This is because, these methods are based on the Fourier transform which results in lack of time-resolution required to detect such-duration ERP components.

• It was found that VCUS effects on conventional wavelet coherence of REEG signals decreases as interelectrode distance increases in some fixed direction. However, this study provided various results which showed increase in VCUS effects on this coherence when interelectrode distance was increased in different directions. It is important to mention here that existing EEG coherence studies also predict this result but these studies assume decrease in VCUS effects irrespective of an interelectrode direction (Nunez, 1981; Srinivasan et al., 1998; Nunez and Srinivasan., 2005).

• VCUS effects on the conventional wavelet coherence of REEG signals were found independent of time and frequency. This important result was observed for almost every subject used in this study. It will be proved useful to examine VCUS effects on conventional time-frequency coherence methods of REEG signals, because literature on EEG coherence analysis is based on only frequency-domain methods.

• Results in this study showed significant VCUS effects on statistics of EEG coherence methods based on difference in coherence between coherences of different EEG activities. Moreover these results provided substantial evidence that VCUS effects are not additive and therefore can not be ignored in examining difference between different brain states. Using t test and conven-

[1]Some of these important ERP components were: C110 ranging between 100ms to 200 ms, C175 ranging between 160ms to 190ms, C247 ranging between 220 to 260ms, and P300 around 300ms after the stimulus.

tional wavelet coherence analysis of REEG signals, statistical significance of difference between coherences of alcoholic and non-alcoholic REEG activities was found more than 95 %. This statistical significance was dropped to 50 %, when it was obtained by minimizing VCUS effects on that coherences using our proposed wavelet coherence method of SL. Therefore this result brings the importance[1] of minimizing VCUS effects on EEG coherence analysis.

8.3 Clinical applications of results

Results obtained in this study show the importance of our proposed method in clinical neuroscience. One of important applications of these results arises in the study of functional connectivity between various lobes of the brain, which is discussed below.

Various neurological disorders can be efficiently diagnosed by examining increase in their functional connectivity using wavelet coherence analysis of REEG signals (Lin and Chen, 1996; Blanco et al., 1997; Czinege and Bloom, 1997; Chille et al., 2003; Hassanpour et al., 2004; Kiymik et al., 2005; Markazi et al., 2005; Xiaoli Li et al., 2006). A major problem arises, when this coherence is highly affected by VCUS, which results in biased estimates of that coherence. Literature on EEG coherence analysis does not provide a solution that can be used to minimize VCUS effects on this coherence method. This study presents a solution to this problem by proposing the wavelet coherence method of SL. Results obtained in this study have provided sufficient evidence that the proposed wavelet coherence method provides robust measures of coherence with minimum VCUS effects. In addition, it offers an optimal time-frequency resolution at low and high frequency ranges, which can be proved useful for those neurological disorders which have important signatures both at low and high frequencies. In brief, results of this study have provided a substantial amount of evidence that the wavelet coherence analysis of SL can provide important clinical contributions.

[1]Most of EEG coherence studies avoid the issue of VCUS effects using the assumption that VCUS effects are additive (Andrew et al., 1996; Clarke et al., 2001; Moselhy et al., 2001; Baltas et al., 2002; Winterer et al., 2003; Marsdlek et al., 2006).

8.4 Limitations

Following are the limitations of this research.

- **Number of recording electrodes**:

Accuracy of estimating SL tends to increase as interelectrode distance decreases. This is because, large interelectrode distance may contaminate estimates of SL by various other features rather than reflecting radial scalp current density (true SL) at corresponding electrodes (Nunez et al., 1997). Interelectrode distance can be decreased by using the larger number of recording electrodes. The EEG recording system based on the extended 10-20 system of 64 electrodes was used in this study, because it provides satisfactory estimates of SL (Nunez et al., 1997). However, accuracy of SL estimates can be further improved by increasing the number of recording electrodes.

- **Neighboring electrodes**:

Hjorth method based on local methods (Hjorth, 1975) was used in the estimation of SL. This method provides satisfactory estimates of SL, but main disadvantage of this method is its lack of ability to estimate SL for every electrode position on the scalp. This method requires neighboring electrodes having equal distance from a central electrode. The electrode system used in this study does not fulfil this requirement for every electrode position, because it has various electrode positions whose neighboring electrodes are not at equal distance. Therefore, this study has selected those electrode positions whose neighboring electrodes are at equal distance. However, this disadvantage can be removed using more advanced techniques, for example, local methods, which use the actual distance from a central electrode (Lagerlund et al., 1995). These actual distance are usually estimated using the magnetic resonance imaging technique.

8.5 Recommendations for future research

There are still topics related to this work, which would require further investigation. Among them, I stress the following issues:

- **Identification of deep cortical sources:**

EEG coherence analysis can be used to detect an epileptic focus, located deep in the brain, but major problem arises due to superficial sources. These superficial sources biases results of coherence analysis by introducing effects of superficial epileptogenic foci on it (Gerch and Goddard, 1970; Brazier, 1972; Gotman, 1983, 1987).

The physical quantity formed by subtracting coherence of SL from coherence of REEG may be proved useful to minimize these effects. This simply follows from the SL whose sensitivity decreases as distance of corresponding EEG sources from electrode positions increases. It becomes negligible, when corresponding EEG sources are located very deep (more than half of the head radius (Oostendorp and Van Oosterom, 1996; Pernier et al., 1988). Thus it leads to the conclusion that the coherence of SL does not include effects of EEG sources located deep in the brain. Therefore, the difference in coherence between coherences of SL and REEG represents only effects of deep EEG sources and can be used to locate epileptic focus, located deep in the brain. Further research on this, especially in terms of intracranial EEG, may provide clinically significance results.

- **Classification system:**

As mentioned earlier that coherence analysis of SL can not be the complete alternative of coherence analysis of REEG. Each coherence method has its advantages and disadvantages. If corresponding electrode pairs are not affected by VCUS, then REEG-based coherence is better choice than SL-based coherence. It is because, SL-based coherence filters out genuine coherences due to deep EEG sources whereas REEG-based coherence pickups coherences from both local and deep sources (Nunez, 1981). On the other hand, when VCUS effects are high at corresponding pair of electrodes, most of REEG-based coherence is due to VCUS effects and therefore it does not reveal true coherence. Use of SL-based coherence especially when corresponding sources are local, is appropriate in such a situation. Therefore in order to detect true coherence at particular electrodes, choice of the suitable coherence method

between coherences of SL and REEG is important. However, this procedure can be very difficult and time-consuming. Research can be done on this issue especially in terms of some classification system. For example, a classification system based on classifier such as artificial neural networks, Fuzzy logic, hidden Markov would provide the simplest way to detect robust coherences.

Appendix A

Introduction

This appendix presents a detailed discussion on background theory of coherence analysis in EEG studies.

Parametric methods of signal processing

There are several ways to interpret the EEG signal, among them the first approach started from the visual inspection of EEG signals. However the visual inspection of EEG have some disadvantages, for example different types of neurological diseases may show same abnormalities and in result different interpretation of same record can be made (Gevins, 1987a). These drawbacks have been overcome by various signal processing techniques. Signal processing techniques in EEG analysis can be divided into two classes: parametric methods and non-parametric methods. Parametric methods describe a signal in terms of mathematical model characterized by a set of parameters (Lopes Da Silva and Mars, 1987). For example, parametric models represent samples of EEG signals by the following linear relation (Issakson et al., 1981)

$$x_k + a_1 x_{k-1} + \ldots + a_p x_{x-p} = e_x + b_1 e_{k-1} + \ldots + b_q e_{k-q} \qquad \text{(A-1)}$$

Where a_s and b_s are the coefficients of the model which are fixed using the characteristics of EEG signal under consideration and p is the model order. EEG signal is recorded for a fixed interval of time to achieve the estimate of these coefficients (Issakson et al., 1981). The basic strategy is shown in figure A-1

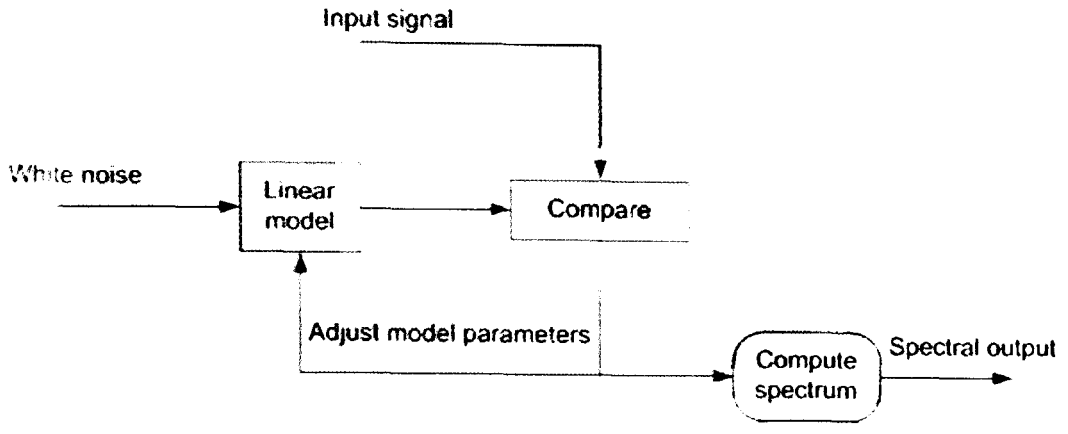

Figure A-1: Block diagram of Model-based approach of spectral estimation. Semmlow, 2004

The model is driven by white noise[1]. Output and input signals are compared with each other to achieve the nearest match between output of the model and the signal under consideration. The model is called an autoregressive model if polynomial of transfer function of model lie in the denominator of transfer function and only a constant in the denominator and the model is called the moving average model if the transfer function of the model has only numerator polynomial (Semmlow, 2004). A model that contain both autoregressive and the moving average characteristics is called an autoregressive moving average model. The autoregressive model of EEG signals has been used in many branches of neuroscience. For example, studies of sleep (Isakssan, 1981; Jansen et al., 1981; Ning and Bronzino, 1987; Simonsen et al., 1987; Amir and Gath, 1989), brain ischemia (Czinege and Bloom, 1997; Hao et al., 1997), seizure (Remond, 1977; Rogowski et al., 1981; Vaz and Principe, 1987; Gersch, 1988; Gath et al., 1992; Franaszczuk et al., 1994; Panzica et al., 1998; Salant et al., 1998; Jouny et al., 2005; Subasi at al., 2005), anesthesia (Bender et al., 1992; Sharma et al., 1992; Jensen et al., 1996; Sharma and Roy, 1997; Muthuswamy and Roy, 1999), Alzheimer's disease (Locatelli et al., 1998), newborn seizure (Roessgen and Boashash, 1995; Roessgen et al., 1998; Boashash and Keir, 1999; Celka and Colditz, 2002) and cognitive processes (Anderson and Sijercic, 1996; Bigan and Woolfson, 2000; Svoboda, 2006; Maiorescu et al., 2003; Curran et al., 2004). Various studies have proved superiority of model-based approaches over Fourier-based methods. For example, Fourier-based methods require fairly long observation time about 30 seconds or more to achieve good spectral resolution. This may eas-

[1]White noise contains equal energy at all frequencies

ily come into conflict with non-stationary behavior of EEG. This advantage is largely overcome by using parametric models (Isaksson et al., 1981). For example, Roessgen and Boashash (1995) compared EEGs of seizure and non-seizure of one newborn by modeling the model of Lopes da Silva et al. (1974) for seizure activity by adding another input signal of seizure characteristics to the model of Lopes da Silva. Their results demonstrated the superiority of model-based approach over the Fourier-based approach. Fourier-based auto-spectrum could not reveal important seizure characteristics such as the repetitive waveforms were not present and also the significant amount of spectral overlap between seizure and non-seizure activity was present. On the other hand model-based parameters clearly demonstrated the seizure activity of newborn seizure and showed the significant level of difference between seizure and non-seizure activity for the low frequency seizure activity. Grewal et al. (1998) using the Fourier-based and autoregressive techniques of signal processing measured the coherence function of EEG signals of rat during the vigilance states of quiet waking, slow wave sleep and rapid eye movement sleep. Coherence function in autoregressive model was calculated using the technique developed by the (Nuttall, 1976). During the quite waking sleep and slow wave sleep, coherence was low for both techniques but there was significant amount of coherence nearly o.8 in the theta range. Compared to the Fourier-based method, coherence function measured by the autoregressive technique, provided the smother value of coherence with a higher resolution and low variance. The major disadvantage of the parametric techniques is that these techniques are computationally more expensive than the non-parametric techniques (Gath et al., 1992; Pardey et al., 1996). For example, Gersch, (1987) suggested the time varying autoregressive model for the EEG signals but it was useful only for modeling of only small number of EEG channels as'the number of parameters fitted to the model were proportional to the the square of the number of the EEG channels (Gath et al., 1992).

Non-parametric methods of signal processing

Time-domain signal processing methods

A very simple, but surprisingly effective method of analysis of EEG signals in non-parametric method is based upon the averaging technique in which number of brief time series are averaged (Scott, 1976). Values of mean amplitude, variance, skewness are calculated for each electrode site. The calculated vari-

ables are then analyzed. Another existing method in the literature is known as the zero-crossing method or periodic analysis (Lim and Winters, 1980). In this method, individual waves are analyzed by counting the zero-crossing of the original wave, the time interval between a positive to negative voltage transition to next positive to negative voltage is called the zero crossing (Henderson et al., 2006). The total number of counts within each period, over the analysis epoch, then displayed in a histogram format which shows the distribution of the counts for a specified frequency category, or as a percentage of time occupied by the count in that category. This method is widely used to test the effect of the psychoactive drugs. However, this method has drawbacks, such as sensitivity to noise and other artifacts and also results are difficult to interpret in the spectral terms. Several attempts have been made to improve the technique, for example iterative technique has been used but main difficulties remains.

Another method is autocorrelation analysis (Brazier and Casby, 1952). The application of autocorrelation analysis to brain potentials was first reported by Imahori and Suhara (1949 cited in Gevins, 1987b). The autocorrelation function measures the degree of similarity between an EEG signal and its replica at successive time delays and it also emphasizes the periodic component of an EEG segments and suppresses non-periodic components, by comparing the EEG time series with itself at sequential time delays (Gavins, 1987b). The autocorrelation function of discrete stochastic time series $x(n)$ is defined as (Lynn, 1992)

$$R_{xx}(d) = \frac{1}{N} \sum_{n=1}^{n=N} x(n)x(n+d), \tag{A-2}$$

where N is the total number of samples present in time series $x(n)$ and d shows time shift in time series $x(n)$. Eq. (A-2) indicates that the autocorrelation function is the average product of the sample $x(n)$ with a time-shifted version of itself. EEG autocorrelation function function for epilepsy patients has been reported to be regular than those of normals (Yamamoto, 1960 cited in Gevins, 1987b) as shown in Figure A-2.

Another important measure is a cross-correlation function. A cross-correlation function measures the similarity in waveform of two EEG segments, usually from different recording sites. It is given by the following relation:

$$R_{xy}(d) = \frac{1}{N} \sum_{n=1}^{n=N} x(n)y(n+d), \tag{A-3}$$

where R_{xy} is the cross-correlation function of time series $x(n)$ and $y(n)$. Eqs. (A-2) and (A-3) are based upon the stationarity assumption of the EEG signals and therefore correlation analysis is a function of the time delay only. Another disadvantage is that the autocorrelation of two different signals of nearly equal amplitudes but having different rhythmic or frequency components basically represents the superposition of two separate rhythmic components and this result in the loss of individual frequency components. Correlation analysis is confined to only time-domain. Frequency-domain information of EEG signals is also important (Vincent et al., 1995; Akin, 2002).

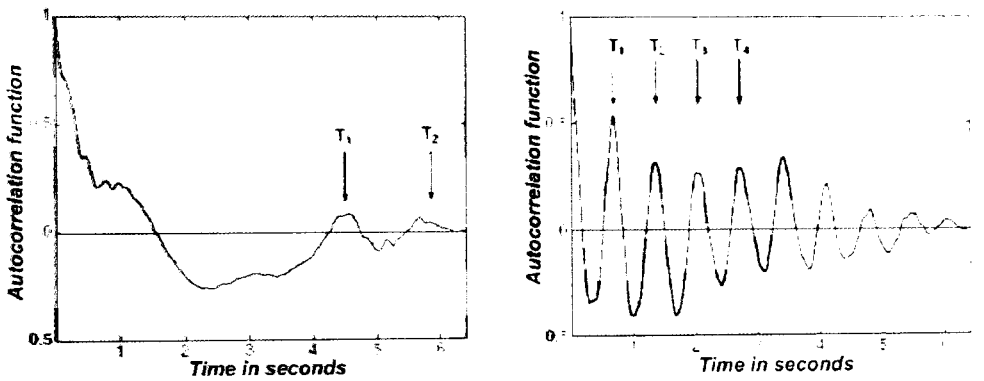

Figure A-2: The autocorrelation of normal EEG (left figure) and seizure EEG. The moment centres are marked. Seizure EEG has periodic peaks and the normal EEG has irregular peaks. Liu et al., 1992

Frequency-domain signal processing methods

Signal in the time-domain is represented by means of its value on the time axis. It is possible to use another representation for the same signal: that is the frequency-domain representation. The Fourier transform is used to transform the time-domain signal into the frequency-domain. The Fourier transform was developed by (Jean Baptiste Fourier (1768-1830)) and reached innumerable applications in mathematics, physics and natural sciences. Furthermore, the Fourier transform is computationally very attractive since it can be calculated by using an extremely efficient algorithm called the Fast Fourier transform (Cooley and Tukey, 1965). The Fourier transform describes

a signal $x(t)$ as a linear superposition of sines and cosines characterized by their frequency ω

$$X(\omega) = \int_{-\infty}^{\infty} x(t)e^{-i\omega t}dt, \tag{A-4}$$

The inverse Fourier transform is given,

$$x(t) = \int_{-\infty}^{\infty} X(\omega)e^{i\omega t}d\omega, \tag{A-5}$$

Eq. (A-4) is the continuous Fourier transform of the signal $x(t)$. Let us consider in the following that the signal consists of N discrete values, sampled every time Δt, denoted by $x(n)$ The discrete Fourier transform of this signal is defined as:

$$X(m) = \sum_{n=1}^{N} x(n)e^{-i2\pi mn/N}, \tag{A-6}$$

where $m = 0, \ldots, N-1$ and its inverse as:

$$x(n) = \frac{1}{N}\sum_{m=0}^{N-1} X(m)e^{i2\pi mn/N}. \tag{A-7}$$

From the complex coefficients of Eq. (A-6), the periodogram can be obtained as:

$$P_{xx}(m) = \mid X(m) \mid^2 = X(m) \cdot X^*(m), \tag{A-8}$$

where asterisk stands for complex conjugate operation. Eq. (A-8) is called the auto-spectrum. Cross-spectrum can be similarly defined by making the product of Eq. (A-8) between time series $x(n)$ and $y(n)$ as follows:

$$P_{xy}(m) = X(m)Y^*(m), \tag{A-9}$$

where $X(m)$ and $Y(m)$ are the Fourier transforms of $x(t)$ and $y(t)$ respectively. The sample cross spectrum gives a measure of the linear correlation between two signals for different frequencies. The estimate of the auto-spectra or cross-spectra from N data points of given stationary process do not provide the consistent estimate. For example, estimation of auto-spectrum from three different segments of 1024 point produces different results. Therefore different methods to estimate the auto-spectrum have been described, among them is the Blackman and Turkey method (Blackman and Turkey, 1959). This method is based upon the Wiener-Khinchin theorum which states that auto-spectrum of stationary random process is defined to be the Fourier transform of its autocorrelation function. In this method, auto-spectrum is estimated by calculating the corresponding autocorrelation function. Another approach is based upon the Welsh periodogram method in which several calculation of

the periodogram are made from the data and then periodogram are averaged to obtain an improved estimate of auto-spectrum.

Various studies have shown the relation of different frequency bands and the learning abilities of children. The decrease in the alpha and beta bands of auto-spectrum with the increase in the activity in the delta band of auto-spectrum in the children having the difficulties in learning, spelling, reading, writing and speech has been reported (John et al., 1980; Harmony et al., 1990; Byring et al., 1991; Ackermann et al., 1995). The later study by Schmid et al. (2002) performed on the group of 155 clinically healthy normal children in the awake state of vigilance with the eyes closed having the IQ less than 90 and greater than 90 showed the decrease of delta and theta bands of auto-spectrum with the increase in the activity in the alpha band especially for the parietooccipital region of the brain for verbal IQ. Auto-spectrum has been used for the quantitative analysis of EEG during sleep studies (Gath, 1980; Hadjiyannakis et al., 1997; Ferri et al., 2000; Wichniak et al., 2003; Madan et al., 2004; Taikang and Nhon, 2004; Ferri et al., 2005). The Fourier-based auto-spectrum has been used for the quantitative analysis of epileptic seizures (Gotman, 1982; Gotman et al., 1995; Gath, 1992; Asano et al., 2004). The technique developed by the Gotman (1982) for epileptic seizures is based upon calculating various features from the auto-spectrum e.g. frequency and the width of the dominant spectral peak, ratio of the power in the dominant spectral peak to that in the same frequency band of the background spectrum, etc. These various spectral features are calculated for the EEG of the normal and the epileptic seizures and then compared with each other as shown in Figure A-3

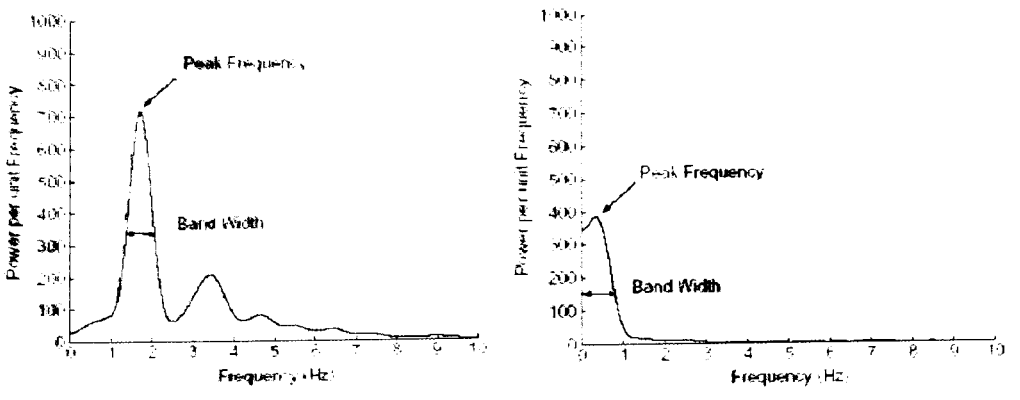

Figure A-3: The auto-spectrum of seizure EEG (left figure) and the normal EEG. Gotman, 1982

The auto-spectrum has been used to study the effects of ischemic brain injury. Hypoxic-ischemic encephalopathy is damage to cells in the central nervous system (the brain and spinal cord) from inadequate oxygen. Hypoxic-ischemic encephalopathy may be cause of death in newborns. Significantly reduced variance in the auto-spectrum of EEG of hypoxic-ischemic encephalopathy of newborns as compared to the variance in the auto-spectrum of EEG of healthy newborns has been reported (Wong et al., article in press). Even though the auto-spectrum has been successfully used for the study of various cognitive processes and neurological disorders. However the change of auto-spectrum for different kinds of the EEG signals does not provide the information about the EEG activity in the frequency-domain for the functional relation between different cortical regions of the brain. Cross spectrum analysis given by the Eq. (A-9) provides the means to measure the functional relation between different cortical regions in the frequency-domain (Gath et al., 1992; Ferri et al., 2000; Ning and Trinh, 2004). The cross spectrum of time series $x(n)$ and $y(n)$ normalized by the square root of the product of auto-spectra of that time series is called coherence function in EEG studies.

Appendix B

Physical basis of the SL

Two dimensional SL (SL) of scalp potential v at electrode position E whose cartesian coordinates are x and y is given by,

$$L_E(v) = \frac{\partial^2}{\partial x^2} + \frac{\partial^2}{\partial y^2}(v) \tag{B-1}$$

Ohm's law provides the physical basis of SL in terms of surface current density. According to the Ohm's law, scalp current density $\vec{J}$, the electric field $\vec{E}$ and conductivity c are related by the following relation:

$$\vec{J} = c\vec{E} \tag{B-2}$$

Using the divergence on both sides of Eq. (B-2)

$$\nabla.\vec{J} = \nabla(c\vec{E}) \tag{B-3}$$

For an isotropic linear volume, conductivity is constant, it can be removed out from the divergence operator.

$$\nabla.\vec{J} = c\nabla.\vec{E} \tag{B-4}$$

Substituting $E = -\nabla(v)$ into the Eq. (B-4), we get

$$\nabla.\vec{J} = -c\nabla^2(v) \tag{B-5}$$

Where ∇^2 is mathematical operator and is equal to

$$\frac{\partial^2}{\partial x^2} + \frac{\partial^2}{\partial y^2} \tag{B-6}$$

Putting B-6 into the Eq. (B-5), we get

$$\nabla.\vec{J} = -c\frac{\partial^2}{\partial x^2} + \frac{\partial^2}{\partial y^2}(v) = -cL_E(v) \tag{B-7}$$

Therefore we can say that divergence of current density is proportional to minus the Laplacian of electric potential (Perrin et al., 1987). The term divergence of current density actually refers to the change in the current density. At a location where there are no underlying current sources, the Laplacian would be zero, while it would be maximal directly over a source (Nunez and Srinivasan, 2005). That simply means thtat the Laplacian of the potential may be used to localize the underlying generators of the EEG.

Relation between SL and cortical potential

The SL can also be explained in terms of cortical potential. Cortical potential is measured at the surface surrounding the volume of the brain (Towie et al., 1998). Srinivasan(1999) explains that "potential measured at smooth surface surrounding the volume of the brain, as in direct recordings from the human brain in surgical patients with surface grids, without accounting for the folds of the cortical surface"" (page 1). Based on Ohms Law and current conservation the following relationship can be derived (Katznelson, 1981; Srinivasan, 1999):

$$V_{CSF} = V_{skull} + \frac{\rho_{skull}}{\rho_{scalp}} d_{skull} d_{scalp} L_{scalp} \tag{B-8}$$

Here d_{skull} and d_{scalp} stand for the thicknesses of the skull and scalp respectively; V_{CSF} and V_{skull} stand for potential at the inner and outer surface of skull respectively; ρ_{skull} and ρ_{scalp} stand for the resistivities of skull and scalp respectively and surface Laplacain

$$L_{scalp} = \nabla^2 V_{scalp} \tag{B-9}$$

.

And also from (Srinivasan, 1999)

$$V_{CSF} \sim V_{cortex} \tag{B-10}$$

$$V_{skull} \ll V_{CSF} \tag{B-11}$$

so that above equation becomes

$$L_{scalp} \propto V_{cortex} \tag{B-12}$$

Thus, the SL of the scalp potentials can be used to estimate the cortical surface potentials.

Hjorth Method

The nearest neighbor method (Hjorth, 1975; Wallin and Stalberg, 1980) is the most popular method to derive Laplacian. This method approximates the Laplacian at electrode o as the sum of the potentials at the four nearest neighbors to electrode o minus four times the potential at electrode o. Nunez and Srinivasan, (2005) have explained the method of computing SL using Hjorth method, which is explained here. In Figure B-1, the brain region is divided into two parts: skull and scalp.

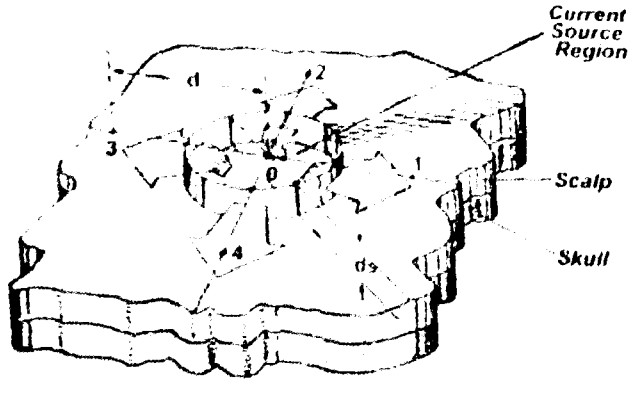

Figure B-1: The brain region is divided into two parts: skull and scalp. Katznelson(1981)

It has been assumed that electrode o is placed at a scalp position right above the source s, located inside the brain. A small cylinder of scalp tissue of thickness d_s with principle axis positioned at electrode o perpendicular to the scalp surface is assumed. Four more electrodes named as 1 to 4 from a equal tangential distance d from electrode o are assumed here. The main goal is to compute SL or value of current density due to the source s. The cylinder is divided into four equal parts as shown in Figure B-1. The current $\vec{I}_s$ flowing from the cylinder walls of each section into the nonlocal scalp can be obtained by the surface integral of its current density $\vec{J}_s$, that is

$$\vec{I}_s = \int\int_C \vec{J}_s.\vec{d}_s \tag{B-13}$$

Using $\vec{J}_s = c\ \vec{E}_s$ Ohm's law[1] and Eq. (B-13),

$$\vec{I}_s = \int\int_C \vec{J}_s.\vec{d}_s = c\int\int_C \vec{E}_s.\vec{d}_s \tag{B-14}$$

Where c and $\vec{E}_s$ represent the conductivity constant and the value of electric field for each section respectively. The electric fields for each section is calculated at the center of each distance say point p between electrode o and other electrodes named as 1, 2, 3 and 4. The electric field $\vec{E}_{01}$ at point p between electrode o and electrode 1 at the center along a distance d is equal to the difference of potentials at an electrodes o and electrode 1 divided by the sum of the distances between the point p and its distances from electrode o and 1, here the distance between point p and each electrode, for example, from point p to 1 is equal to the $d/2$. Therefore the value of $\vec{E}_{01}$ is given as $\vec{E}_{01} = \frac{v_0 - v_1}{d/2+d/2}$. The values of the electric field between an electrode o and electrodes 2, 3 and 4 can be calculated in the similar way. One can represent the value of electric field E_s for any of four regions of cylinder as $\frac{(v_0 - v_j)}{d}$, where j runs from 1 to 4. Therefore replacing the integral sign with summation sign in the right hand side of Eq. B-14, we can write Eq. (B-14) as

$$\vec{I} \approx c\sum_{j=1}^{4} \frac{(v_0 - v_j)}{d}\frac{S}{4} \approx c[4v_0 - v_1 - v_2 - v_3 - v_4]\frac{\pi d_s}{4} \tag{B-15}$$

Eq. (B-15) can be written in terms of scalp current density by dividing both sides with the surface area of the cylinder $\pi(\frac{d}{2})^2$

$$J \approx \frac{I}{\pi(\frac{d}{2})^2} \approx cd_s\frac{[4v_0 - v_1 - v_2 - v_3 - v_4]}{d^2} \tag{B-16}$$

The Laplacian in Eq. (B-1) or in general form represents the continuous partial derivative but based on the limited number of samples, it can be approximated by means of the finite differences(Korn and Korn., 1968)

$$L_E(v) = \frac{\partial^2}{\partial x^2} + \frac{\partial^2}{\partial y^2}(v) \approx \frac{d^2}{dx^2} + \frac{d^2}{dy^2}(v) \tag{B-17}$$

In our case all four electrodes are placed at equal distance from electrode o, therefore we can write equation B-17 as

$$L_E(v) \approx \frac{dx^2 + dy^2}{d^2}(v) \tag{B-18}$$

[1]According to this law current density $\vec{J}$ is directly proportional to its electric field $\vec{E}$ where the conductivity c remains constant

Electrodes 2, 0 and 4 are considered here along the direction of Y axis and electrodes 1, 0 and 3 are considered here along the direction of X axis as shown in Figure B-2. The second order differences of potentials along the X and Y direction are,

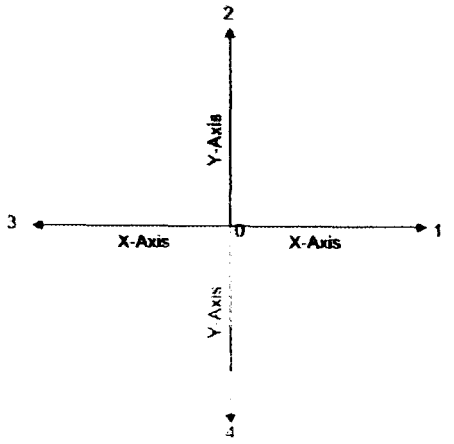

Figure B-2: The electrodes 2, 0 and 4 are placed along the direction of Y axis and the electrodes 1, 0 and 3 are along the direction of X axis

$$dx^2(v) = (v_1 - v_0) - (v_0 - v_3) \tag{B-19}$$

$$dy^2(v) = (v_2 - v_0) - (v_0 - v_4) \tag{B-20}$$

Therefore,

$$\begin{aligned} dx^2 v + dy^2 v &= (v_1 - v_0) - (v_0 - v_3) + (v_2 - v_0) - (v_0 - v_4) \\ &= -4v_0 + v_1 + v_2 + v_3 + v_4 \end{aligned} \tag{B-21}$$

Substituting Eq. (B-21) into Eq. (B-18),

$$L_E(v) \approx \frac{-4v_0 + v_1 + v_2 + v_3 + v_4}{d^2} \tag{B-22}$$

The quantity

$$j_v = -\frac{L_E(v)d^2}{4} = v_0 - \frac{v_1 + v_2 + v_3 + v_4}{4}, \tag{B-23}$$

has been mostly used instead of $L_E(v)$ in EEG studies, because it is more convenient to compare with potential v as it has the units of potential i.e. μv. Substituting the value of Eq. (B-22) into the Eq. (B-16), we get

$$J \approx cd_s L_E(v) \tag{B-24}$$

or

$$J \propto L_E(v) \tag{B-25}$$

Therefore it is clear from the Eq. (B-25) that SL for the electrode o is directly proportional to the current density due to source s.

Appendix C

Experimental setup and data preparation

EEG data is donated by the Dr Henri Begleiter at the Neurodynamics Laboratory at the State University of New York Health Center at Brooklyn and the ERP analysis on this data has been published in Zhang et al., 1995; Ingber, 1997) which is now publicly available at the web page http://kdd.ics.uci.edu//databases/eeg/eeg.html. The method of measuring the EEG data is explained below:

Subjects were divided into two groups: alcoholics and abstinent alcoholics (average 10 years of abstinence). Alcoholics subjects had a history of alcoholism of at least 10 years with an average drinking rate of 45 units per week. One unit of pure alcohol was taken equal to 10 ml. ERPs of 15 subjects, selected from each group, were used in this study. The subjects had no history of chronic somatic or neurological disease. Male subjects with the age range of 16-25 were chosen. They had normal hearing and normal sight. Each subject was exposed to either a single stimulus (S1) or to two stimuli (S1 and S2). These stimulus were 19 pictures of objects chosen from the Snodgrass and Vanderwart., (1980) picture set. The duration for the first S1 and the second S2 picture stimulus in each trial was 300ms. The interval between each trial was fixed to 3.2s. Two picture stimuli appeared in succession with a 1.6 s fixed interstimulus interval. Two pictures were shown in three different ways: First one is called the matched condition, in the matching condition, the S1 was repeated as S2. The Second one is called the non-matched condition when S1 was followed by a picture that was completely different from S1 in terms of its semantic category. Last one is called single trial, when only one picture was shown to the subject. The presentation of these pictures were shown to the subject in the random order. The subjects were 1 meter away from the center of computer display and their task was to decide whether

the second response(S2) was the same as the first one. The subjects were instructed to respond their reaction by pressing the mouse key only if they felt confident about it. If a change occurs(non-matched condition) and they press a button to indicate change, then this is called hit trial. If a change occurs and subject press the button for no change, this is a miss trial. If no change occurs(matched condition) and they press no change, this is correctly detected no change trial whereas if they press change, this is a false alarm. This experiment yielded an ERP waveform consisting of three components which were most clearly discernible at the more posterior electrodes: component I (c110) ranging between 100 and 125 ms, component 2 (c175) ranging between 160 and 190 ms, and component 3 (c247) ranging between 220 and 260 ms.

EEG data was recorded from 64 electrode system based on the extended 10-20 system i.e 10-10 system. AF3 and AF4 are called in 10-10 system of 64 electrodes as the AF1 and AF2 respectively (Oostenveld and Praamstra, 2001). After the EEG signals have been detected by electrodes, these signals were amplified and filtered by 1.00-100Hz band pass filters. The procedure of amplification and filtering of EEG signals is necessary because EEG signals are very small, contain unwanted noise, and can even be masked by other biosignals from different biological phenomena. An A/D converter was used to change the EEG signals from a continuous analog wave form to a digital signal at the sampling rate of 256 Hz (3.9-msec epoch) for one second. Trials with excessive eye and body movements ($\geq$ 73.3 uV) were rejected on-line and also subjects were seated in a reclining chairs located in a sound attenuated RF shielded room. Two additional bipolar deviations were used to record the vertical and horizontal EOG, which were later used for the rejection of eyes artifacts using subtraction method. Following is the brief introduction of artifacts.

EEG recording techniques

Electrical activity of the brain can be recorded by the insertion of needle electrodes into the neural tissue of the brain and this technique is called depth recording. Normally EEG is recorded by affixing an array of electrodes to the scalp.The most widely used placement of electrodes is the so called 10-20 system consisting in 20 electrodes (sometimes less or more) uniformly distributed along the head,generally referenced to 2 electrodes in the earlobes.

Depending upon the choice of reference electrode, EEG recording techniques are divided into different classes. Some popular REEG recording techniques are bipolar recordings, common reference recordings and average reference recordings. In common reference recordings, the terminal of each amplifier is connected to the same electrode, and all other electrodes are measured relative to this single point. In average reference recordings, the outputs of all of the amplifiers are summed and averaged, and this averaged signal is used as the common reference for each amplifier. In bipolar recordings both signals do not have common lead and the electrodes are connected in series to an equal number of amplifiers.

EEG artifacts

One of main problems in the automated EEG analysis is the detection of different kinds of interference waveforms or artifacts added to the EEG signal during the recording sessions. These interference waveforms, the artifacts, are any recorded electrical potentials not originated in the brain. We can divide EEG artifacts into two main classes: (1)artifacts which are exterior to the subject (2) artifacts caused by the subject.

Artifacts exterior to the subject

The artifacts exterior to the subject can be divided into four main classes:

- The leads and the electrodes.
- Electrical interference: this electrical interference is external to the subject or the recording system.
- EEG equipment
- The subject.

The most common electrode artifact is the electrode popping. Morphologically this appears as single or multiple sharp waveforms due to abrupt impedance change. It is identified easily by its characteristic appearance (ie, abrupt vertical transient that does not modify the background activity) and its usual distribution, which is limited to a single electrode In general, sharp transients that occur at a single electrode should be considered artifacts until

proven otherwise. At other times, the impedance change is not so abrupt, and the artifact may mimic a low-voltage arrhythmic delta wave. Another artifact, which we call as alternating current (60-Hz) artifact arises when the impedance of one of active electrodes becomes significantly large between the electrodes and the ground of the amplifier. In this situation, the ground becomes an active electrode that, depending on its location, produces the 60-Hz artifact. The artifact presents at exact frequency 60 Hz, as its name indicates. Adequate grounding on the patient can almost eliminate this type of artifact from power lines. The movements of the other persons around the patient can generate artifacts, usually of capacitive or electrostatic origin. Avoid this type of artifact as much as possible by restricting the movement of other subjects. Another important artifact is caused by the electro-smog. Electro-smog refers to the huge amount of electromagnetic fields (EMF) present literally everywhere on this planet.The interference from high-frequency radiation from radio, TV, hospital paging systems, and other electronic devices can also produce artifacts. Such type of artifacts can be avoided by making all EEG measurement in a shield room blocking electromagnetic radiation from outside. Summarizing the above discussion of artifacts, exterior to the subject, we can say that several technical artifacts such as the electrode-pop artifact, electro smog, etc may be effectively prevented with adequate care in the EEG laboratory. For example use of appropriate electrode/electrolyte combinations, fixation of the leads, shielding of the subject.

Artifacts caused by the subject

Artifacts caused by the subject are of two types: artifacts provoked by subjects movements and artifacts provoked by biological electric phenomena. In order to reduce artifacts caused by movements (gestures, respiration, etc.), it is important that the subject be relaxed and asked not to move during the experiment. Biological phenomena that cause EEG artifacts are: eye movements, muscle activity, cardiac beat, and sweat. In the following, I discuss the most important: eye movement and muscle artifacts.

- Eye movement artifacts

Eye movement artifacts (or ocular artifacts) result from the contamination of the EEG by the electrooculogram (EOG), a potential produced by movement of the eye or eyelid. Several methods have been proposed for removing ocular artifacts from the EEG, most of which make use of a separate EOG

record. One approach to reducing contamination from eye movement artifacts is to regress out reference signals collected near the eyes. Regression methods have been proposed using both time domain and frequency-domain techniques. All regression methods, whether in time or frequency domains, depend on having one or more clean reference channels (e.g. one or more 'EOG' channels) which cannot be further analyzed after regression. Independent Component Analysis ICA is a statistical signal processing technique whose goal is to express a set of random variables as a linear combinations of statistically independent component variables ICA algorithm is used to remove eye artifacts Another most common method is the rejection technique

- Muscle artifacts

Muscle activity produces an electric potential called electromyogram (EMG), which is termed as muscle artifacts in EEG. The muscle artifact is very common and may be many times larger in magnitude than the EEG signal. This artifact is due to contraction of neck and scalp muscles. Further, in a tense subject, the muscle activity is often wide spread though maximal in temporal regions. The muscle artifact is found to affect the EEG spectrum above 14 Hz considerably i.e. the B-activity. In visual analysis, an attempt is often made to reduce the muscle artifact by decreasing the higher cutoff frequency of the recording amplifiers.

Thesis results

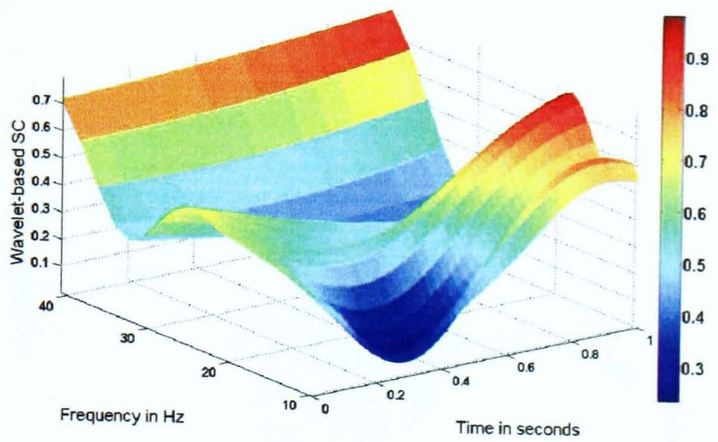

Figure C-1: Subject a681: wavelet squared coherency of REEG between electrodes CP_3 and P_1

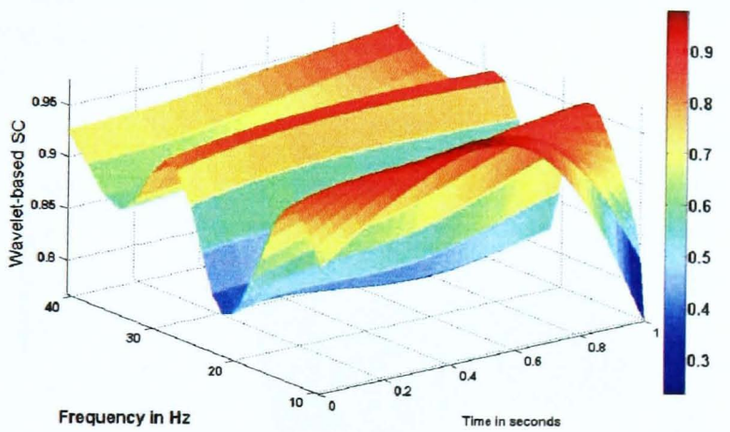

Figure C-2: Subject a681: wavelet squared coherency of REEG between electrodes CP_3 and P_4.

Wavelet squared coherency of REEG due to VCUS effects between electrodes CP_3 and P_1 does not show VCUS effects at any frequency. However VCUS effects around 30 Hz are observed, when interelectrode distance is increased from CP_3 to P_4 in different direction than the direction between CP_3 and P_1.

Effects of interelectrode direction on wavelet coherence analysis of REEG signals

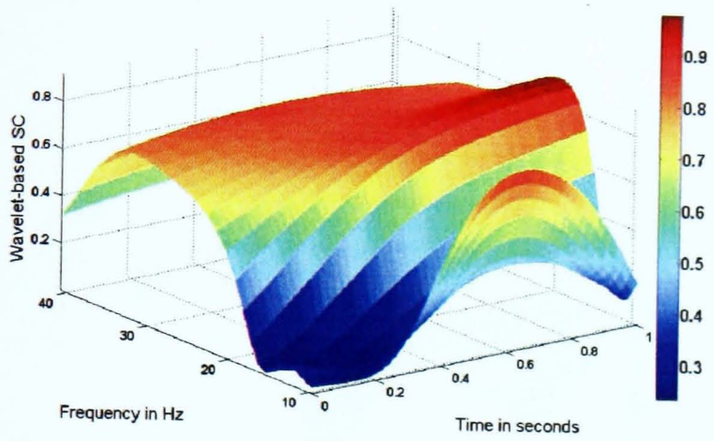

Figure C-3: Subject c381: wavelet squared coherency of REEG between electrodes POz and FCz

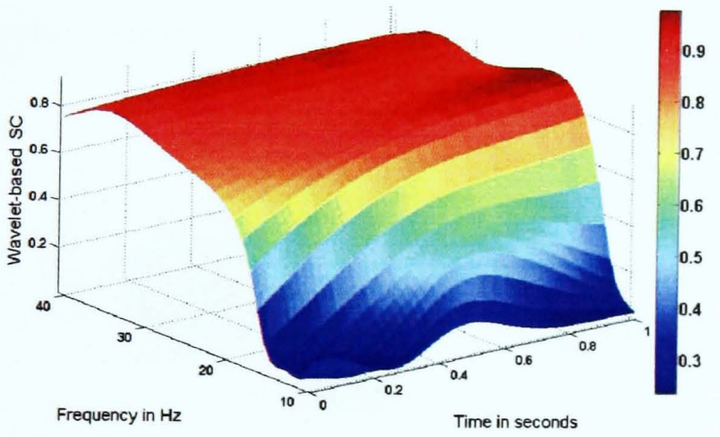

Figure C-4: Subject c381: wavelet squared coherency of REEG between electrodes POz and AF_3

Wavelet squared coherency of REEG due to VCUS between electrodes POz and FCz effects shows constant value of 0.7 between 25 and 35 Hz. This value of coherence is increased up to 0.8, when interelectrode distance is increased from POz to AF_3 in different direction than the direction between POz and FCz.

Wavelet squared coherency of REEG due to VCUS effects decreases as interelectrode increases along some fixed direction

Figures from C-5 to C-6 show the effects of interelectrode distances on the wavelet squared coherency due to VCUS effects. These figures clearly show that coherence due to VCUS effects decreases as the interelectrode distance increases along some fixed direction.

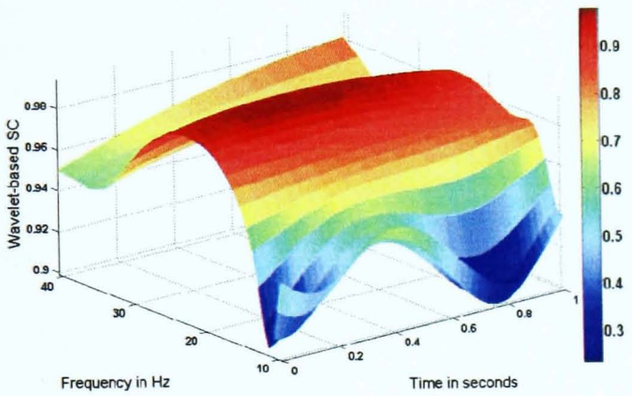

Figure C-5: For the interelectrode distance between POz and Pz, wavelet squared coherency of REEG due to VCUS effects is around 0.98.

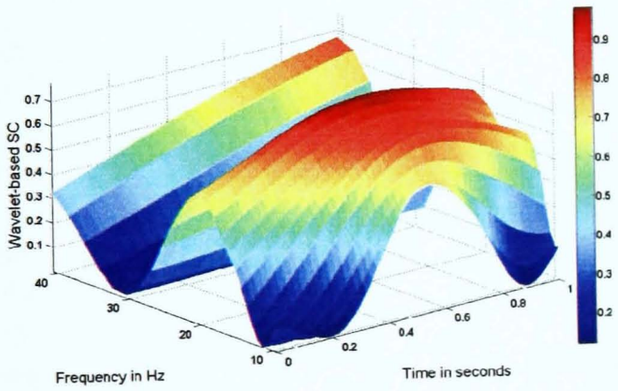

Figure C-6: The distance of POz from Pz is increased up to the distance FPZ. At this distance, wavelet squared coherency of REEG due to VCUS effects is almost disappeared.

AWSCs of REEG and SL between electrodes PZ and remaining 29 electrodes for EEG activities of alcoholics and abstinent alcoholics subjects

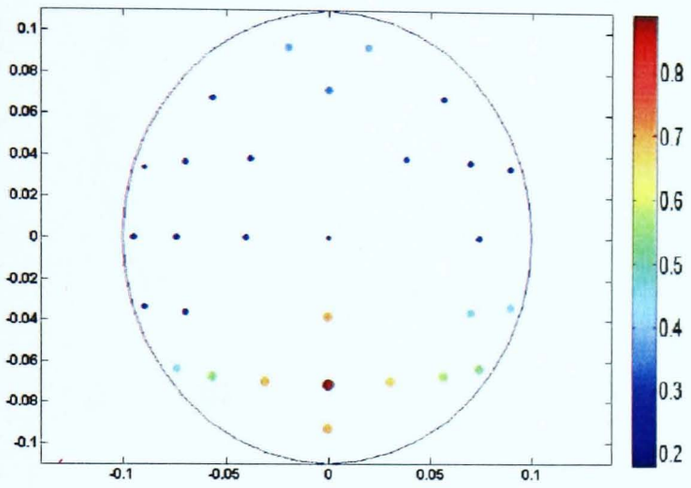

Figure C-7: AWSCs of REEG between electrodes PZ and remaining 29 electrodes for abstinent alcoholic subject c101

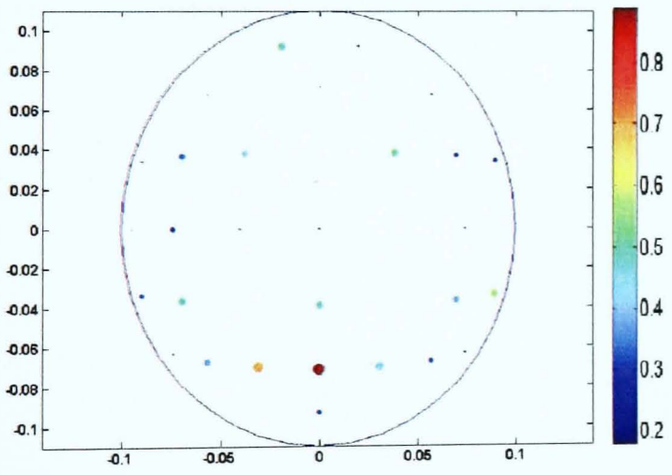

Figure C-8: AWSCs of SL between electrodes PZ and remaining 29 electrodes for abstinent alcoholic subject c101

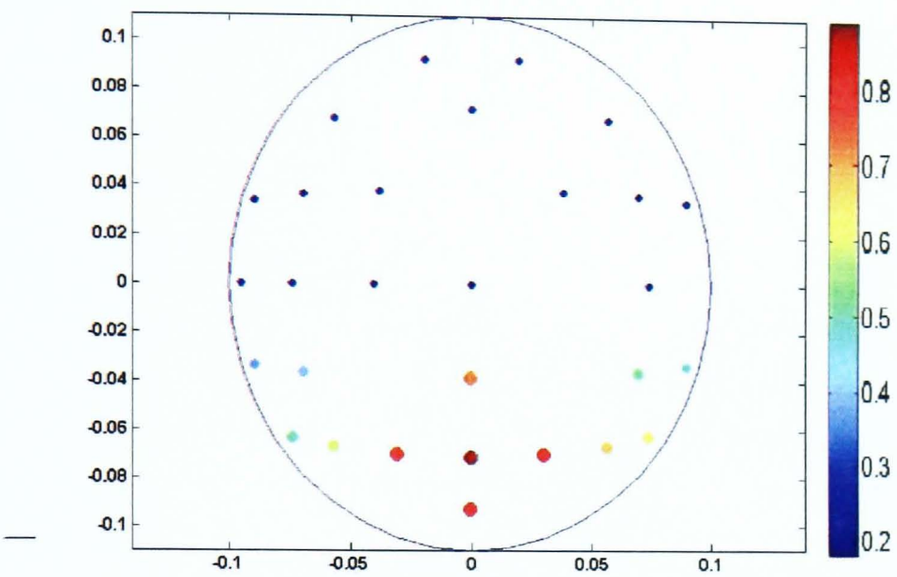

Figure C-9: AWSCs of REEG between electrodes PZ and remaining 29 electrodes for alcoholic subject a101

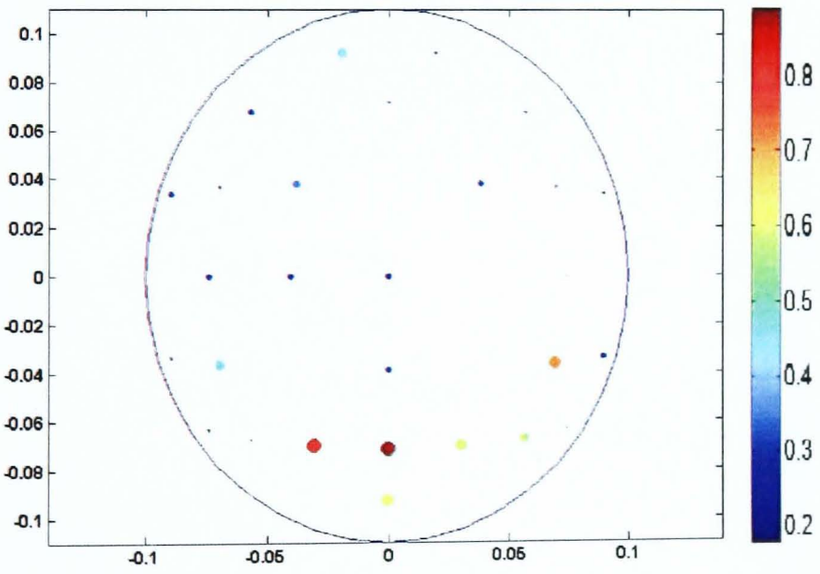

Figure C-10: AWSCs of SL between electrodes PZ and rest of 29 electrodes for alcoholic subject a101

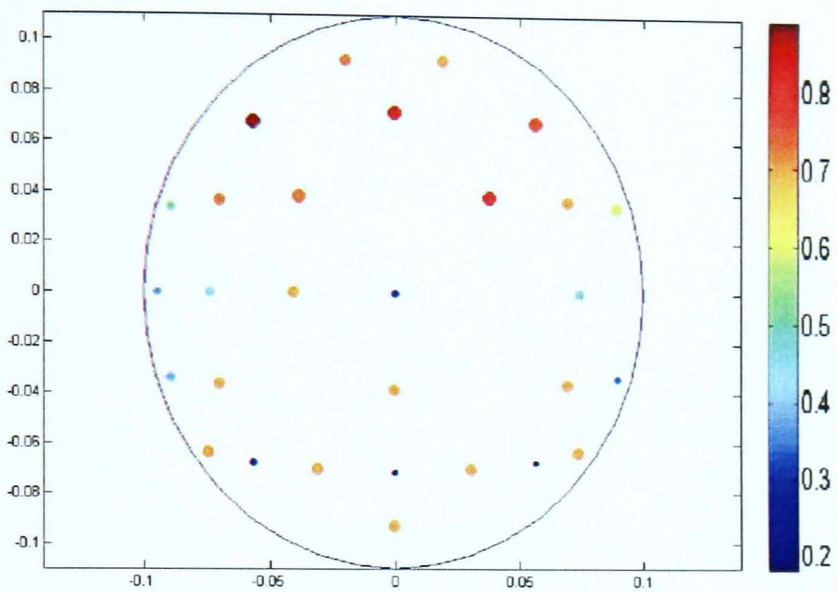

Figure C-11: AWSCs of REEG between electrodes F3 and remaining 29 electrodes for control subject c102

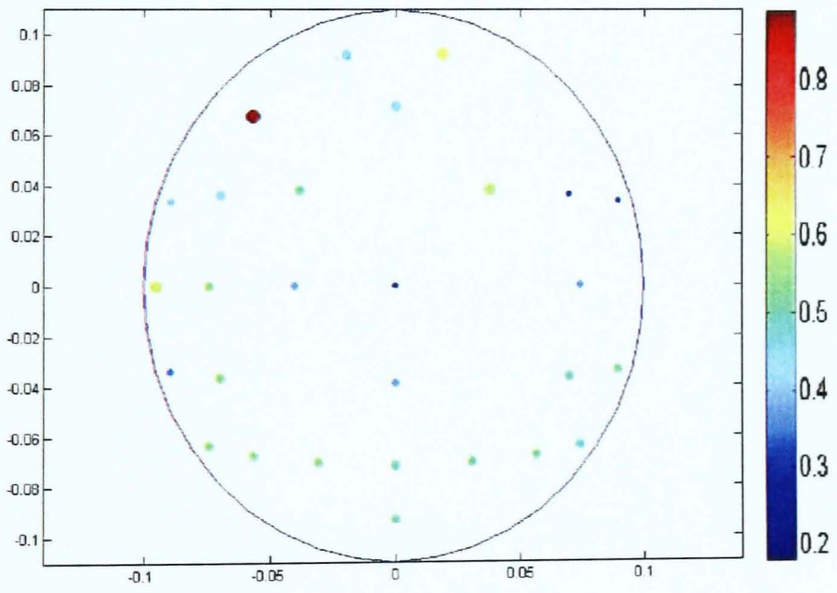

Figure C-12: AWSCs of SL between electrodes F3 and remaining 29 electrodes for control subject c102

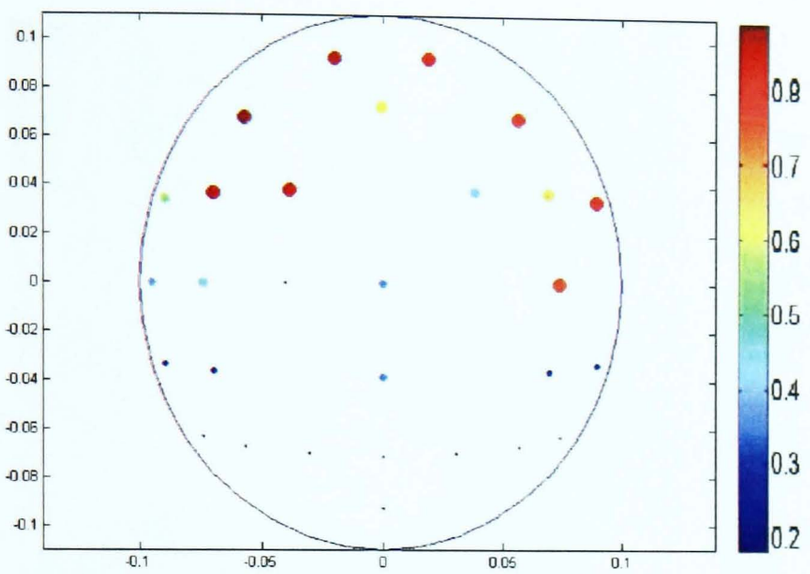

Figure C-13: AWSCs of REEG between electrodes F3 and remaining 29 electrodes for alcoholic subject a102

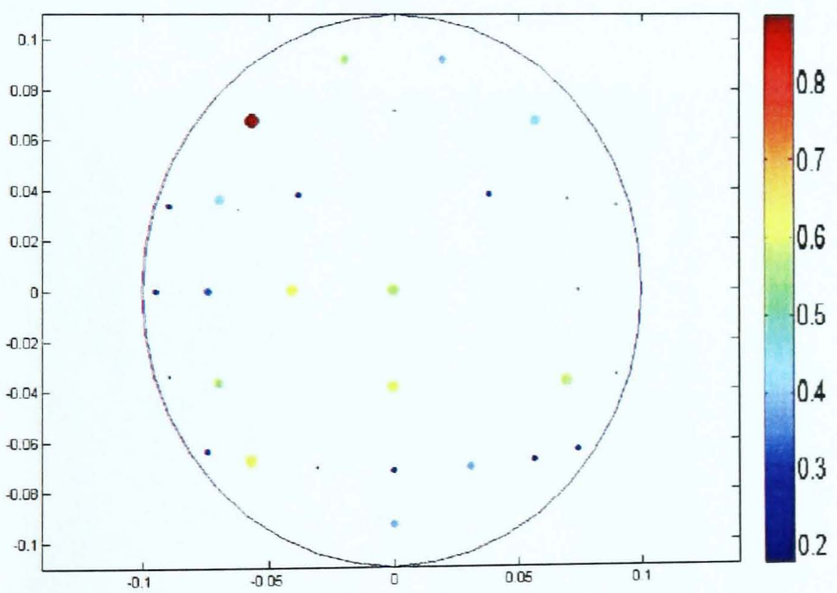

Figure C-14: AWSCs of SL between electrodes F3 and rest of 29 electrodes for alcoholic subject a102

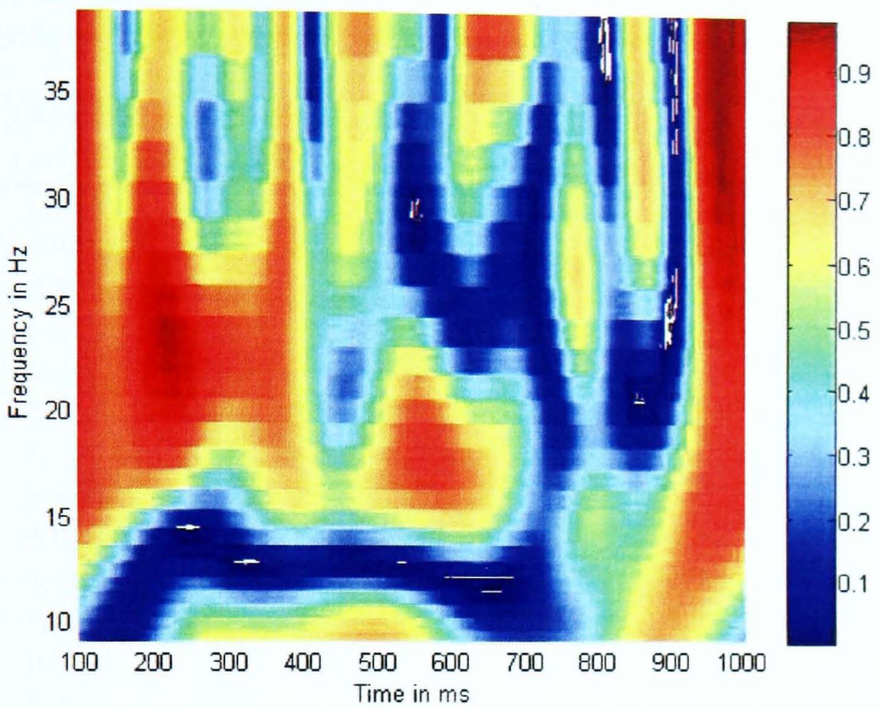

Figure C-15: AWSCc of REEG of alcoholic subject(a402.)

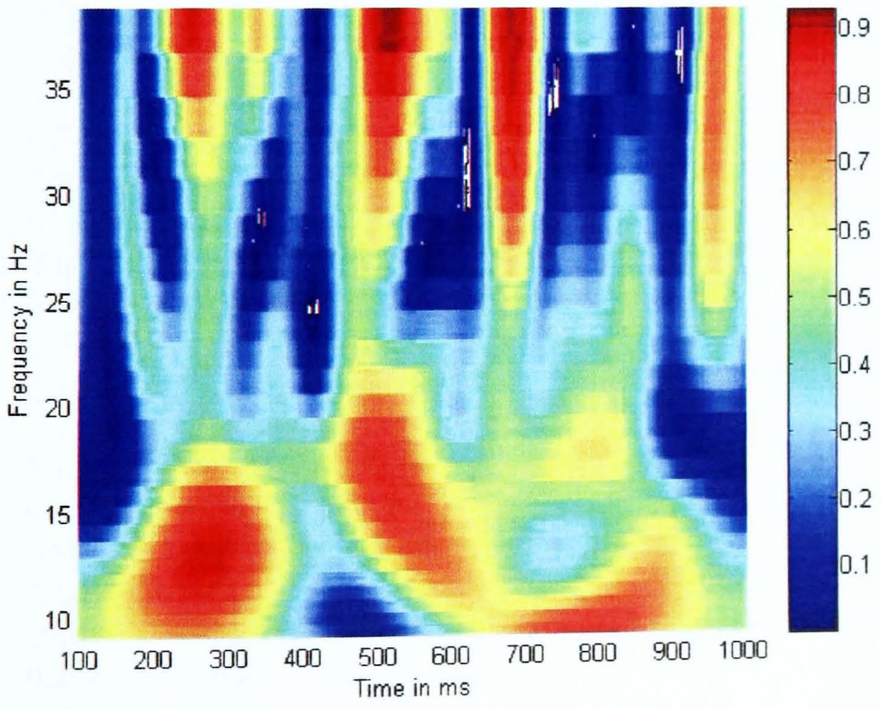

Figure C-16: AWSCc of REEG of abstinent alcoholic subject(c402) which is lower in value, in most of frequencies, than AWSCs of REEG of alcoholic subject (a402)(top figure).

Table 1: *Averaged wavelet squared coherency of REEG is denoted by AWSCE, and averaged wavelet squared coherency of SL is denoted here by AWSCS.*

AWSCS control	AWSCS alcoholic	Electrode pair	Subject name	AWSCE control	AWSCE alcoholic
0.958	0.249	PZ-P1	364	0.127	0.924
0.885	0.109	PZ-P3	364	0.443	0.848
0.947	0.064	PZ-P2	364	0.124	0.972
0.312	0.512	FZ-F4	364	0.481	0.701
0.442	0.761	FZ-AF3	364	0.621	0.991
0.401	0.301	FZ-AF4	364	0.511	0.311
0.311	0.615	AF4-AF3	364	0.261	0.001
0.814	0.215	F4-AF3	364	0.711	0.883
0.816	0.162	F4-AF4	364	0.123	0.436
0.412	0.902	F4-F3	364	0.562	0.733
0.065	0.511	C5-FC6	364	0.732	0.945
0.819	0.425	C5-FC5	364	0.910	0.914
0.332	0.156	C5-P5	364	0.102	0.615
0.215	0.56	C5-P6	364	0.511	0.410
0.528	0.516	P5-FC6	364	0.843	0.134
0.912	0.651	P5-FC5	364	0.415	0.731
0.304	0.442	P5-CP5	364	0.631	0.816
0.431	0.631	P5-P6	364	0.497	0.714
0.801	0.452	P6-FC6	364	0.446	0.441
0.236	0.116	P6-FC5	364	0.788	0.942
0.469	0.316	P6-CP5	364	0.841	0.831
0.313	0.004	PZ-P1	370	0.965	0.913
0.765	0.389	PZ-P3	370	0.878	0.800
0.219	0.032	PZ-P2	370	0.916	0.600
0.912	0.981	FZ-F4	370	0.881	0.812
0.494	0.531	FZ-AF3	370	0.655	0.113
0.712	0.889	FZ-AF4	370	0.625	0.386
0.151	0.531	AF4-AF3	370	0.032	0.519
0.403	0.665	F4-AF3	370	0.281	0.618
0.813	0.806	F4-AF4	370	0.988	0.401
0.115	0.491	F4-F3	370	0.526	0.762
0.211	0.381	C5-FC6	370	0.193	0.436
0.461	0.091	C5-FC5	370	0.557	0.718
0.403	0.612	C5-P5	370	0.302	0.851
0.719	0.771	C5-P6	370	0.114	0.618
0.375	0.392	P5-FC6	370	0.491	0.772
0.375	0.519	P5-FC5	370	0.761	0.619

AWSCS control	AWSCS alcoholic	Electrode pair	Subject name	AWSCE control	AWSCE alcoholic
0.551	0.832	P5-CP5	370	0.806	0.885
0.983	0.441	P5-P6	370	0.428	0.904
0.336	0.826	P6-FC6	370	0.551	0.795
0.714	0.774	P6-FC5	370	0.603	0.439
0.382	0.602	P6-CP5	370	0.182	0.552
0.6887	0.175	PZ-P1	379	0.685	0.849
0.190	0.010	PZ-P2	379	0.719	0.839
0.239	0.156	PZ-P3	379	0.480	0.613
0.304	0.731	FZ-F4	379	0.681	0.953
0.119	0.669	FZ-AF3	379	0.411	0.819
0.516	0.431	FZ-AF4	379	0.631	0.641
0.649	0.364	AF4-AF3	379	0.114	0.387
0.181	0.194	F4-AF3	379	0.671	0.549
0.365	0.228	F4-AF4	379	0.014	0.731
0.508	0.653	F4-F3	379	0.705	0.816
0.228	0.401	C5-FC6	379	0.441	0.495
0.195	0.399	C5-FC5	379	0.301	0.811
0.394	0.751	C5-P5	379	0.557	0.773
0.041	0.917	C5-P6	379	0.961	0.452
0.385	0.301	P5-FC6	379	0.837	0.776
0.957	0.955	P5-FC5	379	0.295	0.714
0.709	0.791	P5-CP5	379	0.559	0.938
0.319	0.628	P5-P6	379	0.724	0.841
0.663	0.841	P6-FC6	379	0.382	0.743
0.487	0.728	P6-FC5	379	0.846	0.206
0.157	0.463	P6-CP5	379	0.731	0.772
0.102	0.164	PZ-P1	381	0.479	0.957
0.1444	0.015	PZ-P2	381	0.315	0.864
0.0032	0.036	PZ-P3	381	0.355	0.700
0.396	0.473	FZ-F4	381	0.109	0.331
0.913	0.744	FZ-AF3	381	0.913	0.713
0.405	0.857	FZ-AF4	381	0.744	0.819
0.538	0.544	AF4-AF3	381	0.331	0.992
0.071	0.341	F4-AF3	381	0.439	0.714
0.254	0.496	F4-AF4	381	0.651	0.415
0.285	0.913	F4-F3	381	0.443	0.743
0.802	0.694	C5-FC6	381	0.536	0.822
0.483	0.457	C5-FC5	381	0.475	0.569
0.031	0.473	C5-P5	381	0.713	0.984
0.515	0.614	C5-P6	381	0.801	0.316

AWSCS control	AWSCS alcoholic	Electrode pair	Subject name	AWSCE control	AWSCE alcoholic
0.655	0.317	P5-FC6	381	0.159	0.205
0.753	0.283	P5-FC5	381	0.416	0.531
0.451	0.432	P5-CP5	381	0.281	0.397
0.157	0.492	P5-P6	381	0.761	0.997
0.717	0.194	P6-FC6	381	0.637	0.969
0.819	0.711	P6-FC5	381	0.445	0.418
0.692	0.927	P6-CP5	381	0.737	0.741
0.533	0.068	PZ-P1	382	0.879	0.943
0.0199	0.0433	PZ-P2	382	0.806	0.948
0.177	0.048	PZ-P3	382	0.492	0.781
0.273	0.374	FZ-F4	382	0.912	0.813
0.701	0.855	FZ-AF3	382	0.447	0.734
0.203	0.847	FZ-AF4	382	0.431	0.921
0.417	0.441	AF4-AF3	382	0.547	0.473
0.170	0.596	F4-AF3	382	0.604	0.971
0.411	0.436	F4-AF4	382	0.831	0.416
0.273	0.319	F4-F3	382	0.312	0.775
0.911	0.512	C5-FC6	382	0.513	0.931
0.302	0.813	C5-FC5	382	0.811	0.611
0.768	0.751	C5-P5	382	0.552	0.895
0.851	0.416	C5-P6	382	0.769	0.263
0.512	0.654	P5-FC6	382	0.813	0.394
0.867	0.793	P5-FC5	382	0.935	0.362
0.657	0.173	P5-CP5	382	0.771	0.778
0.271	0.791	P5-P6	382	0.432	0.972
0.453	0.831	P6-FC6	382	0.332	0.872
0.371	0.233	P6-FC5	382	0.817	0.881
0.907	0.153	P6-CP5	382	0.845	0.973
0.303	0.714	PZ-P1	384	0.038	0.893
0.635	0.031	PZ-P2	384	0.119	0.835
0.042	0.022	PZ-P3	384	0.036	0.917
0.007	0.006	P1-P3	384	0.465	0.568
0.061	0.391	FZ-F4	384	0.414	0.937
0.034	0.164	FZ-AF3	384	0.574	0.994
0.344	0.573	FZ-AF4	384	0.533	0.871
0.871	0.271	AF4-AF3	384	0.213	0.779
0.433	0.694	F4-AF3	384	0.617	0.653
0.215	0.541	F4-AF4	384	0.881	0.582
0.817	0.983	F4-F3	384	0.643	0.683
0.914	0.951	C5-FC6	384	0.795	0.483

AWSCS control	AWSCS alcoholic	Electrode pair	Subject name	AWSCE control	AWSCE alcoholic
0.411	0.613	C5-FC5	384	0.611	0.411
0.172	0.783	C5-P5	384	0.321	0.331
0.413	0.559	C5-P6	384	0.892	0.538
0.664	0.783	P5-FC6	384	0.512	0.379
0.988	0.997	P5-FC5	384	0.227	0.791
0.819	0.534	P5-CP5	384	0.358	0.471
0.339	0.473	P5-P6	384	0.663	0.982
0.458	0.725	P6-FC6	384	0.291	0.773
0.619	0.905	P6-FC5	384	0.496	0.533
0.324	0.872	P6-CP5	384	0.442	0.729
0.162	0.004	PZ-P1	387	0.902	0.936
0.203	0.001	PZ-P2	387	0.913	0.916
0.028	0.016	PZ-P3	387	0.620	0.849
0.167	0.052	P1-P3	387	0.873	0.935
0.342	0.331	FZ-F4	387	0.614	0.729
0.541	0.521	FZ-AF3	387	0.749	0.843
0.331	0.943	FZ-AF4	387	0.538	0.884
0.514	0.719	AF4-AF3	387	0.505	0.652
0.839	0.891	F4-AF3	387	0.411	0.932
0.271	0.721	F4-AF4	387	0.338	0.308
0.704	0.954	F4-F3	387	0.927	0.207
0.991	0.608	C5-FC6	387	0.639	0.651
0.103	0.783	C5-FC5	387	0.324	0.447
0.247	0.559	C5-P5	387	0.391	0.937
0.438	0.613	C5-P6	387	0.663	0.822
0.915	0.818	P5-FC6	387	0.198	0.493
0.764	0.431	P5-FC5	387	0.597	0.431
0.813	0.233	P5-CP5	387	0.826	0.849
0.215	0.348	P5-P6	387	0.176	0.344
0.681	0.922	P6-FC6	387	0.438	0.094
0.517	0.582	P6-FC5	387	0.510	0.577
0.145	0.351	P6-CP5	387	0.243	0.862
0.109	0.117	PZ-P1	392	0.971	0.900
0.095	0.832	PZ-P2	392	0.910	0.389
0.233	0.104	PZ-P3	392	0.922	0.834
0.141	0.509	P1-P3	392	0.965	0.880
0.549	0.042	FZ-F4	392	0.641	0.934
0.951	0.741	FZ-AF3	392	0.763	0.775
0.216	0.669	FZ-AF4	392	0.443	0.947
0.375	0.581	AF4-AF3	392	0.856	0.862

AWSCS control	AWSCS alcoholic	Electrode pair	Subject name	AWSCE control	AWSCE alcoholic
0.711	0.599	F4-AF3	392	0.471	0.996
0.907	0.738	F4-AF4	392	0.592	0.419
0.431	0.253	F4-F3	392	0.477	0.206
0.611	0.647	C5-FC6	392	0.629	0.338
0.599	0.706	C5-FC5	392	0.305	0.561
0.682	0.661	C5-P5	392	0.449	0.734
0.779	0.974	C5-P6	392	0.762	0.801
0.208	0.483	P5-FC6	392	0.814	0.883
0.394	0.611	P5-FC5	392	0.541	0.757
0.553	0.273	P5-CP5	392	0.331	0.529
0.622	0.753	P5-P6	392	0.637	0.722
0.884	0.864	P6-FC6	392	0.546	0.597
0.501	0.739	P6-FC5	392	0.759	0.832
0.528	0.619	P6-CP5	392	0.662	0.863
0.154	0.481	PZ-P1	394	0.861	0.882
0.095	0.116	PZ-P2	394	0.899	0.847
0.001	0.047	PZ-P3	394	0.755	0.664
0 .077	0.068	P1-P3	394	0.967	0.890
0.813	0.715	FZ-F4	394	0.904	0.875
0.811	0.942	FZ-AF3	394	0.894	0.881
0.705	0.406	FZ-AF4	394	0.769	0.973
0.314	0.564	AF4-AF3	394	0.791	0.584
0.012	0.773	F4-AF3	394	0.521	0.218
0.631	0.672	F4-AF4	394	0.236	0.447
0.441	0.547	F4-F3	394	0.94	0.396
0.384	0.487	C5-FC6	394	0.279	0.661
0.302	0.886	C5-FC5	394	0.483	0.374
0.761	0.681	C5-P5	394	0.788	0.799
0.415	0.239	C5-P6	394	0.561	0.764
0.186	0.773	P5-FC6	394	0.367	0.493
0.716	0.629	P5-FC5	394	0.716	0.778
0.549	0.409	P5-CP5	394	0.655	0.718
0.166	0.553	P5-P6	394	0.416	0.537
0.187	0.681	P6-FC6	394	0.261	0.374
0.531	0.422	P6-FC5	394	0.358	0.591
0.237	0.537	P6-CP5	394	0.758	0.796
0.023	0.016	PZ-P1	395	0.805	0.578
0.280	0.172	PZ-P2	395	0.897	0.366
0.053	0.072	PZ-P3	395	0.727	0.708
0.485	0.412	P1-P3	395	0.841	0.497

AWSCS control	AWSCS alcoholic	Electrode pair	Subject name	AWSCE control	AWSCE alcoholic
0.006	0.562	FZ-F4	395	0.418	0.887
0.072	0.481	FZ-AF3	395	0.945	0.749
0.413	0.915	FZ-AF4	395	0.768	0.973
0.138	0.549	AF4-AF3	395	0.576	0.559
0.861	0.771	F4-AF3	395	0.886	0.798
0.425	0.561	F4-AF4	395	0.513	0.596
0.143	0.056	F4-F3	395	0.331	0.371
0.513	0.591	C5-FC6	395	0.502	0.758
0.572	0.776	C5-FC5	395	0.592	0.841
0.447	0.859	C5-P5	395	0.773	0.876
0.718	0.641	C5-P6	395	0.562	0.795
0.581	0.966	P5-FC6	395	0.784	0.379
0.913	0.754	P5-FC5	395	0.091	0.441
0.668	0.687	P5-CP5	395	0.446	0.638
0.183	0.554	P5-P6	395	0.359	0.815
0.458	0.372	P6-FC6	395	0.918	0.396
0.254	0.663	P6-FC5	395	0.403	0.855
0.762	0.349	P6-CP5	395	0.794	0.617
0.523	0.620	PZ-P1	396	0.917	0.422
0.192	0.933	PZ-P2	396	0.846	0.344
0.002	0.240	PZ-P3	396	0.675	0.437
0.132	0.847	P1-P3	396	0.855	0.734
0.435	0.512	FZ-F4	396	0.638	0.523
0.339	0.417	FZ-AF3	396	0.713	0.964
0.614	0.332	FZ-AF4	396	0.527	0.839
0.724	0.692	AF4-AF3	396	0.613	0.792
0.549	0.714	F4-AF3	396	0.894	0.547
0.275	0.481	F4-AF4	396	0.392	0.699
0.316	0.532	F4-F3	396	0.241	0.747
0.792	0.761	C5-FC6	396	0.407	0.809
0.887	0.973	C5-FC5	396	0.751	0.751
0.425	0.629	C5-P5	396	0.645	0.647
0.406	0.938	C5-P6	396	0.591	0.792
0.265	0.539	P5-FC6	396	0.743	0.658
0.619	0.776	P5-FC5	396	0.629	0.415
0.227	0.463	P5-CP5	396	0.948	0.529
0.317	0.375	P5-P6	396	0.741	0.294
0.764	0.844	P6-FC6	396	0.337	0.684
0.194	0.386	P6-FC5	396	0.463	0.744
0.418	0.522	P6-CP5	396	0.645	0.846

AWSCS control	AWSCS alcoholic	Electrode pair	Subject name	AWSCE control	AWSCE alcoholic
0.113	0.018	PZ-P1	402	0.401	0.995
0.025	0.017	PZ-P3	402	0.214	0.850
0.134	0.779	P1-P3	402	0.750	0.870
0.193	0.776	FZ-F4	402	0.482	0.639
0.662	0.832	FZ-AF3	402	0.366	0.219
0.863	0.403	FZ-AF4	402	0.752	0.783
0.324	0.361	AF4-AF3	402	0.546	0.962
0.225	0.219	F4-AF3	402	0.418	0.761
0.346	0.203	F4-AF4	402	0.753	0.817
0.158	0.577	F4-F3	402	0.462	0.659
0.683	0.783	C5-FC6	402	0.614	0.669
0.531	0.624	C5-FC5	402	0.791	0.891
0.725	0.891	C5-P5	402	0.853	0.967
0.716	0.881	C5-P6	402	0.653	0.827
0.158	0.921	P5-FC6	402	0.397	0.603
0.359	0.726	P5-FC5	402	0.586	0.799
0.749	0.914	P5-CP5	402	0.795	0.975
0.853	0.892	P5-P6	402	0.963	0.762
0.488	0.736	P6-FC6	402	0.631	0.688
0.365	0.451	P6-FC5	402	0.581	0.973
0.638	0.638	P6-CP5	402	0.686	0.513

MATLAB Codes

The MATLAB[1] computing language has been used for our study because it is a computer language, which is especially designed for the high-performance numerical computation and visualization and as compared to other computational languages, it provides a large number of functions for math computations, data analysis and processing, visualization and graphics and signal processing. Therefore it is comparatively easy to use and learn for our proposed method, which requires various mathematical and signal processing tools. Another reason of choosing the MATLAB is that the large number of software packages exist in MATLAB for computing and analyzing the signal processing tools which are also used in our study.

We have developed some easy to use MATLAB codes for the computation of

[1]The name MATLAB stands for matrix laboratory.

the wavelet-based, STFT-based and the Fourier-based coherencies of scalp current densities and the EEG signal. These MATLAB codes are basically written as script file, once the script file runs, it automatically asks for the inputs required for the computation of outputs. The detail of the inputs have been explained in the following section. The inputs are denoted by bold and the italic letters.

Assume, ***xp*** and ***yp*** as two time series corresponding to two electrodes x and y respectively, which are placed on the head of subject. The number of epochs recorded in each electrode is denoted by ***noep*** . Each electrode records the same type of trials for several times, the number of these repeated trials for each subject is different and is denoted by ***dim.*** The time series of four nearest electrodes to x are represented by ***n1SL1, n2SL1, n3SL1*** and ***n4SL1.*** Similarly, the time series of four nearest electrodes to y are represented by the ***n1SL2, n2SL2, n3SL2*** and ***n4SL2.*** For the estimation of STFT-based and Fourier-based coherencies, the Hanning window was used whose length is denoted by the ***length-window***. The number of overlapping epochs and FFT points used during the STFT and Furier transform are denoted by ***noverlap*** and ***nfft*** respectively. The more detailed description is given within the codes. The following are the MATLAB codes.

Bibliography

ABASOLO, D., HORNERO, R., ESPINO, P., ALVAREZ, D. and POZA, J., 2006. Entropy analysis of the EEG background activity in Alzheimer's disease patients. *Physiological Measurement,* **27**(3), pp. 241-53.

ACKERMANN, P.T., DYKMAN, R.A., OGLESBY, D.M. and NEWTON, J.E., 1995. EEG power spectra of dysphonetic and nondysphonetic poor readers. *Brain Language,* **49**, pp. 140-152.

ADLER, G., BRASSEN, S. and JAJCEVIC, A., 2003. EEG coherence in Alzheimer's dementia. *Journal of neural transmission,* **110**, pp. 1051-1058.

AKAY, M., AKAY, Y.M., CHENG, P. and SZETO, H.H., 1994. Time-frequency analysis of the electrocortical activity during maturation using wavelet transform. *Biological cybernetics,* **71**(2), pp. 169-76.

AKIN, M., 2002. Comparison of wavelet transform and FFT methods in the analysis of EEG signals. *Journal of medical systems,* **26**(3), pp. 241-7.

ALARCON, G., GUY, C.N., BINNIE, C.D., WALKER, S.R., ELWES, R.D. and POLKEY, C.E., 1994. Intercerebral propagation of interictal activity in partial epilepsy: implications for source localisation. *J Neurol Neurosurg Psychiatry,* **57**, pp. 435-449.

AMIR, N. and GATH, I., 1989. Segmentation of EEG during sleep using time-varying autoregressive modeling. *Biological cybernetics,* **61**(6), pp. 447-55.

ANDERSON, C.W. and SIJERCIC, Z., 1996. Classification of EEG signals from four subjects during five mental tasks, *Solving Engineering Problems with Neural Networks. Proceedings of the International Conference on Engineering Applications of Neural Networks, 17-19 June 1996,* / 1996, Syst. Eng. Assoc pp407-14.

ANDREW, C. and PFURTSCHELLER, G., 1996. Coherence analysis of movement-related EEG, *Proceedings of the Third International Hans Berger Congress,* 1996, .

ANDREW, C.N.C., RAPPELSBERGER, P. and FILZ , O., 1998. Topology of EEG Coherence Changes May reflect differential Neural Network Activation in Cold and Pain Perception *Brain Topography,* **11**, pp. 125-135.

ASANO, E., MUZIK, O., SHAH, A., JUHASZ, C., CHUGANI, D.C., KAGAWA, K., BENEDEK, K., SOOD, S., GOTMAN, J. and CHUGANI, H.T., 2004. Quantitative

visualization of ictal subdural EEG changes in children with neocortical focal seizures. *Clinical Neurophysiology,* **115**(12), pp. 2718-2727.

BABILONI, F., BABILONI, C., FATTORINI, L., CARDUCCI, F., ONORATI, P. and URBANO, A., 1995. Performances of surface Laplacian estimators: A study of simulated and real scalp potential distributions. *Brain Topography,* **8**(1), pp. 35-45.

BABILONI, F., BABILONI, C., LOCCHE, L., CINCOTTI, F., ROSSINI, P.M. and CARDUCCI, F., 2000. High-resolution electro-encephalogram: source estimates of Laplacian-transformed
somatosensory-evoked potentials using a realistic subject head model constructed from magnetic resonance images. *Med Biol Eng Comput.,* **38**(5), pp. 512-519.

BABILONI, F., BABILONI, C., CARDUCCI, F., FATTORINI, L., ONORATI, P. and URBANO, A., 1996. Spline Laplacian estimate of EEG potentials over a realistic magnetic resonance-constructed scalp surface model. *Electroencephalography and Clinical Neurophysiology,* **98**(4), pp. 363-373.

BAHCIVAN, H., NING ZHANG, MIRSKI, M.A. and SHERMAN, D., 2001. Cross-correlation analysis of epileptiform propagation using wavelets, *2001 Conference Proceedings of the 23rd Annual International Conference of the IEEE Engineering n Medicine and Biology Society, 25-28 Oct. 2001,* / 2001, IEEE pp1804-7.

BALIAN, E.S., 1988. How to design analyze, and write doctoral or master's research. 2nd edition edn. London, Enland: University press of America.

BALTAS, E., BENTLEY, D., JONES, A., REOULLAS, A., STERGIOULAS, L.K., XYDEAS, C.S. and YOUELL, P., 2002. An LVQ classifier of EEG coherence patterns for pain detection, *Proceedings of Third International Symposium on Communication Systems Networks and Digital Signal Processing, 15-17 July 2002,* / 2002, Sheffield Hallam Univ. Press Learning Centre pp248-51.

BARLOW, J.S., 1959a. Autocorrelation and correlation analysis in electroencephalography. *IRE. Trans. Med. Electron,* **ME-6**, pp. 179-183.

BARLOW, J.S., 1967. Correlation analysis of EEG-tremor relationships in man. *Electroencephalography and Clinical Neurophysiology,* **25**, pp. 167-177.

BARLOW, J.S. and FREEMAN, M.Z., 1959b. Comparison of EEG activity recorded from homologous locations on the scalp by means of autocorrelation and crosscorrelation analysis. *Res. Lab. of Electronics, Quart. Prog. Rep.*, **54**, pp. 173-181.

BENDAT, J.S. and PIERSOL, A.G., 2001. Random data analysis and measurement procedures. 3rd edn. New York: Wiley.

BENDER, R., SCHULTZ, B., SCHULTZ, A. and PICHLMAYR, I., 1992. Testing the Gaussianity of the human EEG during anesthesia. *Methods of information in medicine,* **31**(1), pp. 56-9.

BIGAN, C. and WOOLFSON, M.S., 2000. Time-frequency analysis of short segments of biomedical data, *First International Conference on Advances in Medical Signal and Information Processing, 4-6 Sept. 2000,* / 2000, IEE pp150-7.

BIGGINS, C.A., EZEKIEL, F. and FEIN , G., 1992. Spline computation of scalp current density and coherence: a reply to Perrin. *Electroencephalography and Clinical Neurophysiology.*, **83**(2), pp. 172-174.

BIGGINS, C.A. and FEIN, G., 1993. Spline computation of scalp current density and coherence: a reply to Pascual-Marqui. *Electroencephalography and Clinical Neurophysiology,* **87**(1), pp. 65-66.

BIGGINS, C.A., FEIN, G., RAZ, J. and AMIR, A., 1991. Artifactually high coherences result from using spherical spline computation of scalp current density. *Electroencephalography and Clinical Neurophysiology,* **79**(5), pp. 413-419.

BLACKMAN, R.B. and TUKEY, W., 1959. The measurement of power spectrum from the point of view of comunications engineering. New York: Dover Publications.

BLANCO, S., D'ATTELLIS, C.E., ISAACSON, S.I., ROSSO, O.A. and SIRNE, R.O., 1996. Time-frequency analysis of electroencephalogram series. II. Gabor and wavelet transforms. *Physical Review E (Statistical Physics, Plasmas, Fluids, and Related Interdisciplinary Topics),* **54**(6), pp. 6661-72.

BOASHASH, B. and KEIR, M., 1999. Design of a DSP system for automatic detection of seizure signals in newborns, *Proceedings of Fifth International Symposium on Signal Processing and its Applications, 22-25 Aug. 1999,* / 1999, Queensland Univ. Technol pp351-4.

BOASHASH, B. and MESBAH, M., 2001. A time-frequency approach for newborn seizure detection. *IEEE Engineering in Medicine and Biology Magazine,* **20**(5), pp. 54-64.

BODENSTEIN, G. and PRAETORIUS, H.M., 1977. Feature extraction from the electroencephalogram by adaptive segmentation. *Proceedings of the IEEE,* **65**(5), pp. 642-52.

BODENSTEIN, G. and PRAETORIUS, H.M., 1977. Feature extraction from the electroencephalogram by adaptive segmentation. *Proceedings of the IEEE,* **65**(5), pp. 642-52.

BRAZIER, M.A.B., 1972. Spread of seizure discharges in epilepsy: anatomical and electrophysiological consideration. **36**, pp. 263.

BRAZIER, M.A.B. and CASBY, J.U., 1952. Crosscorrelation and autocorrelation studies of electroencephalographic potentials. *Electroencephalography and Clinical Neurophysiology,* **4**(2), pp. 201-211.

BRAZIER, M.A.B. and BARLOW, J.S., 1956. Some applications of correlation analysis to clinical problems in electroencephalography, *Electroencephalography and Clinical Neurophysiology,* **8**(2), pp. 325-331.

BRUNS, A., 2004. Fourier-, Hilbert- and wavelet-based signal analysis: are they really different approaches? *Journal of Neuroscience Methods,* **137**(2), pp. 321-332.

BYRING, R.F., SALMI, T.K., SAINIO, K.O. and ORN, H.P., 1991. EEG in children with spelling disabilities. *Electroencephalography and Clinical Neurophysiology,* **79**, pp. 247-255.

CALLAWAY, E., HALLIDAY, R. and NAYLOR, H., 1983. Hyperactive children's event-related potentials fail to support underarousal and maturational-lag theories. *Arch Gen Psychiatry,* **40**, pp. 1243-1248.

CARTER, G., KNAPP, C. and NUTTALL, A., 1973. Estimation of the magnitude-squared coherence function via overlapped fast Fourier transform processing. *Audio and Electroacoustics, IEEE Transactions on,* **21**(4), pp. 337-344.

CELKA, P. and COLDITZ, P., 2002. Nonlinear nonstationary Wiener model of infant EEG seizures. *IEEE Transactions on Biomedical Engineering,* **49**(6), pp. 556-64.

CHABOT, R.J. and SERFONTEIN, G., 1996. Quantitative electroencephalographic profiles of children with attention deficit disorder. *Biological Psychiatry,* **40**(10), pp. 951-963.

CHALLIS, R.E. and KITNEY, R.I., 1991. Biomedical Signal Processing. part 3.The Power Spectrum and Coherence Function. *Med. Biol.Eng. Comput,* **29**, pp. 225-241.

CHAN, H.L., LIN, M.A. and FANG, S.C., 2004. Linear and nonlinear analysis of electroencephalogram of the coma, *Conference Proceedings - 26th Annual International Conference of the IEEE Engineering in Medicine and Biology Society, EMBC 2004, Sep 1-5 2004,* 2004, Institute of Electrical and Electronics Engineers Inc., Piscataway, NJ 08855-1331, United States pp593-595.

CHILLE, S., BALOCCHI, R., DI GARBO, A., D'ATTELLIS, C.E., GIGOLA, S., KOCHEN, S. and SILVA, W., 2003. Discriminating preictal from interictal states by using coherence measures, *Proceedings of the 25th Annual International Conference of the IEEE Engineering in Medicine and Biology Society, 17-21 Sept. 2003,* / 2003, IEEE pp2319-22.

CHUI, C., 1992. An introduction to wavelets. San Diego: Academic Press.

CIESIELSKI, K.T., WALDORF, A.V. and JUNG, R.E., 1995. Anterior brain dificits in chronic alcoholism. Cause or effect ? *J Nerv Ment Dis,* **183**, pp. 756-761.

CLAASSEN, J., HIRSCH, L.J., KREITER, K.T., DU, E.Y., CONNOLLY, E.S., EMERSON, R.G. and MAYER, S.A., 2004. Quantitative continuous EEG for detecting delayed cerebral ischemia in patients with poor-grade subarachnoid hemorrhage. *Clinical Neurophysiology,* **115**(12), pp. 2699-710.

CLARKE, A., BARRY, R., MCCARTHY, R. and SELIKOWITZ, M., 2002. EEG analysis of children with attention-deficit/hyperactivity disorder and comorbid reading disabilities. *J Learn Disabil,* **35**, pp. 276-285.

CLARKE, A.R., BARRY, R.J., MCCARTHY, R. and SELIKOWITZ, M., 2001. Age and sex effects in the EEG: differences in two subtypes of attention-deficit/hyperactivity disorder. *Clinical Neurophysiology,* **112**(5), pp. 815-26.

CLARKE, A.R., BARRY, R.J., MCCARTHY, R. and SELIKOWITZ, M., 1998. EEG analysis in Attention-Deficit/Hyperactivity Disorder: a comparative study of two subtypes. *Psychiatry Research,* **81**(1), pp. 19-29.

COBEN, L.A., DANZIGER, W. and STORANDT , M., 1985. A longitudinal EEG study of mild senile dementia of Alzheimer type: changes at 1 year and at 2.5 years. *Electroencephalography and Clinical Neurophysiology,* **61**(2), pp. 101-112.

COHEN, A., 1986. Biomedical signal processing: compression and automatic recognition. Florida.: CRC Press.

COHEN, L., 1995. Time-frequency analysis. New Jersey: Prentice-Hall.

COHN, R. and LEADER, H.S., 1967. Synchronization characteristics of paroxysmal EEG activity. *Electroencephalography and Clinical Neurophysiology,* **22**(5), pp. 421-428.

COOLEY, J.W. and TUKEY, J.W., 1965. An algorithm for the machine calculation of complex Fourier series. *Mathematics of Computation,* **19**, pp. 297-301.

COOPER, R., 1974. Direct computer processing. In: M.A.B. BRAZIER and LOPES DA SILVA, F., eds, *Hand book of electroencephalography and clinical neurophysiology.* Amsterdam: Elsevier, pp. 42-58.

COPER, R., WINTER, A.L., CROW, H.J. and WALTER, W.J., 1965. Comparison of subcortical, cortical and scalp activity using chronically indwelling electrodes in man. *Electroencephalography and clinical Neurophysiology.,* **18**, pp. 217-228.

CORSINI, J., SHOKER, L., SANEI, S. and ALARCON, G., 2006. Epileptic seizure predictablity from scalp EEG incorporating constrained blind source operation. *IEEE transactions on biomedical engineering.,* **53**(5),.

COSTA, L. and BAUER, L., 1997. Quantitative electroencephalographic differences associated with alcohol, cocaine, heroin and dual-substance dependence. *Drug and Alcohol Dependence,* **46**(1-2), pp. 87-93.

CURRAN, E., SYKACEK, P., STOKES, M., ROBERTS, S.J., PENNY, W., JOHNSRUDE, I. and OWEN, A.M., 2004. Cognitive tasks for driving a brain-computer interfacing system: a pilot study. *IEEE Transactions on Neural Systems and Rehabilitation Engineering,* **12**(1), pp. 48-54.

CZINEGE, L., 1997. Autoregressive coefficient changes of EEG signal model. *Information Technology Applications in Biomedicine. ITAB '97. Proceedings of the IEEE*

Engineering in Medicine and Biology Society Region 8 International Conference, 7-9 Sept. 1997, / 1997, IEEE pp60-1.

CZINEGE, L., URBANICS, R. and FARKAS, Z., 1997. Multi-channel activity correlation analysis-a method to detect ischemic changes of the EEG, *Proceedings of 17th International Conference of the Engineering in Medicine and Biology Society, 20-23 Sept. 1995,* / 1997, IEEE pp735-6.

CZINEGE, L. and BLOOM, M.J., 1997. Wavelet-based spectral analysis of the electroencephalogram under brain ischemia. *Annual International Conference of the IEEE Engineering in Medicine and Biology - Proceedings,* **3**, pp. 1293-1296.

D'ANGIULLI, A., GRUNAU, P., MAGGI, S. and HERDMAN, A., Electroencephalographic correlates of prenatal exposure to alcohol in infants and children: a review of findings and implications for neurocognitive development. *Alcohol,* **In Press, Corrected Proof.**

DANIEL, R.S., 1966. Electroencephalographic pattern quantification and the arousal continuum. *Psychophysiology,* **1**, pp. 337.

DE BRUIN, E.A., BIJL, S., STAM, C.J., BÖCKER, K.B.E., LEON KENEMANS, J. and VERBATEN, M.N., 2004. Abnormal EEG synchronisation in heavily drinking students. *Clinical Neurophysiology,* **115**(9), pp. 2048-2055.

DE BRUIN, E.A., STAM, C.J., BIJL, S., VERBATEN, M.N. and KENEMANS, J.L., 2006/6. Moderate-to-heavy alcohol intake is associated with differences in synchronization of brain activity during rest and mental rehearsal. *International Journal of Psychophysiology,* **60**(3), pp. 304-314.

DEMIRALP, T., ISTEFANOPULOS, Y., ADEMOGLU, A., YORDANOVA, J. and KOLEV, V., 1998. Analysis of functional components of P300 by wavelet transform, *Proceedings of the 1998 20th Annual International Conference of the IEEE Engineering in Medicine and Biology Society. Part 4 (of 6), Oct 29-Nov 1 1998,* 1998, IEEE, Piscataway, NJ, USA pp1992-1995.

DIAMBRA, L. and MALTA, C.P., 1999. Nonlinear models for detecting epileptic spikes. *Physical Review E (Statistical Physics, Plasmas, Fluids, and Related Interdisciplinary Topics),* **59**(1, pt.A-B), pp. 929-37.

DIGGLE, P., 1990. Time Series: A A Biostatistical Introduction. Oxford: Clarendon Press,.

EICHLER, M., DAHLHAUS, R. and SANDKUHLER, J., 2003. Partial correlation analysis for the identification of synaptic connections. *Biological cybernetics,* **89**(4), pp. 289-302.

EISELT, M., SCHENDEL, M., WITTE, H., DORSCHEL, J., CURZI-DASCALOVA, L., D'ALLEST, A.M. and ZWIENER, U., 1997. Quantitative analysis of discontinuous EEG in premature and full-term newborns during quiet sleep. *Electroencephalography and clinical neurophysiology,* **103**(5), pp. 528-34.

ELLIS, R.J. and OSCAR_BERMAN, M., 1989. Alcoholism, aging, and functional cerebral asymmetries. *Psychological Bulletin.,* **106**(1), pp. 128-147.

FATOURECHI, M., MASON, S.G., BIRCH, G.E. and WARD, R.K., 2004. A wavelet-based approach for the extraction of event related potentials from EEG, *2004 IEEE International Conference on Acoustics, Speech, and Signal Processing, 17-21 May 2004,* / 2004, IEEE pp737-40.

FEIN, G., RAZ, J., BROWN, F.F. and MERRIN, E.L., 1988. Common reference coherence data are confounded by power and phase effects . *Electroencephalography and Clinical Neurophysiology,* **69**, pp. 581-584.

FENG, Z. and ZHENG, X., 2002. Changes in complexities and power spectrum of rat electroencephalogram under various anesthesia depth, *Proceedings of the 2002 IEEE Engineering in Medicine and Biology 24th Annual Conference and the 2002 Fall Meeting of the Biomedical Engineering Society (BMES / EMBS), Oct 23-26 2002,* 2002, Institute of Electrical and Electronics Engineers Inc pp145-146.

FERRI, R., BRUNI, O., MIANO, S., PLAZZI, G. and TERZANO, M.G., 2005. All-night EEG power spectral analysis of the cyclic alternating pattern components in young adult subjects. *Clinical Neurophysiology,* **116**(10), pp. 2429-40.

FERRI, R., CHIARAMONTI, R., ELIA, M., MUSUMECI, S.A., RAGAZZONI, A. and STAM, C.J., 2003. Nonlinear EEG analysis during sleep in premature and full-term newborns. *Clinical Neurophysiology,* **114**(7), pp. 1176-80.

FERRI, R., ELIA, M., MUSUMECI, S.A. and PETTINATO, S., 2000. The time course of high-frequency bands (15-45 Hz) in all-night spectral analysis of sleep EEG. *Clinical Neurophysiology,* **111**(7), pp. 1258-65.

FERRI, R., PETTINATO, S., ALICATA, F., DEL GRACCO, S., ELIA, M. and MUSUMECI, A., 1998. Correlation dimension of EEG slow-wave activity during sleep in children and young adults. *Electroencephalography and clinical neurophysiology,* **106**(5), pp. 424-8.

FILIPOVIC, S.R., COVICKOVIC-STERNIC, N., STOJANOVIC-SVETEL, M., LECIC, D. and KOSTIC, V.S., 1998/12. Depression in Parkinson's disease: an EEG frequency analysis study. *Parkinsonism & Related Disorders,* **4**(4), pp. 171-178.

FINK, M., 1974. Cerebral electrometry-quantitative EEG applied to human psychopharmacology. In: G. DOLCE and H. KIINKEL, eds, *CEAN-Computerized EEG Analysis.* Stuttgart Germany: Gustav Fwcher Verlag, pp. 2711-288.

FLETCHER, E.M., KUSSMAUL, C.L. and MANGUN, G.R., 1996/5. Estimation of interpolation errors in scalp topographic mapping. *Electroencephalography and Clinical Neurophysiology,* **98**(5), pp. 422-434.

FRANASZCZUK, P.J., BERGEY, G.K. and KAMINISKI, M.J., 1994. Analysis of mesial temporal seizure onset and propagation using the directed transfer function method. *Electroencephalography and clinical neurophysiology,* **91**(6), pp. 413-27.

FRENCH, C.C. and BEAUMONT, J.G., 1984. A critical review of EEG coherence studies of hemisphereic function. *International journal of Psychophysiology,* **1**, pp. 241-254.

GARDNER, W.A., 1992. A unifying view of coherence in signal processing. *Signal Processing,* , pp. 113-140.

GATH, I. and BAR-ON, E., 1980. Computerized method for scoring of polygraphic sleep recordings. *Computer programs in biomedicine,* **11**(3), pp. 217-23.

GATH, I., FEUERSTEIN, C., PHAM, D.T. and RONDOUIN, G., 1992. On the tracking of rapid dynamic changes in seizure EEG. *IEEE Transactions on Biomedical Engineering,* **39**(9), pp. 952-8.

GATH, I., MICHAELI, A. and FEUERSTEIN, C., 1991. A model for dua' channel segmentation of the EEG signal. *Biological cybernetics,* **64**(3), pp. 225-30.

GERSCH, W., 1987. Non stationary multiichannel time series analysis. In: A.S. GEVINS and A. REMOND, eds, *Handbook of electroencephalography and clinical neurophysiology.* Amsterdam: Elsevier, pp. 261-296.

GERSCH, W., 1988. Linear dependency structure of covariance nonstationary time series, *IEEE 1988 International Symposium on Information Theory - Abstracts of papers, Jun 19-24 1988,* 1988, Publ by IEEE, New York, NY, USA pp237.

GEVINS, A.S., 1987a. Introduction. In: A. GEVINS and A. REMOND, eds, *Handbook of electroencephalography and clinicalneurophysiology.* Amsterdam: Elsevier, pp. 1-14.

GEVINS, A.S., 1987b. Correlation analysis. In: A.S. GEVINS and A. REMOND, eds, *Handbook of electroencephalography and clinical neurophysiology.* Amsterdam: Elsevier, pp. 171-193.

GEVINS, A.S., 1987c. Overview of computer analysis. In: A. GEVINS and A. REMOND, eds, *Methods of Analysis of Brain Electrical and Magnetic Signals: Handbook of Electroencephalography and Clinical Neurophysiology.* Amsterdam: Elsevier, pp. 31-83.

GEVINS, A.S., 1989. Dynamic functional topography of cognitive tasks. *Brain Topography,* **2**(1-2), pp. 37-56.

GEVINS, A.S., 1996. High resolution evoked potentials of cognition. *Brain Topography,* **8**(3), pp. 189-199.

GEVINS, A.S., BRICKETT, P., COSTALES, B., LE, J. and AND REUTTER, B., 1990. Beyond topographic mapping: towards functional anatomicalimaging with 124 channel EEGs and 3-D MRIs. *Brain Topography,* **3**, pp. 53-64.

GEVINS, A.S., LE, J., BRICKETT, P., REUTTER, B. and DESMOND, J., 1991. Seeing through the skull: advanced EEGs use MIRs to accurately measure cortical activity from the scalp. *Brain Topography,* **4**(2), pp. 125-131.

GEVINS, A., JIAN LE, MARTIN, N.K., BRICKETT, P., DESMOND, J. and REUTTER, B., 1994. High resolution EEG: 124-channel recording, spatial deblurring

and MRI integration methods. *Electroencephalography and clinical neurophysiology,* **90**(5), pp. 337-58.

GEVINS, A., LEONG, H., SMITH, M.E., LE, J. and DU, R., 1995/10. Mapping cognitive brain function with modern high-resolution electroencephalography. *Trends in Neurosciences,* **18**(10), pp. 429-436.

GIANOTTI, L.R.R., KUNIG, G., LEHMANN, D., FABER, P.L., PASCUAL-MARQUI, R.D., KOCHI, K. and SCHREITER-GASSER, U., 2007/1. Correlation between disease severity and brain electric LORETA tomography in Alzheimer's disease. *Clinical Neurophysiology,* **118**(1), pp. 186-196.

GISH, H. and COCHRAN, D., 1988. Generalized coherence. *International conference on acoustics, Speech, and Signal Processing.,* **5**, pp. 2745-2748.

GOTMAN, J., 1987. Interhemispheric interactions in seizures of focal onset: data from human intracranial recordings. *Electroencephalography and Clinical Neurophysiology,* **67**, pp. 120-123.

GOTMAN, J., 1982. Automatic recognition of epileptic seizures in the EEG. *Electroencephalography and clinical neurophysiology,* **54**(5), pp. 530-40.

GOTMAN, J., 1983. Measurement of small time differences between EEG channels: method and application to epileptic seizure propagation. *Electroencephalography and clinical neurophysiology,* **56**(5), pp. 501-14.

GOTMAN, J., ZHANG, J., ROSENBLATT, B. and GOTTESMAN, R., 1995. Automatic seizure detection in newborns and infants, *Proceedings of the 1995 IEEE Engineering in Medicine and Biology 17th Annual Conference and 21st Canadian Medical and Biological Engineering Conference, Sep 20-23 1995,* 1995, pp913-914.

GRAY, C.M. and SINGER, W., 1989. Stimulus-specific neuronal oscillations in orientation columns of cat visual cortex. *Proc Natl Acad Sci USA,* **86**, pp. 1698-1702.

GREWAL, M., NING, T. and BRONZINO, J.D., 1988. Coherence analysis of EEG via multichannel AR modeling, *Proceedings of the Fourteenth Annual Northeast Bioengineering Conference (IEEE Cat. No.88-CH2666-6), 10-11 March 1988,* / 1988, IEEE pp245-8.

GRINDEL, O.M., 1968. The significance of correlation analysis for evaluation of the EEG in man. In: M.N. LIVANOV and V.S. RUSINOV, eds, *Mathematical analysis of the electrical activity of the brain.* Cambridge: Harvard University Press., pp. 10-23.

GRINDEL, O.M., BOLDYREVA, G.N., BURASHNIKOV, E.N. and ANDREEVSKII, V.M., 1965. On the possibility of application of correlation analysis of the human electroencephalogram. *Fed. Proc. Transl,* **24**, pp. 753-757.

HADJIYANNAKIS, K., OGILVIE, R.D., ALLOWAY, C.E.D. and SHAPIRO, C., 1997. FFT analysis of EEG during stage 2-to-REM transitions in narcoleptic patients and normal sleepers. *Electroencephalography and clinical neurophysiology,* **103**(5), pp. 543-53.

HAO, L., GHODADRA, R. and THAKOR, N.V., 1997. Quantification of brain injury by EEG cepstral distance during transient global ischemia, *Proceedings of the 19th Annual International Conference of the IEEE Engineering in Medicine and Biology Society. `Magnificent Milestones and Emerging Opportunities in Medical Engineering', 30 Oct.-2 Nov. 1997,* / 1997, IEEE pp1205-6.

HARMONY, T., HINOJOSA, G., MAROSI, E., BECKER, J., RODRIGUEZ, M., REYES, A. and ROCHA, C., 1990. Correlation between EEG spectral parameters and an educational evaluation. *The International Journal of Neuroscience,* **54**, pp. 147-155.

HASSANPOUR, H., MESBAH, M. and BOASHASH, B., 2004. Time–frequency based newborn EEG seizure detection using low and high frequency signatures. *Physiological Measurement,* **25**, pp. 935-944.

HENDERSON, G., IFEACHOR, E., HUDSON, N., GOH, C., OUTRAM, N., WIMALARATNA, S., DEL PERCIO, C. and VECCHIO, F., 2006. Development and assessment of methods for detecting dementia using the human electroencephalogram. *IEEE Transactions on Biomedical Engineering,* **53**(8), pp. 1557-68.

HJORTH, B., 1975. An on-online transformation of EEG scalp potential into orthogonal source derivation. *Electroencephalography and Clinical Neurophysiology,* **39**, pp. 526-530.

HJORTH, B. and RODIN, E., 1988. Extraction of Deep components from scalp EEG. *Brain Topography,* **1**(1), pp. 65-69.

HORNERO, R., ESPINO, P., ALONSO, A. and LOPEZ, M., 1999. Estimating complexity from EEG background activity of epileptic patients. *IEEE Engineering in Medicine and Biology Magazine,* **18**(6), pp. 73-9.

HOSSMANN, K.A., HEISS, W.D., BEWERMEYER, H. and MIES, M., 1980. EEG frequency analysis in the course of acute ischemic stroke. *Neurosurgical Review,* **3**, pp. 31-36.

IMAHORI, K. and SUHARA, K., 1949. On the statistical method in the brain-wave study. *Folia Psychiatr Neurol Jap,* **3**, pp. 137-155.

INGBER, L., 1997. Statistical mechanics of neocortical interactions: Canonical momenta indicators of electroencephalography. *Physical Review E.,* **55**(4), pp. 4578-4593.

ISAKSSON, A., WENNBERG, A. and ZETTERBERG, L.H., 1981. Computer analysis of EEG signals with parametric models. *Proceedings of the IEEE,* **69**(4), pp. 451-61.

JACQUES, G., FRYMIARE, J.L., KOUNIOS, J., CLARK, C. and POLIKAR, R., 2004. Multiresolution analysis for early diagnosis of Alzheimer's disease, *Conference Proceedings. 26th Annual International Conference of the IEEE Engineering in Medicine and Biology Society, 1-5 Sept. 2004,* / 2004, IEEE pp251-4.

JANSEN, B.H., HASMAN, A., LENTON, R. and VISSER, S.L., 1979. A study of inter and intra individual variability of the EEG of 16 normal subjects by means of segmentation. In: H. LECHNER and A. ARANIBAR, eds, *Electroencephalography and clinical neurophysiology, experts medica.* Amsterdam: .

JANSEN, B.H., HASMAN, A. and LENTEN, R., 1981. Piecewise analysis of EEGs using AR-modeling and clustering. *Computers and Biomedical Research,* **14**(2), pp. 168-78.

JASTROW, J., 1900. Fact and fable in Psychology. England: Oxford.

JEFFREY, A., 2004. Mathematics for engineers and scientists. 6 edn. Chapman and Hall.

JELIC, V., JULIN, P., SHIGETA, M., NORDBERG, A., LANNFELT, L., WINBLAD, B. and WAHLUND, L.O., 1997. Apolipoprotein E 14 allele decreases functional connectivity in Alzheimer's disease as measured by EEG coherence. *Journal of neurology, neurosurgery and Psychiatry,* **63**, pp. 59-65.

JENSEN, E.W., LINDHOLM, P. and HENNEBERG, S.W., 1996. Autoregressive modeling with exogenous input of middle-latency auditory-evoked potentials to measure rapid changes in depth of anesthesia. *Methods of information in medicine,* **35**(3), pp. 256-60.

JIAN LE, MENON, V. and GEVINS, A., 1994. Local estimate of surface Laplacian derivation on a realistically shaped scalp surface and its performance on noisy data. *Electroencephalography and Clinical Neurophysiology, Evoked Potentials,* **92**(5), pp. 433-41.

JIAN-ZHONG XUE, HUI ZHANG, CHONG-XUN ZHENG and XIANG-GUO YAN, 2003. Wavelet packet transform for feature extraction of EEG during mental tasks, *Proceedings of the 2003 International Conference on Machine Learning and Cybernetics, 2-5 Nov. 2003,* / 2003, IEEE pp360-3.

JOHN, E.R., AHN, H., PRICHEP, L., TREPETIN, M., BROWN, D. and KAYE, H., 1980. Developmental equations for the electroencephalogram. *Science,* **210**, pp. 1255-1258.

JOUNY, C.C., FRANASZCZUK, P.J. and BERGEY, G.K., 2005. Signal complexity and synchrony of epileptic seizures: is there an identifiable preictal period? *Clinical Neurophysiology,* **116**(3), pp. 552-8.

KATZNELSON, R.D., 1981. Normal modes of the brain: neuroanatomical basis and a physiological theoretical model. In: P.L. NUNEZ, ed, *Electric Fields of the Brain: The Neurophysics of EEG.* New York: Oxford, .

KAVITHA, V., DUTT, N.D. and PRADHAN, N., 1995. Nonlinear prediction of chaotic electrical activity of the brain, *Proceedings of the 1st 1995 Regional Conference IEEE Engineering in Medicine and Biology Society and 14th Conference of the Biomedical Engineering Society of India, Feb 15-18 1995,* 1995, IEEE pp3-39.

KAY, S.M. and MARPLE, S.L.,JR, 1981. Spectrum analysis-a modern perspective. *Proceedings of the IEEE,* **69**(11), pp. 1380-1419.

KAYSER, J. and TENKE, C.E., 2006. Principal components analysis of Laplacian waveforms as a generic method for identifying ERP generator patterns: II. Adequacy of low-density estimates. *Clinical Neurophysiology,* **117**(2), pp. 369-380.

KELLY, S.P., DOCKREE, P., REILLY, R.B. and ROBERTSON, I.H., 2003. EEG alpha power and coherence time courses in a sustained attention task, *Conference Proceedings. 1st International IEEE EMBS Conference on Neural Engineering 2003, 20-22 March 2003,* / 2003, IEEE pp83-6.

KIYMIK, M.K., GÜLER, İ, DIZIBÜYÜK, A. and AKIN, M., 2005. Comparison of STFT and wavelet transform methods in determining epileptic seizure activity in EEG signals for real-time application. *Computers in Biology and Medicine,* **35**(7), pp. 603-616.

KLEIN, A., SAUER, T., JEDYNAK, A. and SKRANDIES, W., 2006. Conventional and wavelet coherence applied to sensory-evoked electrical brain activity. *IEEE Transactions on Biomedical Engineering,* **53**(2), pp. 266-72.

KNOTT, V., MOHR, E., MAHONEY, C. and ILIVITSKY, V., 2000. Electroencephalographic coherence in Alzheimer's disease: comparisons with a control group and population norms. *Journal of Geriatric Psychiatry and Neurology,* **13**, pp. 1-8.

KORN, G.A. and KORN, T.M., 1968. Mathemetical handbook for scientists and engineers. New York: McGraw-Hill.

KRAMER, M.A. and SZERI, A.J., 2004. Quantitative approximation of the cortical surface potential from EEG and ECoG measurements. *IEEE Transactions on Biomedical Engineering,* **51**(8), pp. 1358-1365.

KUNO, Y., YAGI, T. and UCHIKAWA, Y., 1997. Study toward EEG applications: Event-related potential from posterior parietal cortex. *Annual International Conference of the IEEE Engineering in Medicine and Biology - Proceedings,* **4**, pp. 1551-1553.

LACHAUX, J., LUTZ, A., RUDRAUF, D., COSMELLI, D., QUYEN, M.L.V., MARTINERIE, J. and VARELA, F., June 2002. Estimating the time-course of coherence between single-trial brain signals:an introduction to wavelet coherence. *Neurophysiologie Clinique/ Clinical Neurophysiology,* **32**, pp. 157-174.

LAGERLUND, T.D., SHARBROUGH, F.W., BUSACKER, N.E. and CICORA, K.M., 1995. Interelectrode coherences from nearest-neighbor and spherical harmonic expansion computation of laplacian of scalp potential. *Electroencephalography and clinical neurophysiology,* **95**(3), pp. 178-88.

LAMER, R., LACROIX, D., MEUNIER, J., FRAILE, V. and ALBERT, J., 1994. Imaging of the electrical activity of the brain: a colour display of EEG local coherence,

Proceedings of the 16th Annual International Conference of the IEEE Engineering in Medicine and Biology Society. Part 1 (of 2), Nov 3-6 1994, 1994, IEEE, Piscataway, NJ, USA pp235-236.

LAW, S.K., NUNEZ, P.L., WESTDORP, A.F., NELSON, A.V. and PILGREEN, K.L., 1991. Topographical mapping of brain electrical activity, *Proceedings Visualization '91 (Cat. No.91CH3046-0), 22-25 Oct. 1991,* / 1991, IEEE Comput. Soc. Press pp194-201.

LAW, S.K., NUNEZ, P.L. and WIJESINGHE, R.S., 1993. High-resolution EEG using spline generated surface Laplacians on spherical and ellipsoidal surfaces. *IEEE Transactions on Biomedical Engineering,* **40**(2), pp. 145-53.

LAZZARO, I., GORDON, E., WHITMONT, S., PLAHN, M., LI, W., CLARKE, S., DOSEN, A. and MEARES, R., 1998. Quantitative EEG activity in adolescent attention deficit
hyperactivity disorder. *Clin Electroencephalogr,* **29**, pp. 37-42.

LE , J., MENON, V. and GEVINS, A., 1994. Local estimate of surface Laplacian derivation on a realistically shaped scalp surface and its performance on noisy data. *Electroencephalography and clinical Neurophysiologl.,* **92**, pp. 433-441.

LE, J. and GEVINS, A., 1993. Method to reduce blur distortion from EEG's using a realistic head model. *IEEE Transactions on Biomedical Engineering,* **40**(6), pp. 517-28.

LEHNERTZ, K., 2001. Nonlinear EEG analysis in epilepsy, *2001 Conference Proceedings of the 23rd Annual International Conference of the IEEE Engineering n Medicine and Biology Society, 25-28 Oct. 2001,* / 2001, IEEE pp1546-9.

LEHNERTZ, K., 2002. Nonlinear EEG analysis in epilepsy: from basic research to clinical applications, *Conference Proceedings. Second Joint EMBS-BMES Conference 2002 24th Annual International Conference of the Engineering in Medicine and Biology Society. Annual Fall Meeting of the Biomedical Engineering Society, 23-26 Oct. 2002,* / 2002, IEEE pp25-7.

LEHNERTZ, K., 2002. Nonlinear EEG analysis in epilepsy: from basic research to clinical applications, *Conference Proceedings. Second Joint EMBS-BMES Conference 2002 24th Annual International Conference of the Engineering in Medicine and Biology Society. Annual Fall Meeting of the Biomedical Engineering Society, 23-26 Oct. 2002,* / 2002, IEEE pp25-7.

LEHNERTZ, K. and ELGER, C.E., 1998. Can epileptic seizures be predicted? Evidence from nonlinear time series analysis of brain electrical activity. *Physical Review Letters,* **80**(22), pp. 5019-5022.

LEHNERTZ, K., MORMANN, F., KREUZ, T., ANDRZEJAK, R.G., RIEKE, C., DAVID, P. and ELGER, C.E., 2003. Seizure prediction by nonlinear EEG analysis. *IEEE Engineering in Medicine and Biology Magazine,* **22**(1), pp. 57-63.

LEUCHTER, A.F., SPAR, J.E., WALTER, D.O. and WEINER, H., 1987. Electroencephalographic spectra and coherence in the diagnosis of Alzheimer's-type and multi-infarct dementia. *Arch Gen Psychiatry,* **44**, pp. 993-998.

LIM, A.J. and WINTERS, W.D., 1980. A practical method for automatic real-time EEG sleep state analysis. *IEEE Transactions on Biomedical Engineering,* **BME-27**(4), pp. 212-20.

LIN, Z. and CHEN, J.D., 1996. Advances in time–frequency analysis of biomedical signals. *Critical Reviews in Biomedical Engineering,* **24**(1), pp. 1-72.

LISKE, E., HUGHES, H.M. and STOWE, D.E., 1966. Auto-and cross-coreelation of the EEG following unilateral caloric stimulation of the labyrinth. *Electroencephclography and Clinical Neurophysiology.,* **21**(3), pp. 295-300.

LIU, A., HAHN, J.S., HELDT, G.P. and COEN, R.W., 1992. Detection of neonatal seizures through computerized EEG analysis. *Electroencephalography and clinical neurophysiology,* **82**(1), pp. 30-7.

LOCATELLI, T., CURSI, M., LIBERATI, D., FRANCESCHI, M. and COMI, G., 1998. EEG coherence in Alzheimer's disease. *Electroencephalography and clinical neurophysiology,* **106**(3), pp. 229-37.

LOPES DA SILVA, F. H., VOS, J.E., MOOIBROEK, J. and VAN ROTTERDAM, , 1980. A partial coherence analysis of thalamic and cortical organization of rhythmic activity. In: G. PFURTSCHELLER, P. BUSAR and LOPES DA SILVA, F. H., eds, *Rhythmic EEG activities and cortical functioning.* Amsterdam: Elsevier, pp. 33-59.

LOPES DA SILVA, F.H., HOEKS, A., SMITS, H. and ZETTERBERG, L.H., 1974. Model of brain rhythmic activity: The alpha-rhythm of the thalamus. *Kybernetik,* **15**(1), pp. 27-37.

LOPES DA SILVA, F.H. and MARS, N. J. I., 1987. Parametric methods in EEG analysis. In: A.S. GEVINS and A. REMOND, eds, *Handbook of electroencephalography and clinical neurophysiology: methods of analysis of brain electrical and magnetic signals.* Amsterdam. The Netherland: Elsevier, pp. 243-260.

LV JIU-MING, LUO JING-QING and YUAN XUE-HUA, 2004. Application of chaos analytic methods based on normal EEG, *2004 3rd International Conference on Computational Electromagnetics and its Application, 1-4 Nov. 2004,* / 2004, IEEE pp426-9.

LYNN, P.A., 1992. Digital Signals, processors and noise. Hong Kong.: Macmillan press.

MADAN, T., AGARWAL, R. and SWAMY, M.N.S., 2004. Compression of long-term EEG using power spectral density, *Conference Proceedings. 26th Annual International Conference of the IEEE Engineering in Medicine and Biology Society, 1-5 Sept. 2004,* / 2004, IEEE pp180-3.

MAIORESCU, V.A., SERBAN, M. and LAZAR, A.M., 2003. Classification of EEG signals represented by AR models for cognitive tasks - a neural network based method, *SCS 2003. International Symposium on Signals, Circuits and Systems, 10-11 July 2003,* / 2003, IEEE pp441-4.

MARKAZI, S.A., QAZI, S.A. and STERGIOULAS, L.K., 2005. Study of Change Blindness EEG Synchronisation using Wavelet Coherence Analysis. *Engineering in Medicine and Biology 27th Annual Conference,* September 1-4, 2005 2005, IEEE pp5995-5998.

MAROSI, E., HARMONY, T., SANCHEZ, L., BECKER, J., BERNAL, J., REYES, A., DIAZ DE LEON, A.E., RODRIGUEZ, M. and FERNANDEZ, T., 1992. Maturation of the coherence of EEG activity in normal and learning-disabled children. *Electroencephalography and clinical neurophysiology,* **83**(6), pp. 350-7.

MARPLE, S.L., 1987. Digital spectral analysis with applications. New Jersey: Prentice-Hall.

MARSDLEK, T., MATOUSEK, V., MAUTNER, P., MERTA, M. and MOUCEK, R., 2006. Coherence of EEG signals and biometric signals of handwriting under influence of nicotine, alcohol and light drugs. *Neural Network World,* **16**(1), pp. 41-60.

MEINICKE, P., HERMANN, T., BEKEL, H., MULLER, H.M., WEISS, S. and RITTER, H., 2004. Identification of discriminative features in the EEG. *Intelligent Data Analysis,* **8**(1), pp. 97-107.

MINFEN SHEN, XIANHUI LI and XINJUN ZHANG, 2002. The time-varying coherent analysis of medical signals, *Proceedings of International Conference on Signal Processing (ICSP), 26-30 Aug. 2002,* / 2002, IEEE pp1528-31.

MORMANN, F., LEHNERTZ, K., DAVID, P. and ELGER, C.E., 2000. Mean phase coherence as a measure for phase synchronization and its application to the EEG of epilepsy patients. *Physica D,* **144**(3-4), pp. 358-69.

MOSELHY, H.F., GEORGIOU, G. and KAHN, A., 2001. Frontal lobe changes in alcoholism: A review of the literature. *Alcohol and Alcoholism,* **36**, pp. 357-368.

MOSER, H.R., WEBER, B., WIESER, H.G. and MEIER, P.F., 1999. Electroencephalograms in epilepsy: analysis and seizure prediction within the framework of Lyapunov theory. *Physica D,* **130**(3-4), pp. 291-305.

MURATA, A. and IWASE, H., 1998. Analysis of chaotic dynamics in EEG and its application to assessment of mental workload, *Proceedings of the 20th Annual International Conference of the IEEE Engineering in Medicine and Biology Society. Vol.20 Biomedical Engineering Towards the Year 2000 and Beyond, 29 Oct.-1 Nov. 1998,* / 1998, IEEE pp1579-82.

MUTHUSWAMY, J. and ROY, R.J., 1999. Use of fuzzy integrals and bispectral analysis of the electroencephalogram to predict movement under anesthesia. *IEEE Transactions on Biomedical Engineering,* **46**(3), pp. 291-299.

NAYAK, N., VALENTIN, A., ALARCON, G., GARCIA SEOANE, J. J., FRANZ, B., JULER, J., POLKEY, C.D. and BINNIE, C.D., 2004. Characteristics of scalp electrical fields associated with deep medial temporal epileptiform dischrages. *Clinical Neurophysiology,* **115**, pp. 1423-1435.

NELSON, A.V. and NUNEZ, P.L., 1993. Comparison of the Laplacian with classical recording methods in coherence analysis of EEG, *Proceedings of the 15th Annual International Conference of the IEEE Engineering in Medicine and Biology Society, Oct 28-31 1993,* 1993, Publ by IEEE, Piscataway, NJ, USA pp450-451.

NING, T. and BRONZINO, J.D., 1987. Detection of vigilance states: autoregressive approach, *Proceedings of the Thirteenth Annual Northeast Bioengineering Conference (Cat. No.87CH2436-4), 12-13 March 1987,* / 1987, IEEE pp255-7.

NING, T. and NIKIAS, C.L., 1986. Multichannel AR spectrum estimation: The optimum approach in the reflection coefficient domain. *IEEE Transactions on Acoustics, Speech and Signal Processing,* **ASSP-34**(5), pp. 1139-52.

NING, T. and TRINH, N., 2004. Cross-spectral and cross-bispectral analysis of hippocampal EEG with ICA processing, *Proceedings of the IEEE 30th Annual Northeast Bioengineering Conference, Apr 17-18 2004,* 2004, Institute of Electrical and Electronics Engineers Inc pp102-103.

NUNEZ, P., ed, 1981. *Electric fields of the brain.* New York: Oxford.

NUNEZ, P.L. and PILGREEN, K.L., 1991. The spline-Laplacian in clinical neurophysiology: a method to improve EEG spatial resolution. *Journal of Clinical Neurophysiology.,* , pp. 397-413.

NUNEZ, P.L., SILIBERTEIN, R.B., CDUSH, P.J., WIJESINGHE, R.S. and WESTDROP A. F., 1994. A theoretical and experimental study of high resolution EEG based on surface laplacian and cortical imaging. *Electroenceph clin Neurophysiol,* **90**, pp. 40-57.

NUNEZ, P.L. and SRINIVASAN, R., 2005. Electric fields of the brain. Oxford University Press.

NUNEZ, P.L. and WESTDORP, A.F., 1994. The Surface Laplacian, High Resolution EEG and Controversies. *Brain Topography,* **6**(3), pp. 221-226.

NUNEZ, P.L., ed, 1995. *Neocortical Dynamics and Human EEG Rhythms.* New York: Oxford University Press.

NUNEZ, P.L., 1989. Estimation of large scale neocortical source activity with EEG surface Laplacian. *Brain Topography,* **2**(1), pp. 141-154.

NUNEZ, P.L., 1995. Neocortical Dynamics and Human EEG Rhythms. New York.: Oxford University.

NUNEZ, P.L., SILBERSTEIN, R.B., ZHIPING SHI, CARPENTER, M.R., SRINIVASAN, R., TUCKER, D.M., DORAN, S.M., CADUSCH, P.J. and

WIJESINGHE, R.S., 1999. EEG coherency. II. Experimental comparisons of multiple measures. *Clinical Neurophysiology,* **110**(3), pp. 469-86.

NUNEZ, P.L., SRINIVASAN, R., WESTDORP, A.F., WIJESINGHE, R.S., TUCKER. D.M., SILBERSTEIN, R.B. and CADUSCH, P.J., 1997. EEG coherency. I. Statistics, reference electrode, volume conduction, Laplacians, cortical imaging and interpretation at multiple scales. *Electroencephalography and clinical neurophysiology,* **103**(5), pp. 499-515.

NUTTALL, A.H., 1976. Multivariate linear predictive spectral analysis employing weighted forward and backward averaging:a generalization of Burg's algorithm. *Naval underwater systems center technical report,* **5501**.

NUWER, M.R., COMI, G., EMERSON, R., FUGLSANG-FREDERIKSEN, A., GUERIT, J., HINRICHS, H., IKEDA, A., JOSE C. LUCCAS, F. and RAPPELSBURGER, P., 1998. IFCN standards for digital recording of clinical EEG. *Electroencephalography and Clinical Neurophysiology,* **106**(3), pp. 259-261.

OGO, K. and NAKAGAWA, M., 1995. Chaos and fractal properties in EEG data. *Electronics and Communications in Japan, Part 3 (Fundamental Electronic Science),* **78**(10), pp. 27-36.

OKUDA, K., YASUHARA, A., KAMEI, A., ARAKI, A., KITAMURA, N. and KOBAYASHI, Y., 2000. Successful control with bromide of two patients with malignant migrating partial seizure in infancy. *Brain and development,* **22**, pp. 56-59.

OOSTENDORP, T.F. and VAN OOSTEROM, A., 1996. Surface Laplacian of the potential: theory and application. *IEEE Transactions on Biomedical Engineering,* **43**(4), pp. 394-405.

OOSTENVELD, R. and PRAAMSTRA, P., 2001. The five percent electrode system for high-resolution EEG and ERP measurements. *Clinical Neurophysiology,* **112**(4), pp. 713-719.

PALANIAPPAN, R. and RAVEENDRAN, P., 2001. Cognitive task prediction using parametric spectral analysis of EEG signals. *Malaysian Journal of Computer Science,* **14**(1), pp. 58-67.

PANZICA, F., BINELLI, S., FRANCESCHETTI, S. and AVANZINI, G., 1998. Applicability of autoregressive models to the study of ictal EEG patterns. *Automazione e Strumentazione,* **46**(11), pp. 133-7.

PARDEY, J., ROBERTS, S. and TARASSENKO, L., 1996. A review of parametric modelling techniques for EEG analysis. *Medical engineering & physics,* **18**(1), pp. 2-11.

PERNIER, J., PERRIN, F. and BERTRAND, O., 1988. Scalp current density fields: Concepts and properties. *Electroencephalography and Clinical Neurophysiology,* **69**, pp. 385-389.

PERRIN, F., BERTRAND, O. and PERNIER, J., 1987. Scalp current density mapping: value and estimation from potential data. *IEEE Transactions on Biomedical Engineering,* **BME-34**(4), pp. 283-8.

PERRIN, F., PERNIER, J., BERTRAND, O. and ECHALLIER, J.F., 1989. Spherical splines for scalp potential and current density mapping. *Electroencephalography and clinical neurophysiology,* **72**(2), pp. 184-7.

PRADHAN, N. and NARAYANA DUTT, D., 1993. A nonlinear perspective in understanding the neurodynamics of EEG. *Computers in biology and medicine,* **23**(6), pp. 425-42.

PRIESTLEY, M.B., 1981. Spectral analysis and time series: Multivariate series, prediction and control. London: Academic press.

QUIAN QUIROGA, R., BLANCO, S., ROSSO, O.A., GARCIA, H. and RABINOWICZ, A., 1997. Searching for hidden information with Gabor transform in generalized tonic-clonic seizures. *Electroencephalography and clinical neurophysiology,* **103**(4), pp. 434-9.

QUIAN QUIROGA, R. and SCHURMANN, M., 1999. Functions and sources of event-related EEG alpha oscillations studied with the wavelet transform. *Clinical Neurophysiology,* **110**(4), pp. 643-54.

RANGASWAMY, M., PORJESZ, B., CHORLIAN, D.B., WANG, K., JONES, K.A., BAUER, L.O., ROHRBAUGH, J., O'CONNOR, S.J., KUPERMAN, S., REICH, T. and BEGLEITER, H., 2002. Beta power in the EEG of alcoholics. *Biological Psychiatry,* **52**(8), pp. 831-842.

REMOND, A., ed, 1977. *EEG informatics. a didactic review of methods and applications of EEG data processing.* Amsterdam, ElsevierlNorth-Holland: Biomedical Press.

ROCHA, C., DILLENSEGER, J.-. and COATRIEUX, J.-., 1996. Multi-array EEG signals mapped with three dimensional images for clinical epilepsy studies, *Proceedings of Fourth International Conference on Visualization in Biomedical Computing (VBC'96), 22-25 Sept. 1996,* / 1996, Springer-Verlag pp467-76.

ROESSGEN, M., ZOUBIR, A.M. and BOASHASH, B., 1998. Seizure detection of newborn EEG using a model-based approach. *IEEE Transactions on Biomedical Engineering,* **45**(6), pp. 673-85.

ROESSGEN, M. and BOASHASH, B., 1995. Seizure analysis of newborn EEG using a model based approach, *Proceedings of the 1995 International Conference on Acoustics, Speech, and Signal Processing. Part 3 (of 5), May 9-12 1995,* 1995, IEEE, Piscataway, NJ, USA pp1936-1939.

ROESSGEN, M., ZOUBIR, A.M. and BOASHASH, B., 1998. Seizure detection of newborn EEG using a model-based approach. *IEEE Transactions on Biomedical Engineering,* **45**(6), pp. 673-685.

ROGOWSKI, Z., GATH, I. and BENTAL, E., 1981. On the prediction of epileptic seizures. *Biological cybernetics,* **42**(1), pp. 9-15.

ROMBOUTS, S.A.R.B., KEUNEN, R.W.M. and STAM, C.J., 1995. Investigation of nonlinear structure in multichannel EEG. *Physics Letters A,* **202**(5-6), pp. 352-8.

ROSSO, O.A., BLANCO, S., YORDANOVA, J., KOLEV, V., FIGLIOLA, A., SCHURMANN, M. and BASAR, E., 2001. Wavelet entropy: a new tool for analysis of short duration brain electrical signals. *Journal of neuroscience methods,* **105**(1), pp. 65-75.

ROSSO, O.A. and MAIRAL, M.L., 2002. Characterization of time dynamical evolution of electroencephalographic epileptic records. *Physica A: Statistical Mechanics and its Applications,* **312**(3-4), pp. 469-504.

RUBIN, E., 2000. Figure and ground. In: S. YANTIS, ed, *Key readings in cognittion: Visual perception:* Philadelphia: Psychology Press, pp. 225-229.

RYAN, E.D., CRAMER, J.T., EGAN, A.D., HARTMAN, M.J. and HERDA, T.J., Time and frequency domain responses of the mechanomyogram and electromyogram during isometric ramp contractions: A comparison of the short-time Fourier and continuous wavelet transforms. *Journal of Electromyography and Kinesiology,* **In Press, Corrected Proof.**

RYAN, N., MESBAH, M. and BOASHASH, B., 1999. A review of techniques for automatic detection of neonatal seizure using EEG, *Proceedings of Fifth International Symposium on Signal Processing and its Applications, 22-25 Aug. 1999,* / 1999, Queensland Univ. Technol pp239-42.

RYYNANEN, O.R.M., HYTTINEN, J.A.K., LAARNE, P.H. and MALMIVUO, J.A., 2004. Effect of electrode density and measurement noise on the spatial resolution of cortical potential distribution. *IEEE Transactions on Biomedical Engineering,* **51**(9), pp. 1547-54.

SAIWAKI, N., TSUJIMOTO, H., NISHIDA, S. and INOKUCHI, S., 1997. Directed coherence analysis of EEG recorded during music listening, *Proceedings of 18th Annual International Conference of the IEEE Engineering in Medicine and Biology Society, 31 Oct.-3 Nov. 1996,* / 1997, IEEE pp827-8.

SALANT, Y., GATH, I. and HENRIKSEN, O., 1998. Prediction of epileptic seizures from two-channel EEG. *Medical & biological engineering & computing,* **36**(5), pp. 549-56.

SCHMID, R.G., TIRSCH, W.S. and SCHERB, H., 2002. Correlation between spectral EEG parameters and intelligence test variables in school-age children. *Clinical Neurophysiology,* **113**(10), pp. 1647-1656.

SCOTT, D., 1976. Understanding EEG: an introduction to electroencephalography. Duckworth.

SEMMLOW, J.L., ed, 2004. *Biosignal and biomedical image processing.* New York, U.S.A: Marcel Dekker,Inc.

SHARMA, A., WILSON, S.E. and ROY, R.J., 1992. Autoregressive modeling of EEG signals for monitoring anesthetic levels, *Proceedings of the Eighteenth IEEE Annual Northeast Bioengineering Conference (Cat. No.92CH3238-3), 12-13 March 1992,* / 1992, IEEE pp39-40.

SHARMA, A. and ROY, R.J., 1997. Design of a recognition system to predict movement during anesthesia. *IEEE Transactions on Biomedical Engineering,* **44**(6), pp. 505-511.

SHAW, J.C., 1981. An introduction to the coherence function and its use in EEG signals. *Journal of Medical Engineering and Technology,* **5**, pp. 279-288.

SHERMAN, D.L., CRONE, N.E., BOATMAN, D., GORDON, B., THAKOR, N.V. and HINICH, M.J., 1999. Partial coherence of the event related potential: a new and powerful index of cerebral activation, *Proceedings of the IEEE Signal Processing Workshop on Higher-Order Statistics, 14-16 June 1999,* / 1999, IEEE Comput. Soc pp170-3.

SHERMAN, D.L., TSAI, Y.C., ROSSELL, L.A., MIRSKI, M.A. and THAKOR, N.V., 1997. Spectral analysis of a thalamus-to-cortex seizure pathway. *IEEE Transactions on Biomedical Engineering,* **44**(8), pp. 657-664.

SHIMOYAMA, I., KASAGI, Y., YOSHIDA, S., NAKAZAWA, K., MURATA, A. and ASANO, F., 2004/8. High resolution spectral analysis of visual evoked EEGs for word-recognition "Event-related spectra". *International Congress Series,* **1270**, pp. 213-215.

SIDMAN, R.D., 1991. A method for simulating intracerebral potential fields: the cortical imaging method. *Journal of Clinical Neurophysiology,* **8**, pp. 432-441.

SIMONSEN, E., THOMSEN, C.E. and WILDSCHIODTZ, G., 1987. A generalized model of sleep EEG compared to manual scoring-a sleep analysis method based on autoregressive modeling and cluster analysis, *Proceedings of the Ninth Annual Conference of the IEEE Engineering in Medicine and Biology Society (Cat. No.87CH2513-0), 13-16 Nov. 1987,* / 1987, IEEE pp1272-3.

SNODGRSS, J.G. and VANDERWART, M., 1980. A standardized set of 260 pictures: norms for the naming agreement, familiarity, and visual complexity. *Journal of Experimental Psychology: Human Learning and Memory.,* **6**, pp. 174-215.

SOONG, A.C.K., LIND, J.C., SHAW, G.R. and KOLES, Z.J., 1993. Systematic comparisons of interpolation techniques in topographic brain mapping. *Electroencephalography and clinical neurophysiology,* **87**(4), pp. 185-95.

SREBRO, R., 1985. Localization of visually evolved cortical activity in humans. *Journal of Physiology,* **360**, pp. 233-246.

SRINIVASAN, R., 1999. Methods to Improve the Spatial Resolution of EEG. *International Journal of bioelectromagnetism.*, **1**(1),.

SRINIVASAN, R., NUNEZ, P.L., TUCKER, D.M., SILBERSTEIN, R.B. and CADUSCH, P.J., 1996. Spatial sampling and filtering of EEG with spline Laplacians to estimate cortical potentials. *Brain Topography.*, **8**, pp. 355-366.

SRINIVASAN, R., 2004. Internal and external neural synchronization during conscious perception. *International Journal of Bifurcation and Chaos in Applied Sciences and Engineering,* **14**(2), pp. 825-42.

SRINIVASAN, R., NUNEZ, P.L. and SILBERSTEIN, R.B., 1998. Spatial filtering and neocortical dynamics: estimates of EEG coherence. *IEEE Transactions on Biomedical Engineering,* **45**(7), pp. 814-26.

STAM, C.J., 2003. Chaos, continuous EEG, and cognitive mechanisms: a future for clinical neurophysiology. *American Journal of Electroneurodiagnostic Technology,* **43**(4), pp. 211-27.

SUBASI, A., 2005. Application of classical and model-based spectral methods to describe the state of alertness in EEG. *Journal of medical systems,* **29**(5), pp. 473-86.

SUBASI, A., ALKAN, A., KOKLUKAYA, E. and KIYMIK, M.K., 2005. Wavelet neural network classification of EEG signals by using AR model with MLE preprocessing. *Neural Networks,* **18**(7), pp. 985-97.

SVOBODA, P., 2006. Detection of vigilance changes by linear and nonlinear EEG signal analysis. *Neural Network World,* **16**(1), pp. 61-75.

TA-HSIN LI and KLEMM, W.R., 2000. Detection of cognitive binding during ambiguous figure tasks by wavelet coherence analysis of EEG signals, *Proceedings of 15th International Conference on Pattern Recognition, 3-7 Sept. 2000,* / 2000, IEEE Comput. Soc pp94-7.

TAIKANG NING and NHON TRINH, 2004. Cross-spectral and cross-bispectral analysis of hippocampal EEG with ICA processing, *Proceedings of the IEEE 30th Annual Northeast Bioengineering Conference, 17-18 April 2004,* / 2004, IEEE pp102-3.

TANDONNET, C., BURLE, B., HASBROUCQ, T. and VIDAL, F., 2005/0. Spatial enhancement of EEG traces by surface Laplacian estimation: comparison between local and global methods. *Clinical Neurophysiology,* **116**(1), pp. 18-24.

TAYLOR, M.J. and BALDEWEG, T., 2002. Application of EEG, ERP and intracranial recordings to the investigation of cognitive functions in children. *Developmental science,* **5**(3), pp. 318-334.

THATCHER, R.W., KRAUSE, P.J. and HRYBYK, M., 1986. Cortico-cortical associations and EEG coherence: a two-compartmental model. *Electroencephalography and clinical neurophysiology,* **64**(2), pp. 123-43.

TIERRA, C.J., SIMPSON, D.M. and INFANTOSI, A. F. C., 1996. Surface Laplacian with spline and nearest neighbour interpolations for topographic brain mapping. *18th Annual International Conference of the IEEE Engineering in Medicine and Biology Society.* 1996, .

TORRENCE, C. and COMPO, G.P., 1998. A practical guide to wavelet analysis. *Bulletin of the American meteorological society,* **79**(1), pp. 61-78.

TOWIE, V.L., SYED, I., BERGER, C., GRZESCZCUK, R., MILTON, J., ERICKSON, R.K., COGEN, P., BERKSON, E. and SPIRE, J.-., 1998. Identification of the sensory/motor area and pathologic regions using ECoG coherence. *Electroencephalography and clinical neurophysiology,* **106**(1), pp. 30-9.

TSAI, Y.C., SHERMAN, D.L., ROSSELL, L.A., MIRSKI, M.A. and THAKOR, N.V., 1995. Identification of seizure pathways by spectral analysis of EEG, *Proceedings of the 1995 IEEE Engineering in Medicine and Biology 17th Annual Conference and 21st Canadian Medical and Biological Engineering Conference, Sep 20-23 1995,* 1995, pp897-898.

TUCKER, D.M., DAWSON, S.L., ROTH, D.L. and PENLAND, J.G., 1985. Regional changes in EEG power and coherence during cognition: intensive studies of two individuals. *Behav. Neurosci,* , pp. 564-577.

TUCKER, D.M., ROTH, D.L. and BAIR, T.B., 1986. Functional connections among cortical regions; topography of EEG coherence. *Electroencephalography and clinical neurophysiology,* **63**(3), pp. 242-50.

TUKEL, K. and JASPER, H., 1952. The electroencephalogram in parasagittal lesions. *Electroencephalography and Clinical Neurophysiology,* **4**, pp. 481.-494.

UEDA, S. and MATSUBA, I., 1997. Nonlinear data analysis of EEG. *Transactions of the Institute of Electronics, Information and Communication Engineers A,* **J80-A**(7), pp. 1197-200.

UNSER, M. and ALDROUBI, A., 1996. A review of wavelets in biomedical applications. *Proceedings of the IEEE,* **84**(4), pp. 626-38.

VAN DER HEYDEN, M.J., VELIS, D.N., HOEKSTRA, B.P.T., PIJN, J.P.M., VAN EMDE BOAS, W., VAN VEELEN, C.W.M., VAN RIJEN, P.C., LOPES DA SILVA, F.H. and DEGOEDE, J., 1999. Non-linear analysis of intracranial human EEG in temporal lobe epilepsy. *Clinical Neurophysiology,* **110**(10), pp. 1726-40.

VAZ, F. and PRINCIPE, J.C., 1987. Automatic classification of epileptic seizures in the EEG, *Digital Signal Processing - 87. Proceedings of the International Conference, 7-10 Sept. 1987,* / 1987, North-Holland pp564-7.

VINCENT, J.S., KENNETH, P.S. and MYSORE, R.R., 1995. Multiresolution analysis of event-related potentials by wavelet decomposition. *Brain and Cognition,* , pp. 398-438.

WALLIN, G. and STALBERG, E., 1980. Source derivation in clinical routine EEG. *Electroencephalography and Clinical Neurophysiology.,* **50**, pp. 282-292.

WANG, K. and BEGLEITER, H., 1999. Local Polynomial Estimate of Surface Laplacian. *Brain Topography,* **12**(1), pp. 19-29.

WEISS, N.A. and HASSETT, M.J., 1991. Introductory statistics. 3rd edn. U.S.A: Addison-Wesley publishing company.

WENNBERG, A. and ZETTERBERG, L.H., 1971. Application of a computer-based model for EEG analysis. *Electroencephalography and clinical neurophysiology,* **31**(4), pp. 457-68.

WICHNIAK, A., GEISLER, P., BRUNNER, H., TRACIK, F., CRONLEIN, T., FRIESS, E. and ZULLEY, J., 2003. Spectral composition of NREM sleep in healthy subjects with moderately increased daytime sleepiness. *Clinical Neurophysiology,* **114**(8), pp. 1549-55.

WINTERER, G., ENOCH, M.A., WHITE, K.V., SAYLAN, M., COPPOLA, R. and GOLDMAN, D., 2003. EEG phenotype in alcoholism: increased coherence in the depressive subtype. *Acta Psychiatrica Scandinavica.*, **108**(1), pp. 51-60.

WONG, F.Y., BARFIELD, C.P. and WALKER, A.M., Power spectral analysis of two-channel EEG in hypoxic-ischaemic encephalopathy. *Early Human Development,* **In Press, Corrected Proof**.

WONG, K.F.K., GALKA, A., YAMASHITA, O. and OZAKI, T., 2006. Modelling non-stationary variance in EEG time series by state space GARCH model. *Computers in biology and medicine,* **36**(12), pp. 1327-35.

WU, R., LIANG, S., LIN, C. and HSU, C., 2004. Applications of event-related-potential-based brain computer interface to intelligent transportation systems, *Conference Proceeding - 2004 IEEE International Conference on Networking, Sensing and Control, Mar 21-23 2004,* 2004, Institute of Electrical and Electronics Engineers Inc., Piscataway, United States pp813-818.

XIAOLI LI, XIN YAO, JEFFERYS, J.R.G. and FOX, J., 2006. Computational neuronal oscillations using Morlet wavelet transform, *2005 27th Annual International Conference of the IEEE Engineering in Medicine and Biology Society, 31 Aug.-3 Sept. 2005,* / 2006, IEEE pp4.

YAMAGUCHI, C., 2002. Wavelet analysis of normal and epileptic EEG, *Conference Proceedings. Second Joint EMBS-BMES Conference 2002 24th Annual International Conference of the Engineering in Medicine and Biology Society. Annual Fall Meeting of the Biomedical Engineering Society, 23-26 Oct. 2002,* / 2002, IEEE pp96-7.

YAMAMOTO, T., 1960. Autocorrelation studies of electroencephalograph of normals and epileptics. *Folia Psychiatr Neurol Jap,* **14**, pp. 289-303.

YOSHINAGA, H., KOBAYASHI, K., SATO, M., OKA, E. and OHTAHARA, S., 1996. Investigation of bilateral synchronous spike-wave discharge by EEG topography. *Brain Topography,* **8**, pp. 255-260.

ZHAN, Y., HALLIDAY, D., JIANG, P., LIU, X. and FENG, J., 2006. Detecting time-dependent coherence between non-stationary electrophysiological signals—A combined statistical and time–frequency approach. *Journal of Neuroscience Methods,* **156**(1-2), pp. 322-332.

ZHANG, X.L., BEGLEITER, H., PORJESZ, B., WANG, W. and LITKE. A., 1995. Event related potentials during object recognition tasks. *Brain Research Bulletin.*, **38**(6), pp. 531-538.

ZUMSTEG, D., FRIEDMAN, A., WENNBERG, R.A. and WIESER, H.G., 2005. Source localization of mesial temporal interictal epileptiform discharges: correlation with intracranial foramen ovale electrode recordings. *Clinical Neurophysiology,* **116**(12). pp. 2810-18.